AD A 951 734

AIRCRAFT NAVIGATION AND COMMUNICATIONS INTERFERENCE MITIGATION
(SANGUINE System)

Final Report
(11 December 1969 to 10 March 1971)

March 1971

by

Reuben Goldman
Alfred Eckersley
William W. Cooley

Prepared Under Contract N00039-70-C-1513

for

Naval Electronic Systems Command
Department of the Navy
Washington, D.C. 20360
(Navelex PME117-21)

by

BOEING
Commercial Airplane Group
Seattle, Washington

DTIC FILE COPY

DTIC
ELECTE
JUN 3 1982
S D
D

DISTRIBUTION STATEMENT A
Approved for public release;
Distribution Unlimited

82 04 28 067

FOREWORD

This research--ELF Effects on Avionics--was performed by The Boeing Company, Commercial Airplane Group, Electrodynamics Technology, under Department of the Navy contract N00039-70-C-1513. The program was administered by the Department of the Navy, Naval Electronics Systems Command, Washington, D.C. The naval officer directing the technical aspects of the study was Commander W. K. Hartell (Navelex, PME 117-214). Commander Hartell reports to Captain F. L. Brand, head of the overall Environmental Compatibility Assurance Program (ECAP) of the SANGUINE project, of which this research is a part.

This report recapitulates, unifies, and emphasizes the salient results of the subject study as reported in a comprehensive test plan and 12 monthly reports. The research was performed between December 11, 1969, and March 10, 1971. For the first 8 months of the program--to August 15, 1970--research was conducted under the direction of R. B. Schulz. R. Goldman, principal investigator throughout the program, acted as program manager subsequent to that date.

Dr. William W. Cooley, associate professor of electrical engineering at Seattle University, served as consultant and theoretical analyst in the research. Alfred Eckersley, research specialist with The Boeing Company, collaborated in the research from October 1, 1970 to its completion and in the preparation of this report.

Accession For	
NTIS GRA&I	☒
DTIC TAB	☐
Unannounced	☐
Justification (March 1971)	
By Per Ltr. on file	
Distribution/	
Availability Codes	
Dist	Avail and/or Special
A	

Released

UNANNOUNCED

DTIC COPY INSPECTED 2

ACKNOWLEDGEMENTS

Many Boeing engineers have contributed to this program. The research reported herein involved tests on numerous avionics systems of highly specialized function and of sophisticated design. Engineers knowledgeable in a given avionics system provided technical assistance--often over extended periods--so that research could be performed under realistic conditions. Further, they assisted in the interpretation of laboratory results to ensure that all events requiring mitigation were disclosed.

Appreciation is gratefully extended to the management and engineering personnel of the FAA Air Route Traffic Control Center at Auburn, Washington, for permission to make field measurements in the main control room and to perform tests on elements of avionics ground control equipment. Mr. Len Westbo, engineer in charge of radar equipment maintenance, provided invaluable technical guidance and advice in the performance of SANGUINE-related tests on traffic control equipment and in the interpretation of test results.

The continued direction, critique and advice of naval and IITRI personnel throughout the performance of this study are gratefully acknowledged. Dr. Don A. Miller and Mr. M. Abromavage were the IITRI engineers directly responsible for the technical aspects of this study and for monitoring and approving its direction and content.

Lastly, deep appreciation is expressed to Wayne C. Colley, electronic technician throughout this study, for his industry and innovativeness in devising and constructing test adjuncts and in planning test setups.

CONTENTS

		Page
1.0	INTRODUCTION	1
2.0	LABORATORY PROCEDURES	3
2.1	Statement of Problem	3
2.2	Test Equipment	3
2.2.1	Aircraft Avionics Location	3
2.2.2	Test Field Generation Devices	5
2.2.3	Strip-Line	7
2.2.4	Test Coil	7
2.3	Laboratory Investigation	8
2.3.1	Test Plan	8
2.3.2	Test Procedures: Strip-Line and Magnetic Coil	8
2.3.3	Voltage Injection Tests	9
3.0	SUMMARY OF TEST RESULTS	10
3.1	Voltage Injection on Power and Telephone Lines to Air Traffic Control Equipment	10
3.1.1	Test Equipment and Procedures	11
3.1.2	Test Descriptions and Results	11
3.1.3	Air Route Surveillance Radar Display	13
3.1.4	VHF Communications Receiver	13
3.1.5	Injection Into Telephone Circuit to Remote Air/-Ground Communications Site	14
3.2	Summary of Test Results	15
4.0	VOLTAGES INDUCED IN AIRPLANE WIRING	27
4.1	Introduction	27
4.2	Boeing 747 Aircraft Wiring	27
4.3	Induced Voltages	29
4.4	Airframe Shielding	30
4.5	Summation	31
5.0	FIELDS AT AIRCRAFT ALTITUDE	34

CONTENTS.—Concluded

		Page
6.0	SUSCEPTIBILITY OF ELECTRONIC DISPLAYS	41
6.1	Introduction	41
6.2	Recapitulation of Avionic Display Equipment Susceptibility	41
6.3	Susceptibility of Commercial Test Equipment	41
6.4	Mechanism of Susceptibility	41
6.5	Shielding Effectiveness of CRT Shields	42
6.6	Susceptibility Levels of Oscilloscopes	47
6.7	Conclusions	48
7.0	COMPASS SYSTEM	49
7.1	Introduction	49
7.2	Recapitulation of Earlier Tests and General Background	49
7.3	Impact of SANGUINE System on Navigation	50
7.4	Further Tests	52
7.4.1	Introduction	52
7.4.2	Flux Valve Operation	52
7.4.3	Test Configuration	54
7.5	Test Results	56
7.5.1	Effects of Small DC Fields on Overall System	56
7.5.2	Effects of AC Fields on Overall System	57
7.6	Conclusions	60
8.0	GROUND EQUIPMENT ENVIRONMENT MEASUREMENTS	61
9.0	RESULTS AND RECOMMENDATIONS FOR CONTINUED RESEARCH	62
9.1	Study Results	62
9.2	Recommendations for Continued Research	63
REFERENCES		64
APPENDIX A		65
APPENDIX B		71

FIGURES

No.		Page
1	Electrical/Electronic Equipment Location	4
2	Antenna Locations	5
3	Interior of Power Oscillator	6
4	747 Equipment Location	28
5	Main Equipment Center	28
6	Paths for Overflight of SANGUINE Array	34
7	Geometry for Array	35
8	Fields at Altitude, 10-Element Array--1.5-Mi Spacing, 70 Amp per Element	37
9	Fields at Altitude, 10-Element Array--5-Mi Spacing, 70 Amp per Element	37
10	Fields at Altitude, 10-Element Array--1.5-Mi Spacing, 50 Amp per Element	38
11	Geometry for a Long Wire	39
12	Transverse Variations of Field for Single Antenna Element 20 Mi Long at Altitude	40
13	Tests on CRT Shields	43
14	Mumetal Shield for 3WP1 CRT	44
15	Sketch of Shield for Tektronix 549 CRO Showing Major Openings	45
16	Attenuation of ELF H-Field by 3WP1 CRT Shield	45
17	ELF Magnetic Field Attenuation--Tektronix 549 CRO Tube Shield	46
18	Susceptibility of Cathode Ray Oscilloscopes	47
19	Flux Valve Principles	53
20	Compass System Block Diagrams	54
21	Compass System Test Arrangement	55
22	Compass System--Coupler, Angle Position Indicator, Control Panel, Compensator, and Inertial Navigation System Simulator	55
23	Flux Valve in Test Coil--DC Field Applied	56
24	Airplane Compass System--Oscillogram of Input to Isolation Amplifier Derived from Flux Valve Control Transformer	58
B1	Brake Temperature Monitoring System	71
B2	Test Setup for Brake Temperature Monitor (Wire-by-Wire Voltage Injection Test)	71
B3	Window Heat Control Unit	72
B4	Cockpit Voice Recorder and Control Unit	72
B5	ADF Receiver in Test Coil	72
B6	Block Diagram of Test Setup: RNA-26C VHF Navigation Receiver (Bendix)	73
B7a	Test Setup: RNA-26C VHF Navigation Receiver (Bendix)	74
B7b	Breakout Box for Wire-by-Wire Voltage Injection (VHF Navigation Receiver)	74

Figures.—Continued

No.		Page
B8	Test Setup: MKA-28A Marker Receiver (Bendix)	75
B9	Test Setup: 621A-3 ATC Transponder (Collins)	76
B10	621A-3 ATC Transponder Test Setup	77
B11	ALA-51A Radio Altimeter System	77
B12	Test Setup: ALA-51A Radio Altimeter System (Bendix)	78
B13	Test Setup: Distance Measuring Equipment	79
B14	Test Setup: Loran System 600T, Edo Commercial Corp.	80
B15	Test Setup: Loran Receiver 600T, Edo Commercial Corp.	81
B16	Block Diagram of Test Setup: Weather Radar System, RDR-1E (Bendix)	82
B17	Test Setup: Weather Radar (Coil), RDR-1E (Bendix)	83
B18	Weather Radar System RDR-1E, Main Unit and Radar Control in Coil for Test	83
B19	Weather Radar System RDR-1E Radar Antenna	84
B20	Test Setup: Inertial Navigation System, Strip-Line Testing	84
B21	INS Test Console	85
B22	INS Test Patch Box, Carousel IV	85
B23	INS Control/Display Unit and Mode Selector Unit, Carousel IV	86
B24	Test Equipment for Bendix PB-20 Autopilot Computer (Airborne Computer Unit at Lower Left)	86
B25	Control Panel, PB-20 Autopilot	87
B26	Roll Control Channel for Sperry SP-77 Flight Control System	87
B27a	P13-20 Autopilot Control Panel (in coil)	88
B27b	Test Setup: Flight Recorder System	88
B28	Automatic Test Equipment (T.R.A.C.E.) for Air Data Computer	88
B29	Test Equipment Required to Exercise Air Data Computer	88
B30	Horizontal Display Cabinet, Radar Bright Display RBDE-4	89
B31	Scan Converter Cabinet, Radar Bright Display RBDE-4	89
B32	Rear of Common and Line Compensating Rack, Air Traffic Control Beacon Interrogator, ATCBI-2	90
B33	Rear of Racks Housing VHF and UHF Air-to-Ground Voice Communication Receivers	90
B34	Test Setup: ADF 51Y-4	91
B35	Test Setup: VHF Navigation Receiver (Equipment in Strip-Line Cavity)	92
B36	Test Setup: Wire-by-Wire Voltage Injection Test; Marker Receiver, MKA-28A (Bendix)	92
B37	Marker Receiver and Test Breakout Box	93
B38	Test Setup and Breakout Box for Distance Measuring Equipment DME 860-2 (Collins)	93

FIGURES.--Concluded

No.		Page
B39	Test Setup: Voltage Injection in Power Lines	94
B40	Air Route Surveilance Radar Display	95
B41	Power Line Voltage Injection, Air Route Surveillance Radar	95
B42	Telephone Circuit Test Arrangement	96
B43	FAA Equipment Feeding 1,000-Hz Test Signal into Transmit Line	97
B44	Boeing Test Equipment Injecting Voltages Into Receive Line on FAA Side of Demarcation to Telephone Company Facilities	97
B45	Telephone-Type Level Measuring Equipment	98
B46	Received Signal on Monitor, With 60 Hz Superimposed on 1,000-Hz Test Signal (20 ms/cm; 200 mV/cm)	98
B47	Received Signal on Monitor, With 60 Hz Superimposed on 1,000-Hz Test Signal (700 mV, 60 Hz Injected)	98

TABLES

No.		Page
1	H-Field Exposure Tests--Strip-Line and Coil	17
2	Wire-by-Wire Voltage Injection Tests--Resume and Results	23
3	Induced Voltage (Volts per Gauss) in 747 Wire Runs for Internal Magnetic Field	33
4	Induced Voltage (Volts per Gauss) in 747 Wire Runs for External Magnetic Field	33

1.0 INTRODUCTION

This study is part of a comprehensive Environmental Compatibility Assurance Program (ECAP)of Project SANGUINE. Project SANGUINE is the code designation for a worldwide U.S. Forces communications capability from a single U.S.-based transmitter operating in the extremely-low-frequency (ELF) region.

The ECAP program consists of the research and development required to ensure that an ELF communications system, as designed, installed, and operated, will be compatible with the environment. The total program includes three broad areas: biological and ecological research, facilities construction, and operation planning and interference mitigation development. This document describes research in the latter area--the mitigation of disclosed susceptibilities in aircraft navigation and communications equipment, airborne or ground based, caused by the SANGUINE system. (Studies related to the mitigation of interference to commercial power lines and communications media--TV, radio, telephone--are being performed by other research groups.)

Accordingly, test devices were constructed to generate uniform, controllable fields in the frequency range of 40 to 150 Hz, the bounds within which the SANGUINE operating frequency will be selected. (The discrete frequencies of 42, 56, and 60 Hz are precluded; the first two are telephone ringing-circuit frequencies.) Field strengths were continuously variable to 10+ gauss, an order of magnitude above the nominal 1-gauss "worst-case" criterion given by SANGUINE system design personnel.

Representative avionics subsystems were individually subjected to the test fields and their normal functions exercised. Elements of subsystems were interconnected with wire types (coaxial, shielded, twisted pairs, etc.) and with cable configurations similar to actual installations. Field strengths were increased, and the lowest level producing a malfunction or anomaly--if any--in the functioning of a given piece of equipment was noted. Thresholds of avionics susceptibility to a SANGUINE system field were thus established. The most susceptible items disclosed were the flux valve of the compass system and cathode-ray tube (CRT) indicators used in such systems as Loran and weather radar. Extensive mitigation investigations were conducted on these items; results and a mitigation critique on each item are given herein.

Discrete test frequencies were frequency-shifted ± 5 Hz at a nominal rate of 5 Hz per second to simulate one possible SANGUINE system transmission condition and to observe effects on equipment under test.

Additionally, variable ELF voltages were injected in series with the individual leads comprising interconnection cables, and consequent effects on equipment function were observed. This test simulates, under worst-case conditions (since effects of fuselage shielding and lead twisting are thus negated), voltages induced in avionics cabling in the influence of SANGUINE system-related fields. Results of these tests provided further insight into the performance of an avionics system in an ELF field and helped ensure the disclosure of anomalous events requiring mitigation.

Theoretical studies were made of field strengths about several possible SANGUINE system antenna configurations encompassing a range of aircraft altitudes.

Calculations were made of induced voltages in interconnecting cables in typical large transport airplanes such as the Boeing 747. These calculations were based on actual wiring configurations and equipment locations. It was also necessary to use theoretical concepts (verified in part by laboratory testing on a small model) regarding induced voltages in circuits formed by wires at varying distances from their structure returns. An additional consideration was the shielding provided by the fuselage; values measured with 60-Hz ambients, for Boeing 727 and 747 airplanes, were in good agreement with results obtained from standard formulas in the literature.

The studies discussed above permitted calculating margins by which on-board avionics equipment is protected agairst "worst-case" SANGUINE system fields.

In a sense, this research is a pioneering investigative effort on the electromagnetic compatibility (EMC) aspects of avionics vis-a-vis ELF fields. The EMC discipline is well defined, with its own professional group publication, annual symposia, a voluminous literature, and established procedures; but in most cases lower frequencies of interest have been about 14 kHz, many octaves above the frequencies of interest in this study. Special studies on EMP and on spectral content of lightning and sferics and their effects on electronics have considered frequencies down to about 1 Hz; but virtually nothing exists in current literature on EMC effects on avionics of frequencies under 150 Hz.

A further reason for lack of requirements for ELF susceptibility in commercial avionics is that the minimum frequency normally present in the airplane installation is the 400-Hz power frequency.

A bibliography of documents pertinent to this study is provided in appendix A.

2.0 LABORATORY PROCEDURES

2.1 STATEMENT OF PROBLEM

The SANGUINE system concept is that of an extremely low frequency (ELF) communication system operating at a selected frequency between 40 and 150 Hz. Electromagnetic waves at these frequencies are very long (3×10^6 m at 100 Hz) and require long antennas for efficient transmission. However, ELF waves have certain properties that make them desirable for communicating with submerged submarines on a worldwide basis.

To attain the desired antenna length with the most economical use of real estate, it is envisioned that the antenna conductors will be arranged in a buried grid covering an area possibly as large as 7,000 square miles. Aircraft flying close to or overflying the antenna grid will be traversing a region of maximum field induction, and the function of on-board electronics--avionics--may be affected by interaction with this field. Similar considerations apply to ground control equipment of airfields within or adjacent to the antenna grid.

It is the purpose of this study to ascertain the effects of SANGUINE system field on avionics and ground-based control equipment and to devise mitigative procedures for disclosed malfunctions due to interactions with this field.

Field strengths will, of course, be functions of the antenna configuration and antenna currents (design details are still under consideration) but for purposes of this study, it is assumed that the worst-case magnetic field strength, at the earth's surface directly above the SANGUINE system antenna, will be about 1.0 gauss (although actual design values are presently about an order of magnitude lower). This field should diminish, very roughly, inversely with distance above the earth, so that aircraft overflying the SANGUINE system antenna at normal cruise levels will encounter a SANGUINE field much smaller (< 0.01 gauss) than the earth's magnetic field. However, to ensure that no safety-of-flight conditions are violated, this interference mitigation study has been performed to obtain avionics susceptibility levels. This information will have wide application in subsequent avionic design. Further discussion of these considerations is in sections 4.0 and 5.0.

2.2 TEST EQUIPMENT

2.2.1 Aircraft Avionics Location

The main avionics equipment and antenna locations are shown for a 747, which is typical of late-generation jet aircraft (figs. 1 and 2). Normally, the equipment and installation have fulfilled all electromagnetic compatibility (EMC) requirements as indicated in applicable military, FAA, or airplane company documents. However, these requirements do not require extensive testing in the 40- to 150-Hz region.

Not all the equipment shown in figures 1 and 2 was tested for susceptibility to SANGUINE system frequencies in this study; conversely, tests were performed on some equipment not identified in the equipment breakdown in the figures. Identification and a tabulation of equipment tested is given in section 3.0.

Aircraft avionic equipment may evidence susceptibility to a SANGUINE system field through two mechanisms: either by direct exposure of equipment (black boxes) to the field and consequent induction of EMF's in associated circuitry, or by magnetic induction of voltages into loop circuits consisting of the interconnecting wiring and possibly a structure return. These induced voltages are impressed in series with the equipment terminals (conducted interference). Since time-varying, low-frequency magnetic fields--due to the 400-Hz power system--are already present in aircraft wiring, use of such expedients as twisted pairs (rather than structure return) is common for interface wiring of sensitive systems, to meet established susceptibility requirements. Standard EMC practice, therefore, mitigates some potential SANGUINE system-related problems.

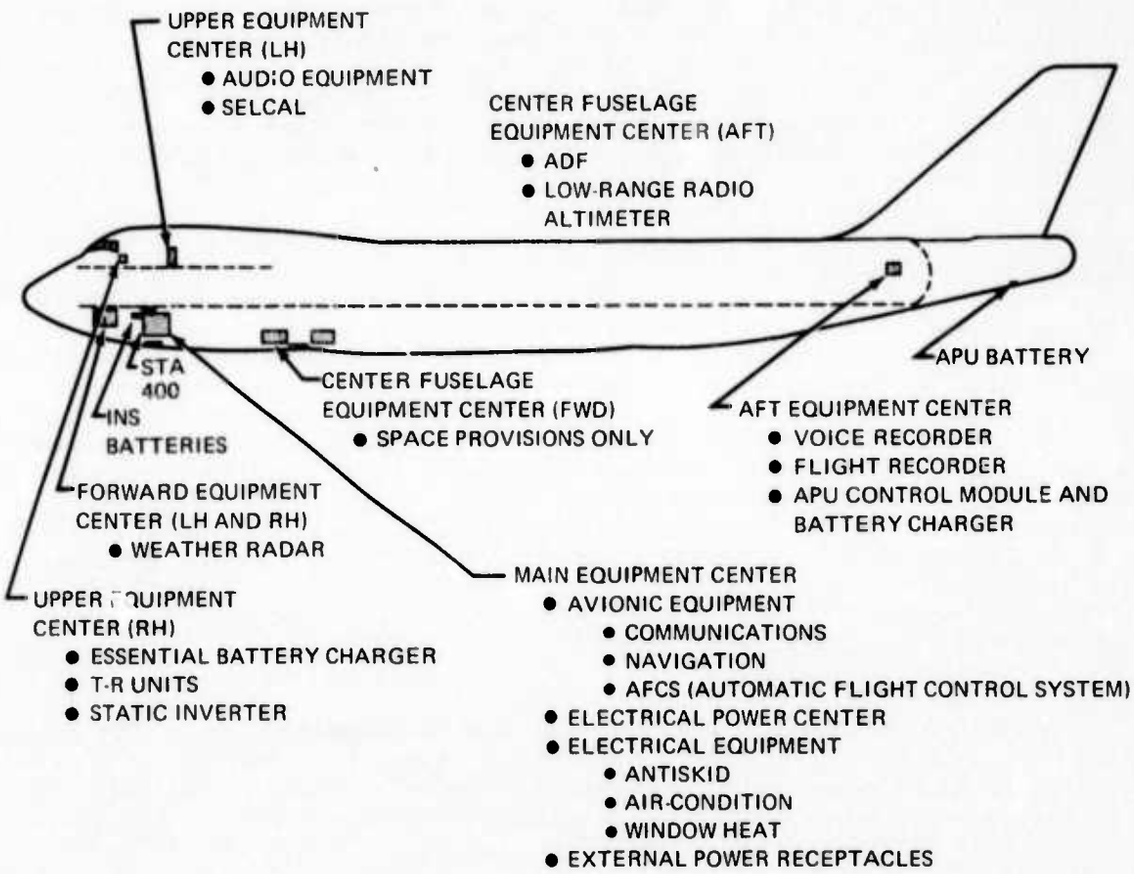

Figure 1. Electrical/Electronic Equipment Location

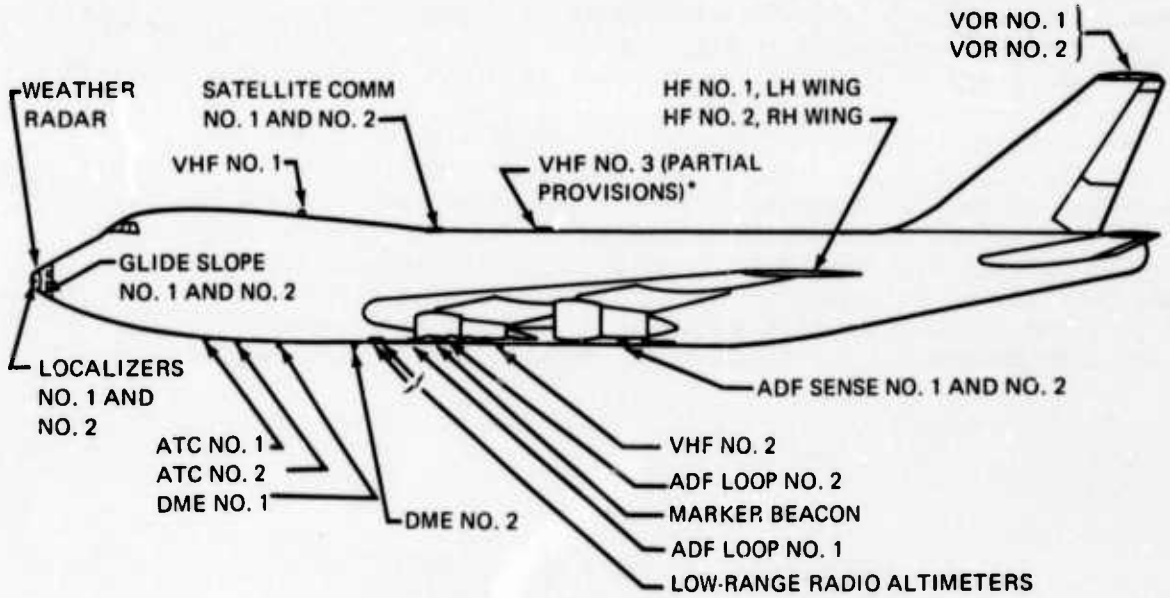

*PARTIAL PROVISIONS CONSIST OF STRUCTURAL PROVISIONS FOR THE ANTENNA PLUS A COAXIAL CABLE BETWEEN THE ANTENNA LOCATION AND THE MAIN EQUIPMENT CENTER

Figure 2. Antenna Locations

A factor that decreases the vulnerability of cables and equipment to ambient fields--SANGUINE system related or other--is the shielding effect of the airplane fuselage (despite its numerous openings and discontinuities). Measurements made on quiescent airplanes (Boeing models 727 and 747) in "noisy" locations, comparing the 60-Hz industrial field ambient just outside a fuselage to that inside show field attenuations averaging 20 dB. Results of calculations made of shielding by a metal cylinder, using typical diameter, skin thickness, and conductivity for an aluminum alloy fuselage, corroborate these attenuation magnitudes (see secs. 4.0 and 5.0).

2.2.2 Test Field Generation Devices

A considerable effort was expended early in the research to develop means for generating uniform, high-level magnetic fields in the 40- to 150-Hz region for avionics equipment susceptibility studies. An immediate difficulty was the lack of a low-frequency current source of sufficient value to generate the desired magnetic fields in a strip-line cavity or within a coil large enough to accommodate the avionics chassis and control elements to be tested. Accordingly, a high power audio-oscillator was constructed. Essentially it is a class AB_2, 250-watt amplifier driven by a Wien bridge oscillator, utilizing negative feedback for low output impedance and constant voltage. Amplifier output consists

of two Eimac type 4CX-250B vacuum tubes. This unit served dependably and with consistent output characteristics throughout the study. Figure 3 shows an interior view of this unit. (Prior to the construction of this power audio-oscillator, a 2,000-watt audio amplifier designed for shaker-pot application was used. It was a fully solid-state device--Unholtz-Dickie--but proved too vulnerable to the thermal stresses induced by rapidly varying loads, as evidenced by the frequent opening of groups of the "fast-blow" fuses required for transistor protection.)

Although the output impedance of the oscillator amplifier was low, mismatch between it and the coil or strip-line that were constructed for this study caused the output voltage to decrease markedly; the output waveform was greatly distorted from a pure sinusoid. Accordingly, it was necessary to construct a transformer to act as an impedance matching device between oscillator and test field generators. A transformer core of generous iron cross section (3.5 in. x 2.5 in.) was adapted for this purpose. The primary and secondary windings were empirically determined for best match between the oscillator-amplifier and the

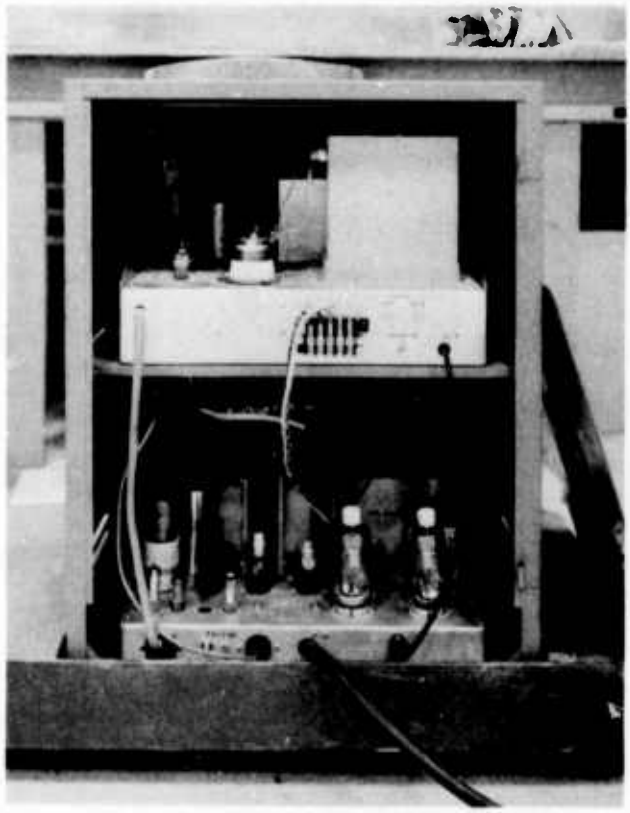

Figure 3. Interior of Power Oscillator

strip-line and coil, respectively. A dual secondary was used; the secondary for the strip-line consisted of a 2-in.-wide, 200-mil-thick copper strap loosely looped about the transformer core. The secondary provided clean sinusoidal current (as observed on an oscilloscope) up to 500 amp. Uniform magnetic fields up to 10 gauss over the frequency range of 40 to 150 Hz were produced within the stip-line "cavity" and could be maintained indefinitely.

The secondary suitable for energizing the test coil consisted of four loose turns of No. 00 wire. Comparable, clean sine-wave currents, up to 50 amp, were available for the coil, producing interior fields up to 20 gauss.

2.2.3 Strip-Line

The strip-line used in this study consists of a 1/4-in.-thick sheet of aluminum, backed with 1/2-in. plywood for rigidity, for the upper plate. Its dimensions are 10 ft long by 2 ft wide. The copper surface or ground plane of the work bench acts as the return or second plate. One end of the upper plate is electrically connected to the work bench by an accordion-pleated copper sheet (50 mils) extending the full width of the upper plate and continuously soldered to a heavy copper bar so that full-surface short-circuit contact is maintained. (The transmission line then functions, at low frequency, as a single-turn coil.) The "pleats" permit varying plate separation; a similar flexible arrangement exists at the input end. All connections are arranged to minimize overall strip-line resistance. The 10-ft cavity length permits immersion of correspondingly long cable lengths in the test field. Details of typical test setups can be seen in several of the photographs in appendix B.

2.2.4 Test Coil

The test coil is an open cylindrical coil form with a cubic aspect ratio; i.e., diameter = length = 24 in. All screws and fasteners are of brass. Twenty-four turns of No. 2 wire were wound on the coil and spaced empirically to result in the most uniform interior field. At maximum available current (50 amp), uniform field strengths up to 20 gauss were produced in the frequency range of 40 to 150 Hz. Dimensions were selected to accommodate a full ATR* enclosure in three orientations of the coil axis with respect to the field. Larger enclosures were placed immediately against the coil face. Full interior field strength persisted to 5 or 6 in. beyond the coil face (by actual measurement). Field strengths within the strip-line cavity or the test coil were measured with an RFL gaussmeter, model 1980. Several probes were available and the probe most suited for ELF magnetic field measurements was used. Rough comparative measurements were made with a Perfection Mica Company AC field evaluator (calibrated for use with a precision millivoltmeter.) These instruments were kept in current calibration by the Boeing Calibration and Certification Laboratories, as was all laboratory equipment used throughout this study.

---

*One ATR (Air Transport Radio unit case) chassis has dimensions: W = 10.125 in., L = 19.5625 in., H = 7.625 in.

2.3 LABORATORY INVESTIGATION

2.3.1 Test Plan

A complete test plan was generated at the outset of this study and forwarded to the contract technical officers for critique and approval. Essentially, it was based on established EMC procedures and practices long in use in the aircraft industry, modified to the frequency range and immediate requirements unique to this research.

In brief, the test plan defined the manner in which selected elements of avionics--particularly those deemed safety-of-flight items by usage and FAA definition--would be subjected to increasing magnetic fields in the 40- to 150-Hz region, while functioning in their normal manner. Thresholds of susceptibility would be determined at discrete frequencies in the test range. This, of course, implies interconnection of a complete subsystem for test, with all proper input voltages, control devices, and output impedance terminations. Interconnecting cables and connector configurations (connector designation, wire type and size, power cable proximity, etc.) were similar to those used in an installation, as determined from aircraft wiring diagrams.

2.3.2 Test Procedures: Strip-Line and Magnetic Coil

In the laboratory, actual test setups for given subsystems varied from equipment to equipment, depending on the equipment function, mode of operation, and form of output. Criteria of malfunction also depended on the form of output--from essentially subjective evaluation, if the output was an audio signal (cockpit voice recorder, PA system, etc.), to a maximum specified deviation on an output indicator or CRT in the cockpit (ILS, VOR, weather radar, etc.). For the subjective evaluations, a degree of objective corroboration was obtained by observing (and photographing, for record) the output waveforms on an oscilloscope. Resultant distortion due to the superimposition of or modulation by the test field, at a given level and frequency, was visually observed on a real-time basis and compared with "no-field" conditions. The magnitude (in microvolts) of the induced voltages (40 to 150 Hz) appearing in the equipment output was measured on a Fairchild EMC-10 interference analyzer (essentially a tunable microvoltmeter).

The general test procedure was as follows: A given avionics subsystem was set up (with required sensors, loads, or stimuli for meaningful exercise) and its normal function checked. Elements of the subsystem--chassis, control heads, indicators, lengths of cable, etc.--were placed in the strip-line cavity, individually and in various combinations. At a given frequency, the test field within the cavity was slowly varied from zero to maximum attainable (>5 gauss for the strip-line). The field intensity (in gauss) at which a malfunction or operating anomaly occurred was noted. This procedure was repeated at each discrete test frequency of 40, 50, 75, 90, 100, 133.3, and 150 Hz (133.3 Hz was chosen as one of the test frequencies because its third harmonic is 400 Hz, a common power frequency on aircraft). The test was repeated for three orthogonal orientations of the main subsystem chassis with respect to the field. (Whenever system output or system characteristics permitted the entire test range--40-150 Hz--was slowly swept at maximum field strengths.)

If no malfunctions occurred during the strip-line test, the equipment comprising the subsystem, in several groupings and orientations, was placed in the test coil where fields of greater strength (>10 gauss) were available. The tests, as described above, were repeated. (Thresholds of susceptibility above 10 gauss in the SANGUINE system frequency domain are of no significance for this investigation.)

The test fields generated in the strip-line cavity and coil interior were not steady-state sine waves at each selected test frequency, but were frequency shifted ±5 Hz about each test frequency at a 5-Hz/sec rate. This more meaningfully simulates a possible SANGUINE system field and explores the modulating effect of the varying field on the subsystem under test.

2.3.3 Voltage Injection Tests

To determine the effects of the SANGUINE system induction field on interconnecting cables and power leads, additional tests were performed. Each lead emanating from an element of a subsystem under test was individually subjected to simulated interference in the SANGUINE system range of test frequencies. This was accomplished by a direct series injection of ELF voltages in each lead. Equipment function was monitored while the magnitude of this voltage was gradually increased. Values at which anomalies occurred were recorded. These voltage values may be translated into SANGUINE system induction field strengths required to generate equivalent voltages, since all pertinent system parameters (i.e., lead lengths, circuit impedances, etc.) that enter into the calculation are determinable. (See section 4.)

To perform these voltage-injection tests, it was necessary to construct "breakout", or access, boxes accommodating the power and signal leads. Each lead was capable of being "opened" within the breakout box constructed and the desired voltage injected in series. The voltage generator for this purpose was a Hewlett-Packard audio generator, model 205 AG. An isolation and impedance-matching transformer, specially constructed for this purpose, was interposed between the audio generator and the lead under test.

The voltage developed by this means in each lead was dependent on the circuit impedance associated with that lead. Often, a "safe" upper limit was predicated on precautions given in the equipment handbook or on results of an analysis of the circuit elements involved. In any event, voltages above 10 volts were not imposed on leads, lest associated circuits be damaged. (Most of the equipment tested was obtained from Boeing stores, and, after suitable quality control and functional check, was returned to stores after test. None of the equipment tested suffered any impairment or damage as a result of these tests.)

3.0 SUMMARY OF TEST RESULTS

The test procedures briefly described in the preceding section were performed on a number of items of equipment or subsystems--avionic and ground based. The latter were installed at the regional FAA Air Traffic Control Center, Auburn, Washington.

For each item of equipment tested, the full test details, test item description, exact test setup, list of test equipment, description of simulated inputs, dummy loads, test result recording, etc., were given in the monthly report corresponding to the time interval in which the test was made. Block diagrams of the test setups and photographs of the elements comprising a given subsystem under test accompanied each test description. Also given were wiring diagrams of all interface connections so that results of wire-by-wire voltage injection tests could be readily interpreted. Given in tables 1 and 2 is a tabular resume of the equipment tested and significant test results. Several representative photographs of equipment and block diagrams of test setups are given in appendix B to illustrate the use of the strip-line and test coil and to show typical breakout boxes required for the wire-by-wire injection tests.

The equipment tested represents an eclectic sampling of latest avionics. The first systems tested were selected because of their relative simplicity of design and function. At the outset of the study, test procedures and test adjuncts required verification of applicability and were subject to refinement. Selection of sophisticated, multi-element subsystems for test would have obscured and complicated these requirements early on the "learning curve." Experience and insights into ELF testing gained in these early tests permitted more rapid progress later in the program. Not all avionics systems requiring test were investigated; time available did not permit their inclusion. Fortunately, only the flux valve (flux gate), a compass system component, evidenced susceptibility at sufficiently low levels of test field intensity (< 0.1 gauss) to require "mitigation" investigation. This effort is described in section 6.0.

Table 1 is a resume of the tests performed by exposing the test items to ELF magnetic fields; frequency-shifted as noted previously.

Table 2 is a similar resume of the "wire-by-wire" voltage injection tests. Again, diagrams identifying all leads tested were given in the pertinent monthly report.

For both tables, only the salient test parameters and test results are given. Reference may be made to the specified monthly report for complete test details.

3.1 VOLTAGE INJECTION ON POWER AND TELEPHONE LINES TO AIR TRAFFIC CONTROL EQUIPMENT

In addition to the ELF field tests summarized in tables 1 and 2, voltage injection tests were performed on power leads of standby and spare ground control equipment and on telephone lines at the FAA Air Route Traffic Control Center (ARTCC) at Auburn, Washington. The need for such tests was discussed with

center management and permission was granted--albeit reluctantly at the outset--to bring test equipment into the facility. Test procedures differed somewhat from those used in the test of avionics elements in Boeing laboratories. A description of these tests, performed at the Auburn ARTCC, is given below.

Discussion with engineers responsible for maintenance of radar and communication equipment at the center revealed that the proposed tests could be performed on equipment in the maintenance area and on operating equipment whose temporary removal from service would not disrupt the activities of the center. Equipment was chosen such that test signals injected would not couple, to any significant degree, into other power or telephone circuits.

3.1.1 Test Equipment and Procedures

Powerline Injection--A simple technique was used as shown in figure B39. A common core links windings in series with the powerline of the unit under test--a monitor winding to which a voltmeter is connected and an injection winding is fed by an audio-oscillator. Frequency shifting was not used for these tests; the oscillator was slowly tuned between 40 and 150 Hz, and effects of injected signals were observed.

The voltmeter indicates the open-circuit voltage injected into the powerline by the oscillator directly when the injection winding is 20 turns; and 6.7 times the injected voltage when the injection winding has three turns. This indication is valid only when the power source is disconnected, since 60 Hz is induced in all windings when the power is on. The reason for using only three turns, rather than 20, on the RBDE-4 equipment (described below) is that its heavy ac power current requirement imposes a potentially destructive (>30 volt) 60-Hz potential on the oscillator output terminals.

The open-circuit injected test voltage is likely to divide in the same ratio as the 60-Hz impedance of power source, injection winding, and equipment terminals so that most of it appears at the RBDE-4 equipment terminals adding to the 115 volts, 60 Hz potential.

An improved test arrangement can be constructed using two transformers in opposition and a dummy load impedance equal to that of the unit under test. This arrangement prevents exposure of the oscillator to 60-Hz line voltages, yet permits large injected voltage levels. Unfortunately, this test equipment was not available for use, although it has been subsequently constructed and tested for applicability.

Telephone Line Injection--The same test arrangement shown in figure B39 was used in series with one side of the line. The voltmeter will indicate the open-circuit induced voltage when there is no telephone traffic.

3.1.2 Test Descriptions and Results

Powerline Injection on Horizontal Display Cabinet--The equipment tested was the horizontal display cabinet, model RDBE-4, manufactured by General Instrument Company (see fig. B30). This equipment, normally used by the air traffic controllers, derived its video input and synchronization from a coaxial jack in the maintenance area; the signals originate from a remote radar.

Equipment power was provided from a 115-volt line through a voltage regulator transformer, a unit of the model RDBE-4. This supplied regulated voltage to part of the unit while other parts used raw power. Injection was then performed on the powerline side, thereby affecting the entire unit.

Vertical jitter of the display resulted from voltage injection. The level at which this jitter would be objectionable to air traffic controllers (who must view the display for long periods) was judged by experienced FAA maintenance employees.

When 0.5 volt was injected into one side of the power input, over the frequency range of 40 to 150 Hz, objectionable jitter was observed only when the frequency was in the immediate vicinity of 75 Hz. Test equipment power limitations prevented injecting greater voltages.

The voltage injection procedure was repeated on the ground line of the equipment. In the maintenance area, where this test was performed, the ground pin of the wall outlet was the only connection from equipment to building ground; thus, the injected voltage did not cause circulation of SANGUINE-frequency test currents in the entire ground system through low-impedance parallel paths.

An injected level of only 30 mv in series with the ground connection caused objectionable vertical jitter at all frequencies between 40 and 175 Hz. Frequencies were noted where increased vulnerability was evident. These were 55, 65, 75, 110, 128, and 175 Hz. The minimum of susceptibility threshold of discernible jitter was as low as 15 mv at these frequencies. The frame frequency of the display is 30 Hz, but is not derived from the powerline. It is thought that either internal synchronization circuits are particularly vulnerable to the listed frequencies or the visual effects are markedly more annoying when low-frequency beats occur.

It is very likely that, if it had been permitted to inject significantly greater voltages on the powerlines, jitter at these singular frequencies would have proven particularly annoying, and the entire range of frequencies would have produced jitter.

It was thus determined that the equipment is vulnerable to 0.5 volt, or more, injected in the powerline at a frequency of 75 Hz. It is also reasonable to conclude that the RBDE-4 unit would be susceptible to powerline injected voltages on the order of 1.0 volt over the range of 40 to 150 Hz.

The extreme vulnerability of the ground connection to injected voltage may well not be a problem in an operational environment because of the multiple paths in the ground system. On the other hand, if there are large ground loops whose planes intercept a SANGUINE system field, conceivably, significant voltage differences could occur between the equipment and the potential to which it should be referenced; more testing and analyses in this area are indicated.

3.1.3 Air Route Surveillance Radar Display

The unit tested is shown in figure B40. The powerline on which voltages were injected serves the console cabinet CA 4081, which is a unit of the ARSR-1 air route surveillance radar, manufactured by Raytheon. The equipment was formerly used by controllers but now is in the equipment area of the center, used to monitor the performance of the Salem, Oregon, radar.

Figure B41 illustrates the injection of voltages into the power panel, where temporary disconnections were made on the equipment side of the circuit breakers. This equipment is powered from wiring in cable trays, and its ground connections are made through various structures rather than through its power cord. For this reason, the tests made on the ground wire of the display unit discussed above could not be performed on this unit.

Using the test arrangement of figure B39, with the powerline of the equipment under test routed through the 20-turn winding, the oscillator was swept from 40 to 150 Hz while injecting a voltage of 5.0 volts minimum. No visible degradation resulted on the display.

The unit is not considered vulnerable to SANGUINE system signals induced on the powerlines.

3.1.4 VHF Communications Receiver

The receiver is a model RV-12, VHF fixed-tuned communication receiver, manufactured by Erco Laboratories. The antenna was temporarily disconnected and input supplied by a signal generator at a 20-microvolt level with 30% modulation at 1,000 Hz. Output was monitored on an oscilloscope. The output power level (0.6 watt to 600 ohm) was also monitored on an output power meter.

An injected level of 7.5 volts on either power lead was just sufficient to cause noticeable envelope distortion (on oscilloscope) or modulation of the power meter reading over the frequency range 40 to 150 Hz.

At specific frequencies, the following observations were made:

- 40 Hz--5.5 volts caused visible distortion
- 44 Hz--5.0 volts caused visible distortion
- 52 Hz--7.5 volts caused visible distortion
- 58 Hz--1.5 volts caused large beat modulation
- 120 Hz--7.5 volts were required to cause weak beat modulation

Since this was operational equipment, time did not permit investigation of the observed maximum vulnerability to frequencies close to 60 Hz. However, the injection level at which it occurred is greater than the mitigation level contemplated (by another investigative group) for powerlines affected by a SANGUINE system field.

3.1.5 Injection into Telephone Circuit to Remote Air/Ground Communications Site

The circuit tested carries two-way voice communication between pilots and controllers and connects the FAA-Auburn ARTCC with a site near Spokane, Washington. Transmitters and receivers at the site are remotely controlled by tones from Auburn. The land distance is approximately 300 miles; the telephone circuit runs as overhead lines for 17 miles at the Spokane end. The block diagram of figure B42 indicates the significant elements in the test.

FAA test equipment was used to insert a signal on the transmit line at the Auburn end, a 1,000-Hz tone of zero dBm (nominal impedance of FAA circuitry is 600 ohms). The same signal was received, attenuated 14 dB (18-dB attenuation is tolerable performance), and injection of the SANGUINE-frequency voltage with Boeing-furnished equipment was accomplished on the receive line. Again, the Boeing equipment was as shown in figure B39, with the 20-turn winding used.

Figure B43 illustrates the FAA equipment feeding the outgoing line; figure B44 shows the Boeing equipment on the FAA side of the demarcation line.

A telephone-system-type level measuring equipment and an oscilloscope, shown in figure B45, were used to monitor the received signals that could also be heard on the speaker of the telephone (controller's position) and speaker amplifier located in the maintenance area. This amplifier appears on the lower right of figure B45.

The output monitored on the oscilloscope appeared as 100 Hz modulated strongly by 60 Hz, as shown in figure B46.

Injection of 0.5 volt at 40 Hz at the point indicated on figure B44 caused noticeable change (distortion) in tone output as well as distortion of the oscilloscope pattern and changes in the monitor indication. The oscilloscope pattern was as shown in figure B47, which was for 700 mv injected at 40 Hz.

To summarize, with injection of 300 mv at 75 Hz, almost 100% modulation resulted. The following levels introduced unacceptable (subjective) distortion:

- 40 Hz--700 mv
- 75 Hz--550 mv
- 100 Hz--550 mv
- 133 Hz--450 mv

An injected signal of 550 mv corresponds to -3 dBm if referred to 600 ohms. Since the overall response of all telephone circuitry is intended to be limited to the 300-Hz to 3-kHz range, signals such as 60 Hz and the SANGUINE system frequencies would be classified as noise on the line. In this particular case, noise injected at, say, 75 to 100 Hz was 11 dB above the signal before it caused annoyance, because of the low-frequency rejection characteristics of the equipment. Another way to state the result of the test is that injected levels greater than that of the 1,000 Hz were needed to compete with the 60-Hz level existing on the line.

The injected level for unacceptable distortion is much greater than the line-to-line mitigation levels established by Navy ECAP reports for telephone circuits exposed to SANGUINE system fields. (Since the injected levels refer to open circuit values, the levels injected across equipment terminating the telepone line are somewhat lower.)

Undesired actuation of the transmitters and receivers would not be expected to result from SANGUINE system signals because the tone frequencies used are greater than 500 Hz.

3.2 SUMMARY OF TEST RESULTS

Analysis of total test results summarized in tables 1 and 2 establishes conclusively that none of the items tested, with two marginal exceptions noted below, is vulnerable, subject to the 1-gauss field strength criterion established by SANGUINE design engineers. In virtually all cases, margins of susceptibility--whether established by exposure of the equipment under test to an ELF test field or through injection of an ELF voltage in an individual lead--were at levels well above those established for SANGUINE system mitigation criteria.

The two exceptions are the magnetic deflection CRT's used as indicators in such systems as Loran and weather radar, and the flux valve (or flux gate) element of the Gyrosyn compass system. Each of these exceptions--by the very nature of its operation--is extremely vulnerable to externally incident magnetic fields. Each system bears an installation legend advising of this vulnerability and cautioning against installation within the influence of external fields. (The weather radar bears the cautionary legend: "Before mounting permanently, determine, by actual operation, that no magnetic interference exists between the radar indicator and other aircraft instruments.")

SANGUINE system-related ELF fields of a magnitude sufficiently great (>0.5 gauss) to distort an avionics CRT display to an unreadable degree would occur only in the immediate vicinity of the SANGUINE antenna. Characteristically, the devices mentioned are used predominantly either at cruise altitudes (weather radar) or over sea routes far from shore (Loran). It is extremely unlikely that a large airfield will be constructed within or close to the SANGUINE antenna grid. Hence, no mitigative modifications are indicated for these systems. At the very worst, their susceptibility will constitute a seldom-occurring, transient nuisance. Results of a shielding investigation for CRT's, aimed toward a possible resolution of this problem, are given in section 7.0.

A similar critique may be given for the flux valve. This device is mounted near a wing tip, isolated from all airplane magnetic fields. In use, internal coils interact with the earth's magnetic field to provide navigation information. Hence, it is extremely susceptible to ambient, varying fields; indeed, its threshold of susceptibility is about an order of magnitude below that for the CRT's--about 0.05 gauss. A discussion of the theory of operation of the flux valve and results of an investigation of possible mitigation expedients are given in section 6.0.

Another instance of apparent extreme vulnerability--low susceptibility threshold--was disclosed during tests on control equipment at the Auburn Air Route Traffic Control Center. Injecting ELF voltages at a level of only 30 mv into the ground line of the horizontal display cabinet of the radar bright display caused objectionable display jitter at all frequencies between 40 and 150 Hz. At certain discrete frequencies, enumerated in the test description, jitter was pronounced at injected voltage values of only 15 mv. These tests were performed near the close of the study interval (December 1970) and at a sensitive area from security and function viewpoints. Tests performed were rather unsophisticated and preliminary; any subsequent tests, if such are required, would be implemented by more sophisticated test adjuncts and would be much more extensive in application. Further tests with newly developed susceptibility test devices would establish definite ground injection susceptibility thresholds.

In any case, it is not likely that ground control equipment of the complexity of the radar bright display would be in the near field of influence of a SANGUINE system. Further, an installation with multiple parallel ground paths, more typical in an operational installation, would not exhibit equivalent low levels of susceptibility. (The radar bright display equipment tested was in a "maintenance" or test area, and was not on-line; hence, the atypical ground configuration.)

A serendipitous fallout of these tests is that they demonstrated to ARTCC management that such tests serve an important purpose and that their conduct will not necessarily dislocate or interfere with ongoing center functions. This rapport and understanding have now been established with both center management and engineering.

Table 1. H-Field Exposure Tests—Strip-Line and Coil

Equipment identification	First sign of malfunction (threshold of susceptibility)		Max field strength used in test	Remarks
	Freq (Hz)	Field strength (B)		
Hydraulic fluid quantity indicator, Gull Airborne Instruments (monthly report 11)	None		12 gauss, 40-150 Hz	
Total air temperature indicator (TAT), Servo Development Corp (monthly report 11)	None		12 gauss, 40-150 Hz	
Oil quantity indicator, Consolidated Airborne Systems	None		12 gauss, 40-150 Hz	
Brake temperature monitoring system, Goodyear (monthly report 11)	None		12 gauss, 40-150 Hz	Refer to figures B1 and B2, appendix B.
Engine tachometer system Tachometer indicator, General Electric Tachometer transmitter, Hamilton Standard (monthly report 11)	None		12 gauss, 40-150 Hz	
Window heat control unit, Garrett Mfg Limited (monthly report 11)	None		12 gauss, 40-150 Hz	Refer to figure B3, appendix B.
Cockpit voice recorder, Fairchild (monthly report 11)	100-150 Hz	4.0 gauss	10 gauss, 40-150 Hz	Frequency shift "beat" and test frequency hum audible at 4.0 gauss, 100-150 Hz. Speech not unintelligible at 10 gauss. Refer to figure B4, appendix B.

Table 1.—Continued

Equipment identification	First sign of malfunction (threshold of susceptibility)		Max field strength used in test	Remarks
	Freq (Hz)	Field strength (B)		
Passenger address amplifier, Collins 346D-1 (monthly report 3)	None		10 gauss, 40-150 Hz	Low frequency test signals visible in PA output on oscilloscope (and measurable by EMC-10), but not discernible to ear. (Response of human ear poor at 40-150 Hz.)
HF transceiver, Collins 618T (monthly reports 4 and 5)	Transmit mode: 40-150 Hz	7.5 gauss	20 gauss, 40-150 Hz	Output of transmitter sensitive to orientation of chassis with respect to test field. Greatest vulnerability when long axis of chassis is perpendicular to field.
	Receive mode: 40-150 Hz	8 gauss		
VHF transceiver, Collins 618M-2B (monthly reports 3 and 4)	None		10 gauss, 40-150 Hz	Barely detectable hum in output (with 1,000 Hz, 30% modulation) at higher field levels (8-10 gauss).
ADF receiver, Collins 51Y-4 (monthly report 4)	None		20 gauss, 40-150 Hz	See figure B5, appendix B.
VHF navigation receiver, Bendix RNA-26C (monthly report 7)	None		10 gauss, 40-150 Hz	See figures B6 and B7, appendix B.
Marker receiver, Bendix MKA-28A and MKA-28C (monthly report 9)	40-150 Hz (MKA-28A)	2.2 gauss	10 gauss, 40-150 Hz	No discernible degradation of audio output to 10 gauss. However, when the marker receiver (MKA-28A) was placed in the strip-line cavity parallel to strip-line and in an upright position, all marker lights blinked at the frequency-shift rate (4 Hz). Varying this rate affected the blink rate directly. This indicator light anomaly occurred only for black box orientation with field noted above. A later model, MKA-28C, did not exhibit this susceptibility.
	None (MKA-28C)		10 gauss, 40-150 Hz	

Table 1.—Continued

Equipment identification	First sign of malfunction (threshold of susceptibility)		Max field strength used in test	Remarks
	Freq (Hz)	Field strength (B)		
ATC transponder, Collins 621A-3. (monthly report 8)	40-150 Hz	12.0 gauss	12 gauss, 40-150 Hz	Barely discernible "lengthening" of output pulses at higher field strengths (only when the long or normal axis of the black box is at right angles to field). See figures B9 and B10, appendix B.
Radio altimeter system, Bendix ALA-51A. (monthly report 8)	None		17 gauss, 40-150 Hz	See figures B11 and B12, appendix B.
Distance measuring equipment, DME 860-2, Collins (monthly reports 6 and 7)	None		16 gauss, 40-150 Hz	See figure B13, appendix B.
Airborne Loran system, 600T, Edo Commercial Corp. (monthly report 10)	40-150 Hz	1.0 gauss (indicator only, see remarks)	10 gauss, 40-150 Hz	The Loran indicator pulse display is on a CRT, employing magnetic deflection. When this CRT was placed in the test field, the display became unstable and "torn" at field strengths of 1.0 gauss at all test frequencies. Isolating the indicator unit from the test field and placing the Loran receiver, control unit, and 3 ft of interconnecting cable in the field produced no display jitter or instability to 10 gauss. See figures B14 and B15, appendix B.
Airborne weather radar system, type RDR-1E (radar and controls), Bendix (monthly report 10)	40-150 Hz	0.5 gauss (PPI only, see remarks)	10 gauss, 40-150 Hz	As was the case with the Loran indicator, the weather radar PPI was affected by relatively weak fields. Field strengths of 0.5 gauss had a noticeable effect on the range marker traces. Trace intensity was modulated (i.e., flickered) at the frequency-shift rate. (There was no displacement of range markers, however.) At increasingly greater field strengths, the traces assumed a beaded or dashed appearance. For field strengths above about 1.5 gauss, PPI traces were distorted and unstable to an unreadable degree. See figures B16, B17, B18, and B19, appendix B.

Table 1.—Continued

Equipment identification	First sign of malfunction (threshold of susceptibility)		Max field strength used in test	Remarks
	Freq (Hz)	Field strength (B)		
Inertial navigation system (INS), Carousel IV, AC Electronics (monthly report 9)	None		12.5 gauss, 40-150 Hz	Most complex of systems tested. No malfunctions or "memory" disturbance at any time during test. See figures B20, B21, B22, and B23, appendix B.
Units of PB20D, automatic pilot system, Bendix: Amplifier and computer* Autopilot control panel** (monthly report 11)				
*Amplifier and computer (monthly report 11)		No malf at	10 gauss, 40-150 Hz	Perceptible null deviation occurred at field strength and frequencies shown (irrespective of frequency-shift application). However, even the 10-gauss field at all frequencies (including 133.3 Hz) failed to perturb the equivalent bank angle more than 1°. (Results given for most susceptible orientations.) See figure B24, appendix B.
	40 Hz	10 gauss		
	70 Hz	8.5 gauss		
	95 Hz	3.0 gauss		
	133.3 Hz	1.0 gauss		
	150 Hz	4.0 gauss		
**Autopilot control panel (monthly report 11)	None		9.5 gauss, 40 Hz 14 gauss, 70 Hz 10 gauss, 100 Hz 7.5 gauss, 133.3 Hz	See figure B25, appendix B.
Roll control channel, part of SP-77 flight control system, Sperry-Phoenix Co. (monthly report 11)	None		5 gauss, 40 Hz 7.5 gauss, 70-90 Hz 8 gauss, 100-120 Hz 6 gauss, 133.3-150 Hz	See figure B26, appendix B.

Table 1.—Continued

Equipment identification	First sign of malfunction (threshold of susceptibility)		Max field strength used in test	Remarks
	Freq (Hz)	Field strength (B)		
Flight data system Flight data recorder Trip and date encoder Accelerometer United Control Corp. (monthly report 11)	None		9 gauss, 40 Hz 12 gauss, 75 Hz 9 gauss, 100 Hz 6.5 gauss, 133.3 Hz 6 gauss, 150 Hz	System operated in simulated flight for 15 min and the tabulated fields applied for several minutes each. Examination of recorder tape showed no deviation from normal "no field" recordings. See figure B27, appendix B.
Air data computer, Honeywell (monthly report 11)	None		13 gauss, 40 Hz 15 gauss, 75 Hz 9.5 gauss, 100 Hz 8 gauss, 133.3 Hz 6 gauss, 150 Hz	The tabulated fields caused no deviation in computer output greater than the inherent repeatability of the computer. See figures B28 and B29, appendix B.
Flux valve, type 59, Sperry-Phoenix Co. (monthly report 11)	<0.1 gauss all freq		(Not applicable)	See section 7.0 for a complete discussion of the flux valve and its susceptibility to SANGUINE system fields.
Susceptibility Tests on Ground Installation Equipment—FAA Air Traffic Control Center (FAA ATTC)				
The following equipment was tested at the FAA ATCC located in Auburn, Washington. We were permitted to bring test equipment into the center and subject the items below to ELF fields.				
Radar bright display, horizontal display cabinet, part of model RBDE-4, General Instrument Co. (monthly report 11)	0.15 gauss 40 Hz 0.6 gauss 75 Hz 1.00 gauss 150 Hz Through lateral side of display cabinet (most vulnerable orientation)		1.50 gauss, 40-150 Hz	Very low field levels, as shown in the tabulation, column 2, produced noticeable jitter of the radar display. The jitter was at the frequency-shift rate; steady state fields (cw) produced no jitter. This result was expected, since the CRT is a magnetic deflection device. See figure B30, appendix B.

Table 1.—Concluded

Equipment identification	First sign of malfunction (threshold of susceptibility)		Max field strength used in test	Remarks
	Freq (Hz)	Field strength (B)		
Scan converter, part of model RBDE-4	0.10 gauss	40-150 Hz	0.5 gauss, 40-150 Hz	Basically, this unit converts radar angle/range data to raster-type display. The scan conversion tube is a magnetic deflection CRT, hence its extreme susceptibility. (The caution notice it bears—mount using nonmagnetic hardware—is apropos.) See figure B31, appendix B.
Transponder decoder unit, part of air traffic control beacon interrogator (ATCBI-2) (monthly report 11)	None (see next column)		2.5 gauss, 40-150 Hz (ATCC engineers cautioned against subjecting this equipment to stronger fields)	Fields as shown in the preceding column had no discernible effect on the decoded output of this equipment (monitored on an oscilloscope for any pulse degradation). See figure B32, appendix B.
VHF receiver, model RV-12, Erco Radio Labs (fixed-tuned: f_o = 126.6 MHz) (monthly report 11)	None		2.5 gauss, 40-150 Hz	Fields of 10 gauss were generated in the coil placed against this equipment in three orientations. Fields at the equipment were 2.5 gauss minimum. See figure B33, appendix B.
UHF receiver, Federal Television Corp. R361-C/GR (monthly report 11)	None		3 gauss (min), 40-150 Hz	See above comment for VHF receiver.

Table 2. Wire-by-Wire Voltage Injection Tests—Resume and Results

Equipment identification	First sign of malfunction		Highest injected voltage		Remarks
	Inj Voltage	Freq	Voltage	Freq	
Hydraulic fluid quantity indicator, Gull Airborne (monthly report 11)	None		9 V	40-150 Hz	Three leads interconnecting calibrated test potentiometer and indicator.
Oil quantity indicator, Consolidated Airborne Systems (monthly report 11)	3.0 V	40-150 Hz	3 V	40-150 Hz	Voltages injected in leads normally connected to the capacitive sensors in oil reservoirs caused indicator needle flutter at about 3 V.
Brake temperature monitoring system, Goodyear (monthly report 11)	2.0 V	40-150 Hz	9.0 V (on nonsusceptible leads)	40-150 Hz	Injected voltages greater than 2 V (irrespective of frequency) on leads associated with sensor output caused an increase in indicated temperature. Refer to figure B2, appendix B.
VHF transceiver, Collins 618M-2B (monthly report 5)	2.5 V 3.5 V	150 Hz 40 Hz	9.5 V (on nonsusceptible leads)	40-150 Hz	All leads pertaining to receiver function were tested. None produced output susceptibility except terminals 22 and 23 on terminal strip J1A; mike audio LO and CT. (See monthly report 5.) (Terminal 21, "audio hi," was not affected.
ADF receiver, Collins 51Y-4 (monthly report 6)	3.0 V	40-133.3 Hz	9.3 V	40-133.3 Hz	Of 35 leads tested (see monthly report 6 for wiring diagram) only three were "susceptible" at levels as shown in column 2. Three of the four lines to the RMI (X, Y, and Z lines on wiring diagram) exhibited susceptibility, in that injected interference voltages in excess of 3 V caused RMI indicator oscillation and slewing (at the test frequencies and for the lengths of leads involved, 3 V is equivalent to an ac field in excess of 30 gauss). See figure B34, appendix B, for block diagram of this test setup.
VHF navigation receiver, Bendix RNA-26C (monthly report 7)	None		9.2 V	40-150 Hz	None of the leads tested caused equipment malfunction below 6 V at any frequency. See figures B6, B7, and B35, appendix B, for test setup and breakout box for wire-by-wire injection test.

Table 2.—Continued

Equipment identification	First sign of malfunction		Highest injected voltage		Remarks
	Inj voltage	Freq	Voltage	Freq	
Marker receiver, Bendix MKA-28A (monthly report 9)	1.0 V 2.0 V	150 Hz 40 Hz (Leads to audio system)	7.5 V (caused no "permanent" malfunction)	40-150 Hz	Injected voltages of 1 V (at 150 Hz) appeared on desired tones (400-Hz tone) in audio output. Injected voltages in excess of 2.2 V in lamp output leads caused lamps (red, amber, and white) to flicker. These voltages, for lead lengths and frequencies involved, do not require mitigative action, since they "represent" effects of fields in excess of 20 gauss. See figures B36 and B37, appendix B, for details of test.
ATC transponder, Collins 621A-3 (monthly report 8)	None below 4.0 V, on any lead (over 40 leads tested)		9.5 V	40-150 Hz	See figures B9 and B10, appendix B, for test details (see monthly report 8 for wiring diagram of leads tested).
Distance measuring equipment, DME 860-2, Collins (monthly reports 6 and 7) (supplementary report to report 7)	0.45 V [in ground lead connector P2 (BP)] (see report 7)	40-150 Hz			Injected voltages between 0.45 V and 1.1 V caused malfunctions when injected in several of the leads (fully tabulated and identified in supplement to monthly report 7). However, analysis shows that, for the lenths of leads involved and their associated circuit impedances (one is a ground lead), conditions disclosed require no mitigative action. In an installation, these leads will be small (<2 ft) and will consist of twisted pairs. See figure B38, appendix B, for details of test setup and breakout box.

Table 2.—Continued

Equipment identification	First sign of malfunction		Highest injected voltage		Remarks
	Inj voltage	Freq.	Voltage	Freq	
Airborne Loran system, 600T, Edo Commercial Corp (monthly report 10)	0.6 V (leads comprising cable to indicator) (wiring diagram in monthly report 10)	40-150 Hz	12.0 V	40-150 Hz	Most of the wires comprising the interconnecting cable to the Loran indicator were susceptible; i.e., injection of small voltages (<1 V) caused display instability. This result was expected, since the Loran CRT display unit was affected by small ambient fields (see table 1). It should be emphasized that the Loran system is not utilized close to an airport but at great distances from shore over sea routes. Hence, the susceptibility of the Loran indicator to weak magnetic fields (<1 gauss) is of minor significance in actual navigation conditions. (Although the fields are designated as "weak" at 1 gauss, this value is at least two orders of magnitude above those encountered by an aircraft at cruise levels, due to a SANGUINE system field.) It is noteworthy that, when the cable containing the susceptible leads was subjected to fields in excess of 12 gauss, no display instabilities were noted. (The indicator proper was shielded from the field.)
Airborne weather radar system, Type RDR-1E, Bendix (monthly report 10)	0.5 V at the discrete frequencies of 40, 50, 67, 134, and 200 Hz (leads associated with CRT display) (diagram in monthly report 10)		10.0 V	40-150 Hz	Only two leads, "azimuth error, PPI," connected to the radar indicator evidenced susceptibility, as indicated in column 2. The notes above for the Loran indicator apply here as well.

Table 2.—Concluded

Equipment identification	First sign of malfunction		Highest injected voltage		Remarks
	Inj voltage	Freq	Voltage	Freq	
Inertial navigation system (INS), Carousel IV, AC Electronics (monthly report 10)	1.5 V	40-150 Hz	9.0 V	40-150 Hz	The wire-by-wire voltage injection test for this critical system was the lengthiest—in time—of all tests performed (see monthly report 9). INS operation, for most wires tested (of the more than 100 individual leads checked), was not affected by injected voltages to 9 V at any test frequency. On a few wires, slight oscillations of the MIN indicator were observed at voltages above 1.5 V (see fig. B23). Again, in an airplane installation, wiring to the equivalent indicators would be rather short (<10 ft) twisted leads. The 1.5 V directly injected to cause the noted oscillation would represent ambient fields—at the test frequencies—of hundreds of gauss.

4.0 VOLTAGES INDUCED IN AIRPLANE WIRING

4.1 INTRODUCTION

Avionics "black box" tests described in section 3 to determine susceptibility levels to ELF voltages impressed on associated wiring in series with the normal inputs are summarized in table 2. It is the purpose of this section to estimate the SANGUINE-system-induced levels of voltages on typical airplane wiring when flying in regions of ELF magnetic fields. Conclusions made for this typical airplane are then extrapolated to conditions of a SANGUINE system environment.

For purposes of illustration, calculations are made for a Boeing 747, which not only has long wire runs because of its size, but also has relatively complex avionics. (Much of the equipment listed in tables 1 and 2 is used on Boeing 747 airplanes.) Similar calculations for other airplanes can be made by the methods indicated. General conclusions are drawn for other aircraft in section 4.5.

Induced voltages may be computed as the product of exposed area and time rate of change of field where, as in most cases, wire runs are close to the skin throughout the airplane. Modifications are needed for nonaluminum airframes because of the lower conductivity of materials such as titanium.

The 747 is 231 ft long and has a wing span of 196 ft. Its body diameter is 23 ft at the center. Since structure imposes limitations on wire routing, wiring, in some parts of the aircraft is as much as 18 in. from any metal.

4.2 BOEING 747 AIRCRAFT WIRING

Wiring interconnecting the several equipment centers, illustrated in figure 4, can have large loop areas exposed to the magnetic fields of a SANGUINE antenna system. Most of the avionics equipment is located in the main equipment center approximately 12 ft aft of and 8 ft below the pilot's instrument panel. The controls and indicators are located in the cockpit.

Figure 5 is a cutaway drawing of the equipment racks in the main equipment center, one deck below the passenger compartment. (The station numbers shown refer to inches measured from an imaginary reference plane about 50 in. in front of the nose of the aircraft. This may seem somewhat ambiguous, but differences in body station numbers give exact separations in inches.) The main equipment center occupies 67 linear in. References to APU power and ac power in figure 5 pertain to circuit-breaker panels and not to generators; main generators are engine mounted, and ac power when engines are off may be supplied from the auxiliary power unit (APU) mounted near the empennage.

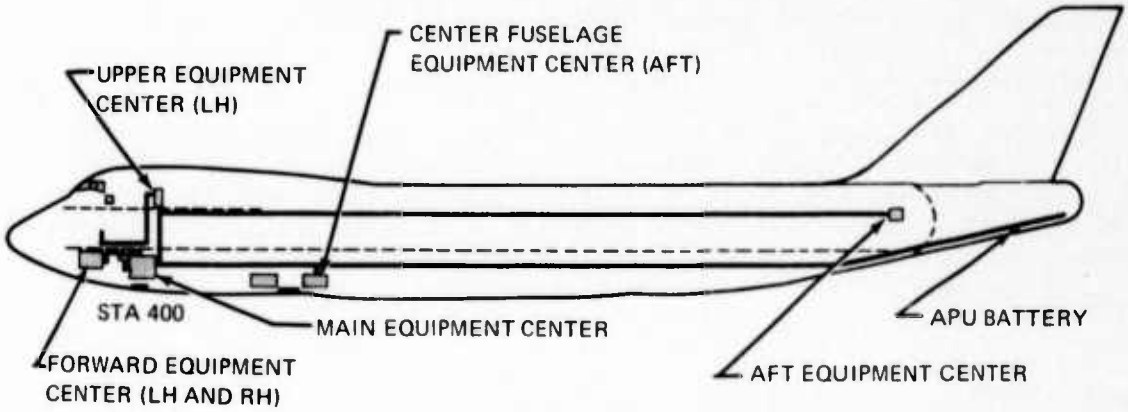

Figure 4. 747 Equipment Location

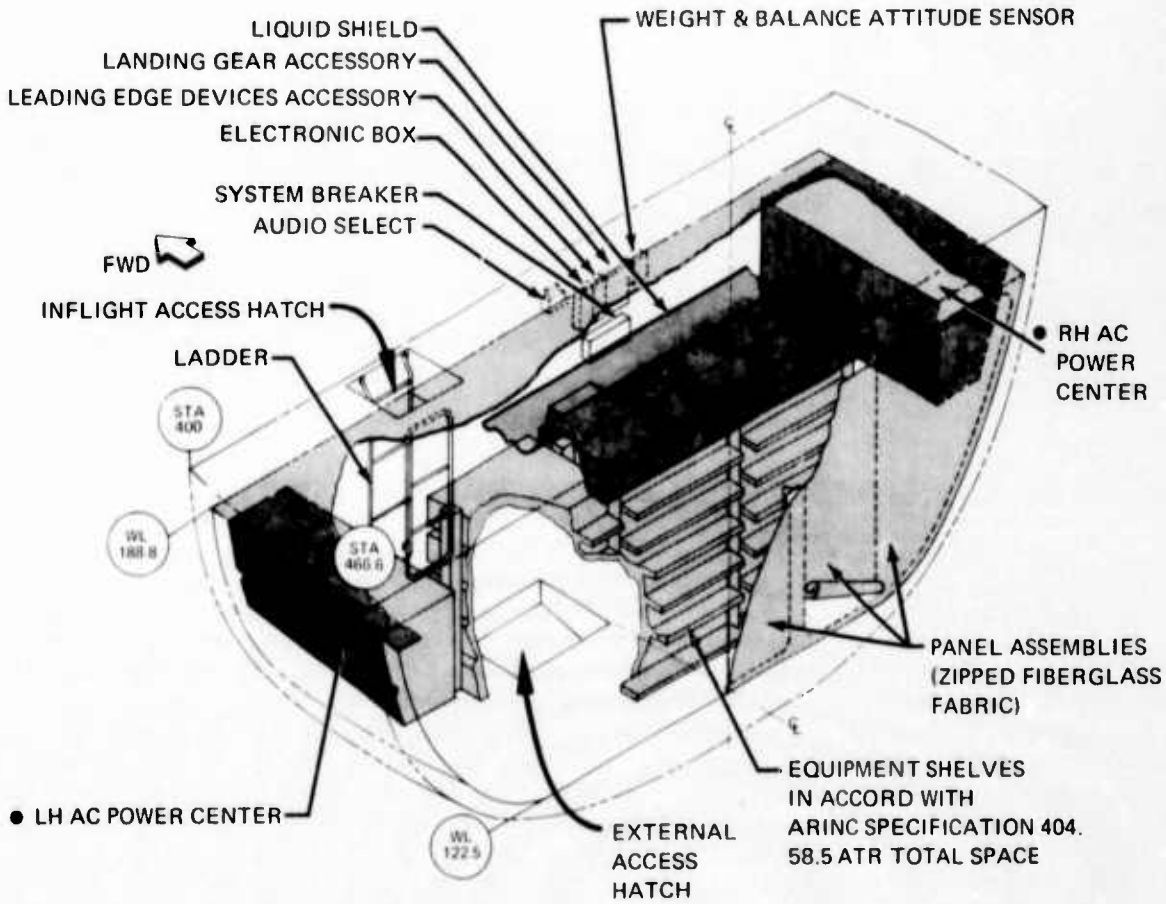

Figure 5. Main Equipment Center

Voltages induced in the interconnection wiring by a SANGUINE system field can be used with results of wire-by-wire laboratory tests to determine where mitigation may be required. Although sensitive wiring is usually twisted, or twisted and shielded, the computations are based upon a single-wire interconnection with a current return path through the aircraft skin. This computation will lead to worst-case conditions; for interconnections where interference exists, a further determination can be made to include the reduction in induced voltage resulting from twisted pairs and shielding. (It should be noted that no induced-voltage interference conditions exist, even for highest estimates of field strength.)

4.3 INDUCED VOLTAGES

The voltage induced in a large loop by a sinusoidal field is given by:

$$V = 2\pi f \iint_{\text{loop}} \hat{B}\cdot\hat{n}ds$$

For estimates in a complex wiring installation far from the SANGUINE system (at least a few hundred feet away), uniform magnetic field strength may be postulated. Since the airplane may have any orientation with respect to the field for a worst-case estimate, the total loop area and maximum field coupling are considered, thus:

$$V = 2\pi fBA$$

which, for 60-Hz frequency, becomes

$$V = (3.502 \times 10^{-3})A \text{ volts/gauss}$$

where A is in square feet.

Loop areas are computed on the basis of average wire separation from aircraft skin. When wire runs are close to skin relative to fuselage diameter, the area will be simply the separation times wire run length. When wires are run far from the skin and near the center of the aircraft, the situation is more complicated and the following discussion is necessary.

For an external uniform magnetic field, the induced voltage in an idealized concentric-cylindrical coaxial system is zero because of symmetry. Therefore, induced voltages will be small when wiring is close to the geometric center of the airplane, even for a structural current return. It was postulated (in monthly report 9) that the induced voltage as a function of wire displacement from the center would vary from zero to a maximum and then go to zero again as the wire approached the outer structure. Tests conducted on a scaled model indicate that this is indeed true for wires near the center, but the experimental points do not approach zero for the wire near structure as they should and the model tests are inconclusive. Intuitively, the coaxial cylinder should behave like a two-wire transmission line, i.e., when the interior wire is near the outside shell the equivalent two-wire line should have a spacing equal to the

distance from wiring to structure; and when the wire is near the center, the equivalent line should be spaced with a separation distance equal to the distance of wiring to the center of the cylinder. An exact formulation for a theoretical study of this problem, presented in report 9, was not pursued to completion, since the experiment partially verifies this intuitive approach and it appears that adequate room for error exists in estimating the voltages liberally. This point is emphasized since the largest voltage for an airplane cable given below resulted from wiring that runs 10 ft from any metal (over the passenger compartment) for a considerable portion of the total wire run.

For each of the interconnection runs between major equipment centers illustrated in figure 4, the exposed area has been computed using the separation from structure appropriate to each run. Wiring is often run close to the nearest structure, and hence the total length is often longer than the sum of longitudinal and transverse distances. Further, each individual run may have differing separations from structure along the run. These factors have been considered and the exposed areas are consistent with measurements made on 747 installations. To present data useful in determining mitigation criteria, two tables have been prepared. Table 3 simply lists the induced voltage per gauss in each interconnection path for a 60-Hz field internal to the aircraft; for other frequencies and magnetic field values, the entries may be modified by direct proportion. The 747 aircraft has about 22-dB shielding at 60 Hz, determined experimentally and consistent with shielding formulas, as described below. Table 4 lists induced voltages per gauss, where the induction field is external to the aircraft.

4.4 AIRFRAME SHIELDING

A theoretical determination of the shielding effectiveness of a long conducting cylinder, as a model of an airplane fuselage, can be approached in two ways. By using a "wave" approach the shielding appears to be small, since the usual aircraft shell thickness is a small fraction of a skin depth at low frequency. As the diameter increases, the fuselage approaches an infinite plane sheet, known to provide but little shielding at low frequencies. A "circuit" approach to this problem indicates that the shielding effectiveness of a long conducting cylindrical shell is

$$|S| = \left|1 + j\, at/\delta^2\right|$$

where a is the diameter, t the shell thickness, and δ the skin depth of penetration of the shell material. From this expression, the shielding effectiveness of a large-diameter cylinder will be large. An experimental program justified the circuit approach to the problem.

Representative values for a Boeing 747 are a = 7 meters, $t = 1.2 \times 10^{-3}$ meters (50-mil skin) and a 60-Hz electrical skin depth of 1.3×10^{-2} meters. The value of S is then 25 dB.

Tests were made on electrically quiescent Boeing 747 and 737 airplanes to determine 60-Hz magnetic shielding effectiveness. The airplanes were made available for these tests at a time when no ground or airplane power was being used, no connections were made to external utilities, and all doors could be closed. In this way, 60-Hz ambient magnetic fields could be used as the "excitation" exterior to the airplane.

Vertically and horizontally polarized components of these fields were measured with a Fairchild EMC-10 interference analyzer at several points around the exterior of the airplane. The range of these measured values was approximately 6 dB. A second set of measurements was then taken inside the airplane, as close as possible to the external measurement points. The polarization of the internal fields was somewhat different from that of the external ones, but again the measurements were within a range of about 10 dB. The high values inside corresponded to high ambient values outside. (The latter represent the net effect of relatively distant power lines and local ground currents.)

The average ratio of the vector fields, outside-to-inside, was 10.5, or approximately 20 dB for the 737. ("Vector" here means the rms of vertical and maximum horizontally polarized components at a given position.) For the 747, the corresponding figure was 22 dB, with a minimum value of 20 dB at one data point. The test procedure was the same for the two airplanes (which were at different airports).

The fairly good agreement between test data (22 dB) and calculations for representative 747 body sections (25 dB) lends credence to the assumption that the theory for conducting cylinders is, at least approximately, applicable to an airframe. The greater the SANGUINE system operating frequency, the greater will be the shielding effectiveness of the airframe. Since the measured values were highly consistent in the fuselage, the ELF shielding value of 22 dB will be used as a basis for discussion of 747 wiring in of this report.

4.5 SUMMATION

A simple example indicates that the induced voltages due to SANGUINE system predicted field values are very small. For a worst-case value of SANGUINE system field strength at low altitude (30 mgauss assumed), a worst-case assumption of wire loop inside the 747 airplane (10-ft spacing from structure, 200 ft long), with a worst-case frequency of 150 Hz, and assuming that the airframe shielding is a worst case (20 dB, the lowest measured value at 60 Hz), the induced voltage on the wiring is calculated as less than 60 mv. No airplane systems tested (table 1) were this susceptible. Therefore, no problems due to induced voltages in airplane wiring are foreseen when overflying the SANGUINE system site, provided that the 30 mgauss is a correct estimate.

The data presented in table 3 do not include airframe shielding and may be extrapolated to aircraft larger or smaller than the 747 by using a factor proportional to overall length. Since smaller aircraft have shorter wire runs and less complicated internal structure to avoid, the exposed loop area reduces faster than the first power of length (i.e., with a power between 1 and 2).

Shielding effectiveness of the fuselage appears to follow that of an infinite cylinder. Hence, for the small range of body sizes encountered, the airframe shielding for aluminum should vary directly with body diameter; smaller aircraft would thus have less shielding. Titanium alloys and stainless steel, increasingly used in airplane manufacture, have electrical skin depths approximately five times those of aluminum alloys. Thus, aircraft sections consisting of these materials will provide little shielding to low-frequency magnetic fields. Extrapolations to other aluminum-skin aircraft can be based on the data of table B1.

Table 4 is representative of a typical large aircraft which, from the above discussion, probably has the largest induced voltages. It may therefore be concluded that there will be no significant voltages induced on wiring on any airplane at cruise altitudes; indications are that even at unusually low altitudes directly over a SANGUINE system antenna, effects of this type will be below the threshold levels for which mitigation would be required. Even if the SANGUINE fields should approach 1 gauss at aircraft altitude, very few items of equipment would require mitigation when aircraft shielding is present.

Table 3. Induced Voltage (Volts per Gauss) in 747 Wire Runs for Internal Magnetic Field

Run to	Run from					
	Forward equipment center	Main	Upper	Center	Aft	APU
Forward equipment center	–	0.08	0.13	0.20	0.80	1.0
Main	–	–	0.05	0.16	2.0	1.0
Upper	–	–	–	0.21	0.75	1.0
Center	–	–	–	–	0.55	0.80
Aft	–	–	–	–	–	0.20

Table 4. Induced Voltage (Volts per Gauss) in 747 Wire Runs for External Magnetic Field

Run to	Run from					
	Forward equipment center	Main	Upper	Center	Aft	APU
Forward equipment center	–	0.006	0.011	0.016	0.066	0.083
Main	–	–	0.004	0.013	0.16	0.083
Upper	–	–	–	0.016	0.062	0.083
Center	–	–	–	–	0.042	0.066
Aft	–	–	–	–	–	0.016

5.0 FIELDS AT AIRCRAFT ALTITUDE

An analysis was performed based on a static field model to provide a more realistic value, for the magnetic flux density at aircraft altitudes, than the 1-gauss worst case considered for laboratory testing. Interest is centered here on field amplitudes and configurational variations in the neighborhood of a SANGUINE system antenna array. The two paths considered, illustrated in figure 6, are representative and yield upper bounds for magnetic field strengths. One path is along the array, equidistant from the ends of the elements, and the other is transverse to the array parallel to a single element of the array. Since worst-case values are sought, earth-return currents are neglected and the model consists of an array of co-phased elements in free space. Although actual soil and rock conductivities will influence field values at aircraft altitude, the

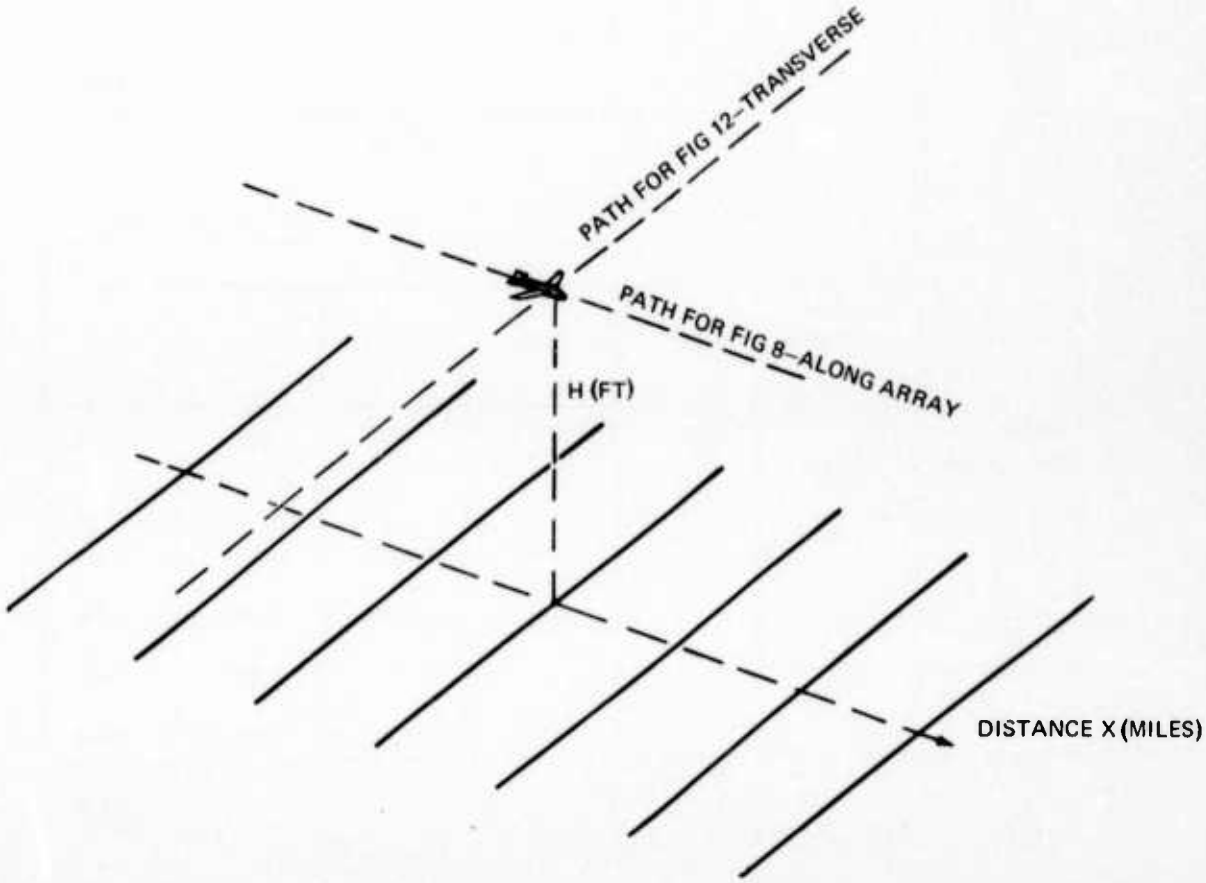

Figure 6. Paths for Overflight of SANGUINE Array

resultant effects will be to reduce the field values. Earth return currents have either vertical components which produce fields tending to zero at aircraft altitude--as will be subsequently clarified--or horizontal components which oppose the fields of the plane array model. All of these qualifications could be removed with a more complete (and more complex) mathematical model. What is here attempted is to show that no significant avionics interactions are likely with fields computed from a simple, first-order mathematical model yielding worst-case results. This will obviate the need to construct a completely rigorous model. For the simplified case, a two-dimensional model, as illustrated in figure 7, will suffice.

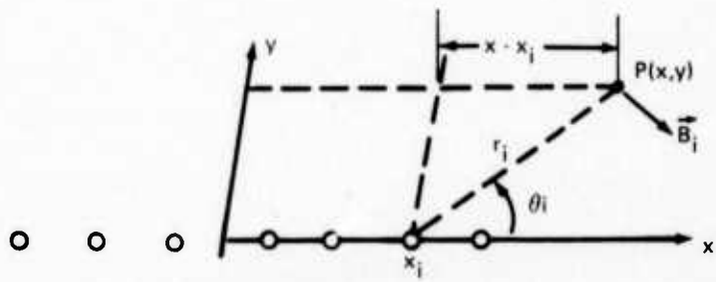

Figure 7. Geometry for Array

Each element of an N-element array produces a magnetic field

$$B_i = \frac{\mu I}{2\pi r_i} \qquad i = 1, 2, 3, \ldots, N.$$

where μ is free space permeability, I is the element current, and r_i is slant distance from the ith element to the observation point. The field direction for each element is perpendicular to the corresponding slant length r_i. It requires a relatively simple computer program to calculate the lengths and angles for an x, y observation point from the geometric relations:

$$r_i = \left[(x - x_i)^2 + y^2\right]^{\frac{1}{2}}$$

$$\theta_i = \arctan \left[\frac{y}{(x - x_i)}\right]$$

The x and y field components

$$B_x = \sum_{i=1}^{N} B_i \cos\theta_i$$

$$B_y = \sum_{i=1}^{N} B_i \sin\theta_1$$

and finally the total

$$|B| = (B_x{}^2 + B_y{}^2)^{\frac{1}{2}}$$

For x and y in miles each element produces

$$B_i = \frac{(4\pi \cdot 10^{-7}) I \; 10^4}{2\pi(1{,}609) r_i} \quad \text{gauss/ampere}$$

A very limited trade study was performed using element currents of 50, 60, and 70 amp and element spacings of 1.5 and 5 miles with several constant altitude flyover paths. Two cases are shown in figures 8 and 9 for 70-amp, 10-element arrays on spacings of 1.5 and 5 miles, respectively. It should be noted that doubling the current will double the field values, so there is little value in varying this parameter except for a check on the computations. Varying the element spacing while keeping the total number of elements constant affects the maximum field values observed, the closest spacing producing the

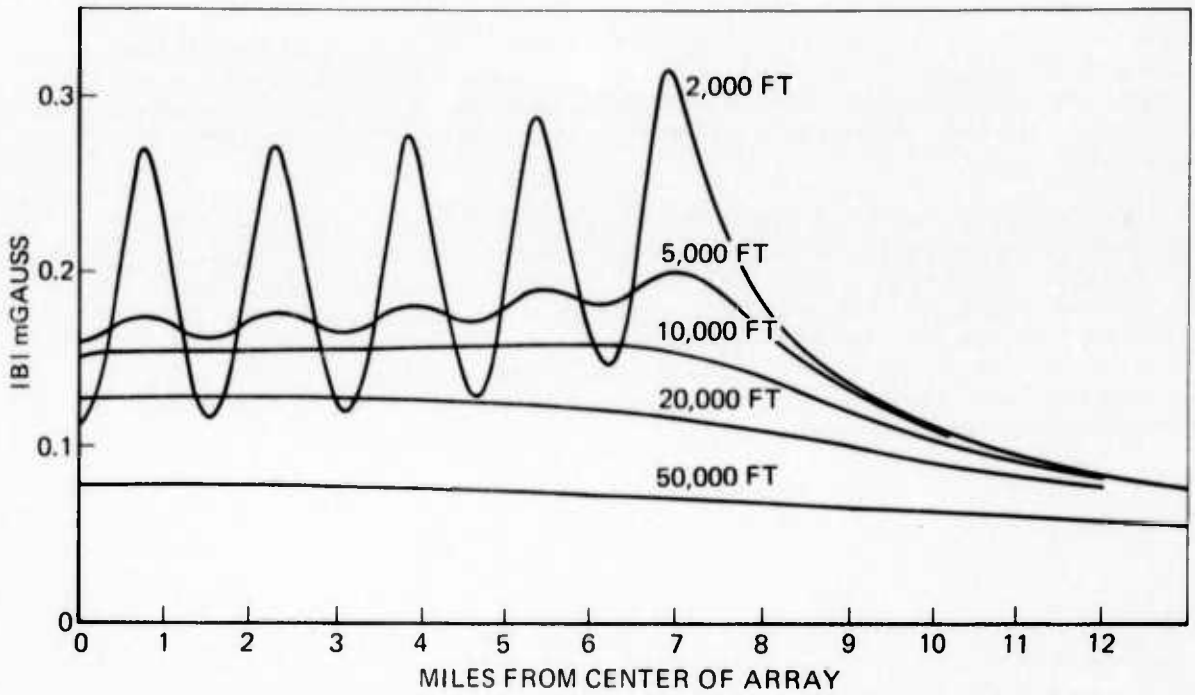

Figure 8. Fields at Altitude, 10-Element Array—1.5-Mi Spacing, 70 Amp per Element

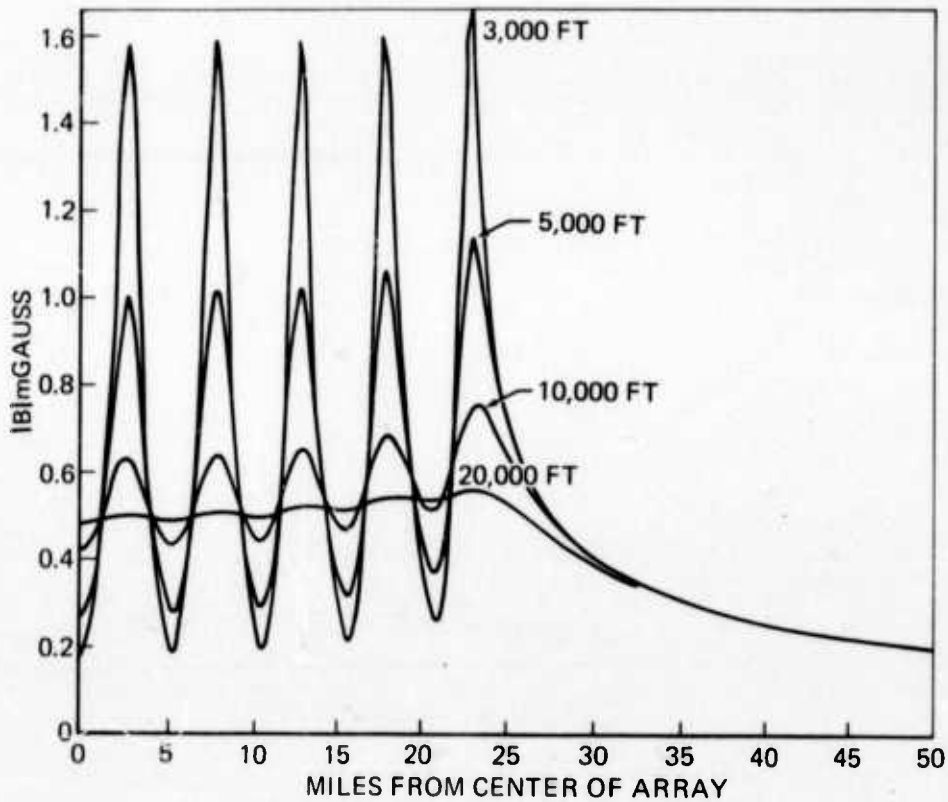

Figure 9. Fields at Altitude, 10-Element Array—5-Mi Spacing, 70 Amp per Element

largest maximum fields. Even for the 1.5-mile spacing, 10-element array, the maximum field at 2,000 ft altitude is less than 1 mgauss. The addition of another orthogonal array to form the SANGUINE antenna grid will add a magnetic field vector at 90°, producing a $\sqrt{2}$ increase in magnetic field strength magnitude.

Searching for the worst case, the field over the end element in the 10-element, 70-amp array was calculated for several very low altitudes: 50, 100, 200, and 500 ft. (See fig. 10.) Over this end element, all the elements produce additive field contributions, although small. One should note the higher peak values over the end element in figures 8 and 9. Near the center of the array, the directions of magnetic field contributions from the end elements are such that they tend to cancel. Thus the end element was chosen as representing the worst case.

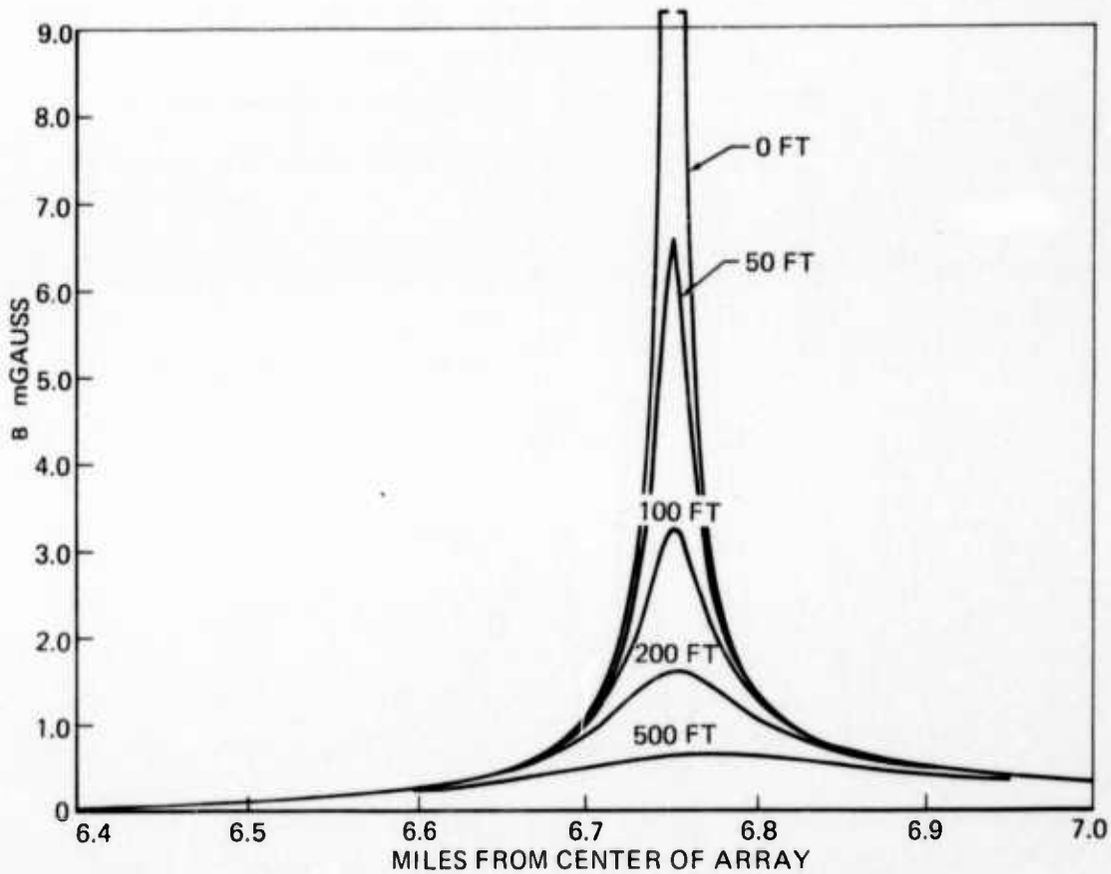

Figure 10. Fields at Altitude, 10-Element Array—1.5-Mi Spacing 50 Amp per Element (Showing Field Near End Element Only)

So far, the field directly centered over the array has been considered. Transverse paths or passes off-center will have reduced field values. To see quantitatively how the field varies, the transverse path illustrated in figure 6 was considered passing over a single element of the array. For this case, the field of a finite straight wire of length L, shown in figure 11, will serve as illustration.

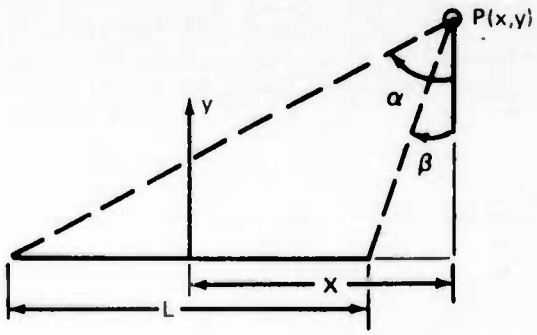

Figure 11. Geometry for a Long Wire

At the observation point P(x,y) the field is perpendicular to the paper and given by

$$B = \frac{\mu I}{4\pi y} (\sin\alpha - \sin\beta)$$

where μ is permeability, I the current, and α and β are angles between the normal and projections from the ends of the wire;

$$\alpha = \arctan\left(\frac{\frac{L}{2} + x}{y}\right)$$

$$\beta = \arctan\left(\frac{\frac{L}{2} - x}{y}\right)$$

Note that directly over the center of the wire $\beta = -\alpha$ and

$$B = \frac{\mu I}{2\pi y} \sin\alpha$$

When y is small compared to L, the angle $\alpha \simeq 90°$, and the field is essentially that of an infinitely long wire. This is justification for neglecting wire length in the previous curves. For a 10-mile-long wire, the field at a 10-mile altitude will be 0.707 times that from an infinitely long wire. This

merely indicates a 3-dB increase overestimate of the fields, and has been shown in figures 7 and 8 for a 50,000-ft overflight with smaller error at lower altitudes.

However, of principal concern are the transverse variations. Figure 12 shows the variation in magnetic field from the center of an element 20 miles long with transverse motion relative to the value at the center of an element. These curves clearly show that for the low altitudes of principal concern the fields previously presented may be considered sharply bounded, i.e., confined to a region of roughly the array dimensions.

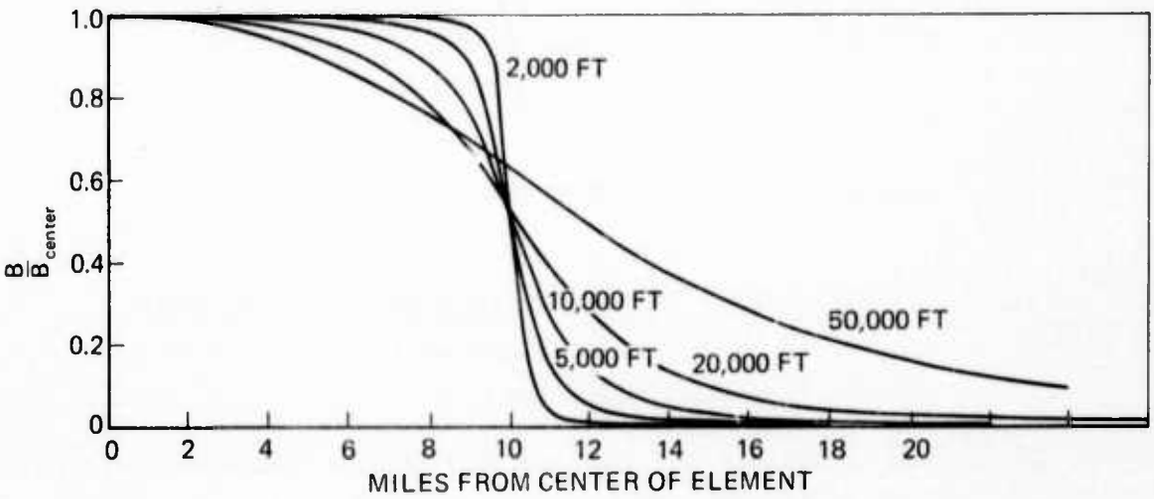

Figure 12. Transverse Variations of Field for Single Antenna Element 20 Mi Long at Altitude

Finally, note that the contribution of vertical currents will be like the transverse variations, with altitude replacing transverse distance. Hence, above the surface in the center of the array, the contribution of vertical currents will reduce rapidly with observation height. Deep horizontal currents will subtract from the values at altitude more than the vertical currents will add. At the antenna currents presently proposed for SANGUINE systems, it was not considered necessary to add significant figures to a problem area where little difficulty exists. Should several orders of magnitude more antenna current be considered, then further clarification should be undertaken, including earth-ionosphere cavity excitation factors.

6.0 SUSCEPTIBILITY OF ELECTRONIC DISPLAYS

6.1 INTRODUCTION

It was discovered in this study that the flux valve, a part of the compass system, was the most susceptible avionics equipment. This topic is discussed in detail in section 7.0. Other susceptible items were CRTs and similar items such as scan converters. This section gives relevant material on these latter items, broadly categorized as electronic displays; tests were made on both airborne equipment and ground-based air traffic control equipment using these devices.

It should be emphasized at the outset that a need for a mitigation program on electronic displays is not foreseen because the worst-case estimate of the susceptibility level of airborne equipment to incident ELF fields is 0.5 to 1 gauss. Not only can it be demonstrated that such levels are found only very close to the buried SANGUINE antenna, but it can also be reasoned that transport airplane equipment would not be exposed to such levels. This is because 20 dB of shielding is demonstrably attributable to the airplane body, and the minimum altitude over the antenna is sufficient to provide protection in itself. Therefore, any apparent residual problems would be with ground-based air traffic control equipment and there are two factors which dispose of this problem: (1) the fact that there are no such facilities within critical distances of the SANGUINE test site, and the expectation that in an operational system such a situation would not be permitted to arise, and (2) the current ability to operate electronic test equipment, such as CRTs, at the SANGUINE test site (ref. 1).

6.2 RECAPITULATION OF AVIONIC DISPLAY EQUIPMENT SUSCEPTIBILITY

As stated in section 3.0, the susceptibility level of (airborne) Loran displays was approximately 1 gauss, and of (airborne) weather radar indications, 0.5 gauss; for types of radar terminal equipment found in an air route traffic control center, the minimum susceptibility level was on the order of 0.15 gauss (see section 3.0).

6.3 SUSCEPTIBILITY OF COMMERCIAL TEST EQUIPMENT

Tests were made in Boeing laboratories on three models of Tektronix oscilloscopes. This equipment was available for a longer time than that referred to in 6.2; the problems are of the same nature, and more detailed appraisals could be made.

When subject to uniform incident ELF magnetic fields on their various axes, the worst-case level of field to cause susceptibility (selected as 0.1 cm jitter in the display) was found to be 0.8 gauss. Details of these tests are discussed below.

6.4 MECHANISM OF SUSCEPTIBILITY

The display jitters in the presence of ELF magnetic fields because the electron beam is deflected in a direction at right angles to its direction of motion and to the instantaneous direction of the field.

Most CRTs in commercial equipment are equipped with magnetic shields, so that the susceptibility to uniform, large-volume ELF fields is dependent on the efficiency of such shielding. The shields are primarily intended to protect the display from magnetic field sources (such as transformers, blower motors, etc.) inside the instrument and to give some protection against ELF (power frequency) fields in the environment where the equipment is used. It is apparent, from the discussion below, that the effectiveness of shields tends to be limited by the need to provide holes in the shields to make connections to electrodes, as well as by the necessarily open ends at the base and face of the tube.

6.5 SHIELDING EFFECTIVENESS OF CRT SHIELDS

The literature (such as refs. 2, 3, and 4) points out practical factors which tend to limit obtainable shielding effectiveness to values much less than those theoretically obtainable for closed volumes of material to which high permeability is attributed. Chief among these factors is the need for openings--at least at the base and faceplate of the tube. The magnetic alloys used in shield construction also characteristically have a shielding effectiveness dependent on the level of induction. (A level of maximum permeability exists somewhere between zero and saturation induction.) The literature emphasizes the need for careful annealing of some materials and details the cost factors for various shapes and materials.

Since it was desirable to be able to explain results on units tested in this research as "black boxes," some experimental work was done on the insides of "boxes," namely, two types of CRT shield.

The test procedure was to place the test shield in appropriate orientation in the test coil (fig. 13), and to measure relative field strengths inside the shield, on the axes, with a magnetic field probe connected to the Fairchild EMC-10 interference analyzer. The probe has 1,000 turns on an average winding diameter of 0.75 in., and a winding length of 0.75 in. It was mounted on a stick with a styrofoam spacer to align it inside the shield. A reference value for the field was obtained in the test coil, with the probe calibrated against the gaussmeter and the shield removed. This latter strategy was required because the shield distorts the otherwise quite uniform field in the coil.

Two items were tested--a shield removed from a 3WP1 CRT, and a shield (loaned by courtesy of Tektronix, Inc.) for a Tektronix 549 cathode-ray oscilloscope. The mechanical characteristics are illustrated in sketches (figs. 14 and 15), and test data for various orientations are given in figures 16 and 17. Frequency was not found to be significant to results to at least 100 Hz; the tests were made at 80 Hz.

Characteristically, as in the literature, certain common characteristics are noted from data of figures 16 and 17:

- Attenuation is significantly better to transverse fields than to axial ones. (Axial field attenuation near the ends is negative.)
- Attenuation is low near the end of the shields.
- Attenuation (in all cases except transverse for the Tektronix shield) depends on induction.

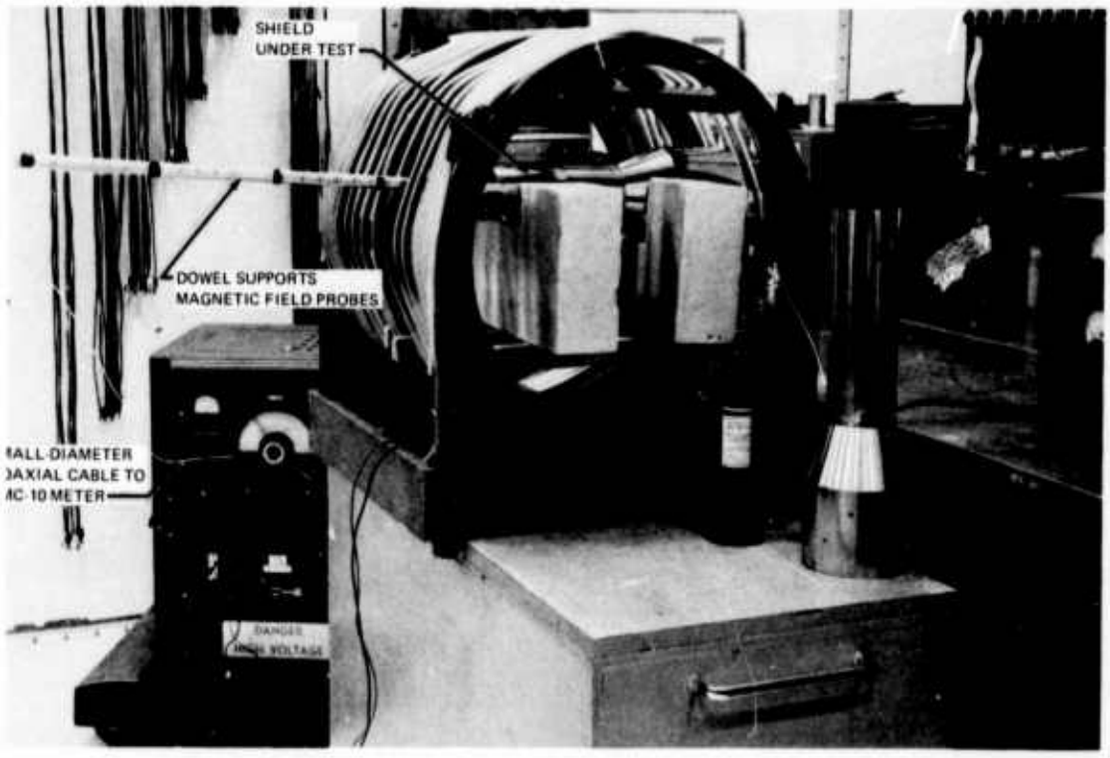

Figure 13. Tests on CRT Shields

The first and last observations are related to the extent that saturation effects tend to limit axial attenuation. Transverse attenuation variation with induction is a function of the alloy properties, such that the Moly-Permalloy did not exhibit significant change from 1- to 10-gauss incident fields.

A detailed look at the data shows a characteristic dip in axial attenuation at high fields between the ends in both cases. This is not attributable to "windows," but was found to be characteristic of tubes of any length of shielding material. Fortunately, axial attenuation is not generally required to be as high as transverse because such field components do not cause serious beam deflection.

The Tektronix shield has a significant dip in attenuation in the Y direction about the slot (whose long direction is peripheral). The 1-in.-square window near the base has only marginal effects (comparing X and Y curves of figure 17), presumably because fringing around the open area at the tube base is the predominant factor in determining shielding at $Z < 3$ in. It was noted during tests not only that the slot is a significant region of leakage, but also that there was some cross-polarization effect; an axial field external to the shield produced a transverse component inside it at this point.

Exploration of the effect of the seam areas on both shields (metal is overlapped at least 0.25 in. and spotwelded) showed that, to transverse fields, rather than leakage, a scarcely perceptible localized increase in attentuation occurred which could be attributed to the double thickness.

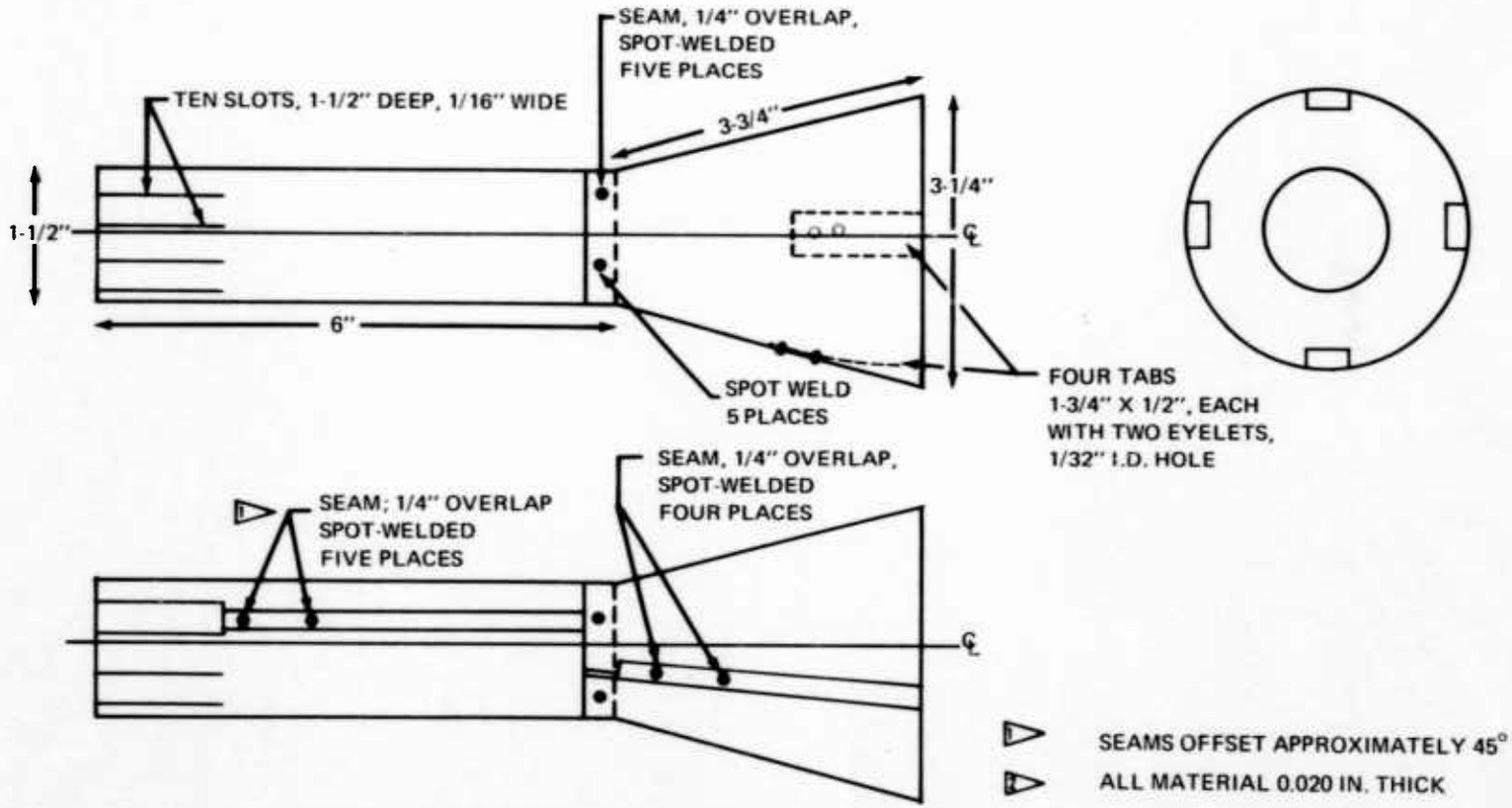

Figure 14. Mumetal Shield for 3WP1 CRT

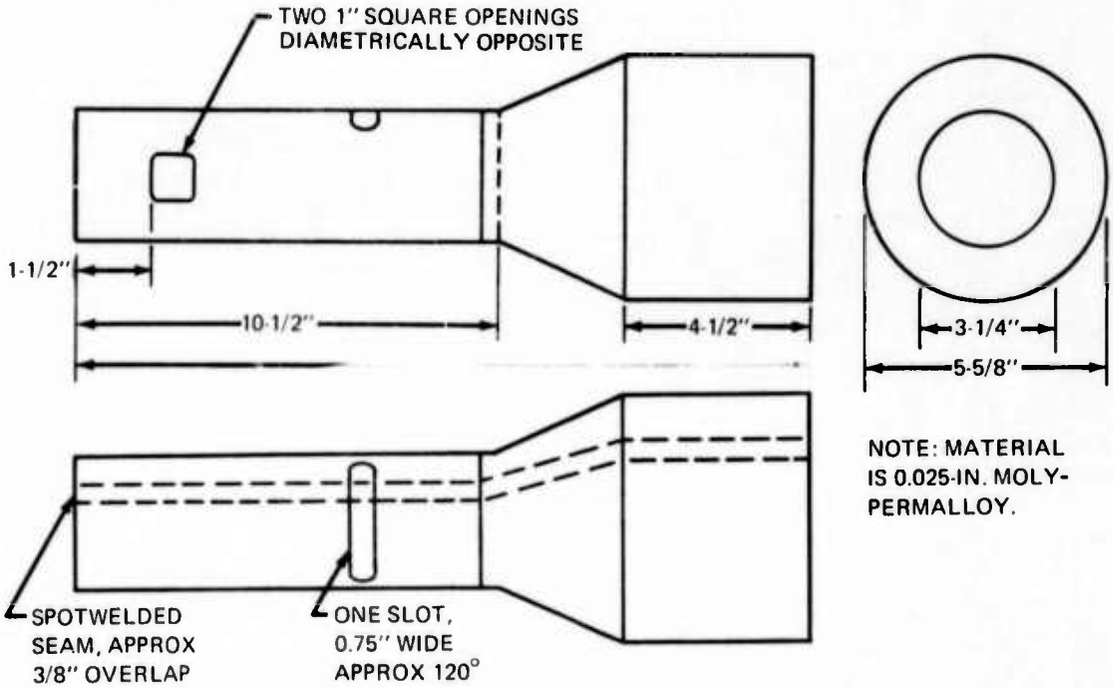

Figure 15. Sketch of Shield for Tektronix 549 CRO Showing Major Openings

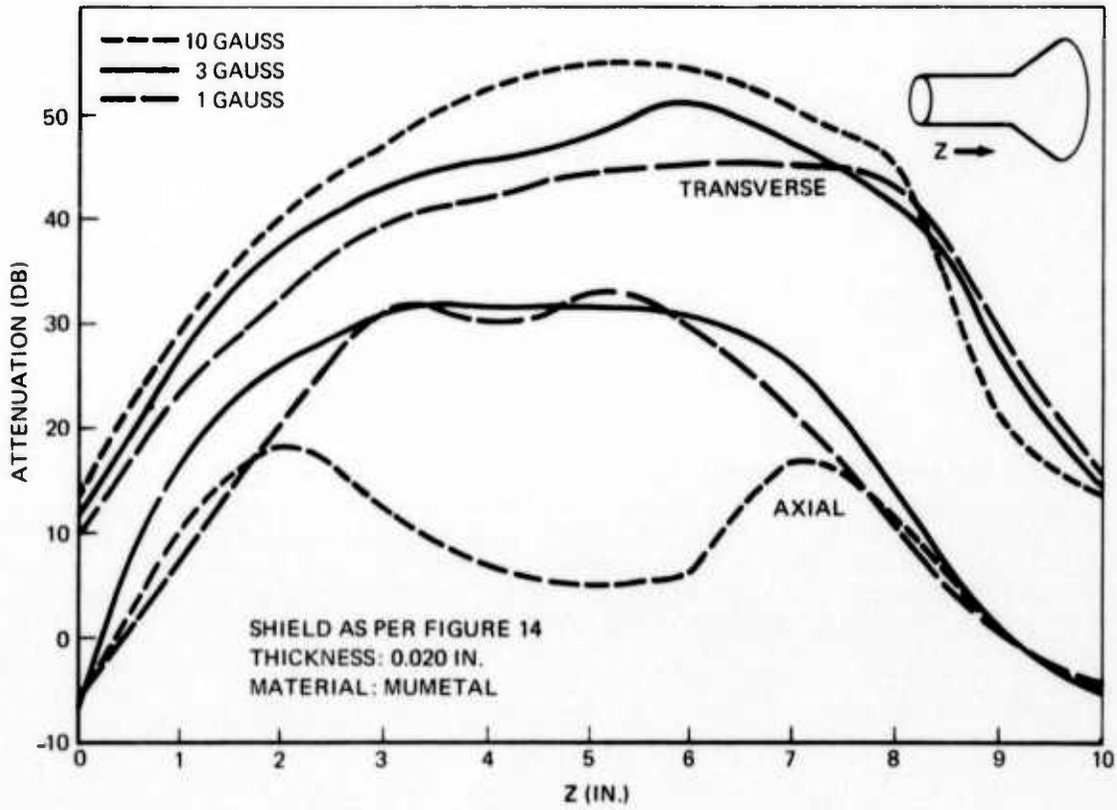

Figure 16. Attenuation of ELF H-Field by 3WP1 CRT Shield

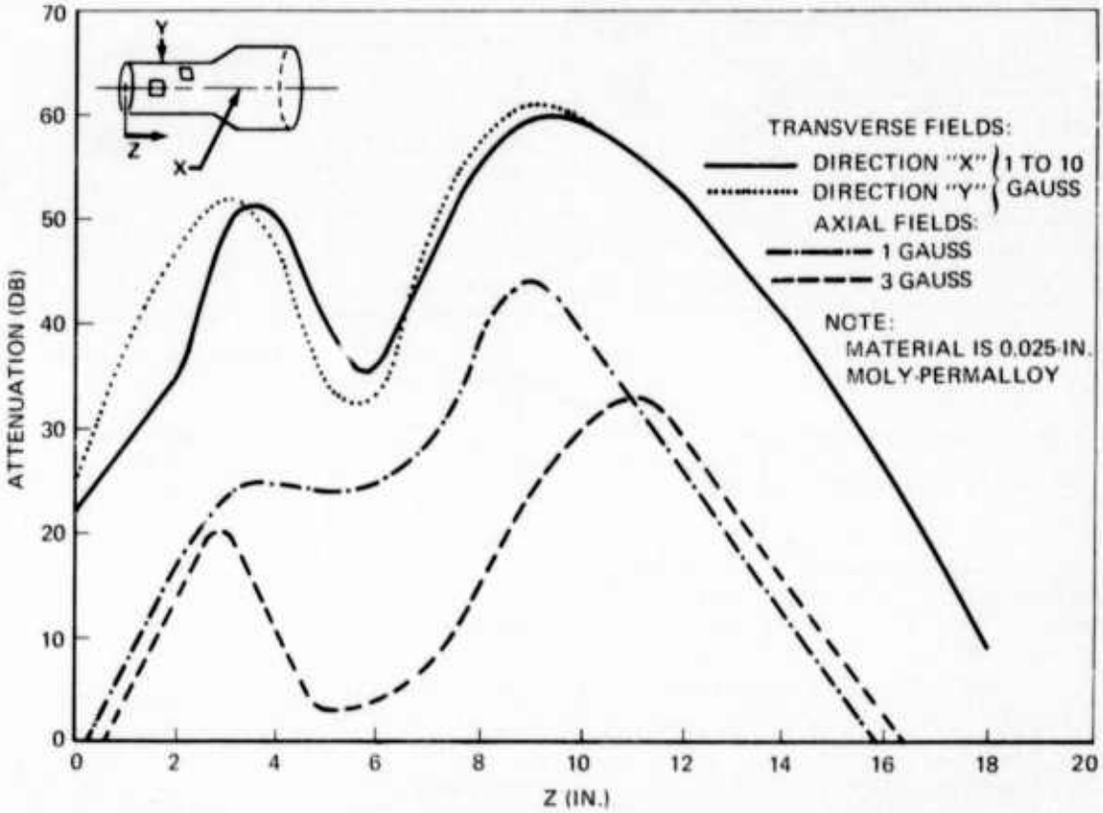

Figure 17. ELF Magnetic Field Attenuation—Tektronix 549 CRO Tube Shield

For a quantitative explanation of the data, first note that the frequently quoted formula for shielding effectiveness of a semi-infinite cylinder with radius R and wall thickness T ($T \ll R$), is

$$S = \frac{\mu T}{2R}$$

where μ is the relative permeability of the material. Insertion of $T = 2 \times 10^{-2}$ in., R = 0.75 in. (neck area of 3WP1 shield), and assuming $\mu = 100{,}000$ for Mumetal makes S equal to 1300 or 62 dB. This is in reasonable accord with the 55 dB of figure 16 for 10 gauss at Z = 5 in. The 7 dB discrepancy can be ascribed either to fringing effects around the end or an effective value for μ which is lower than 100,000 for transverse excitation at this induction.

6.6 SUSCEPTIBILITY LEVELS OF OSCILLOSCOPES

Four types of cathode-ray oscilloscopes (CROs) were exposed to fields from the test coil which illuminated them fairly uniformly along the X, Y, and Z axes. (See figure 18 for definitions.) The field incident on the CRO was measured with the gaussmeter probe close to the oscilloscope cabinet. The CRO was operated with vertical deflection amplifiers desensitized and time base "off," so that a central spot on the screen could be observed. This generally deflected in accordance with the sinusoidal incident field in a direction indicated on figure 18, which presents test results in terms of incident gauss per 1 mm peak-to-peak deflection.

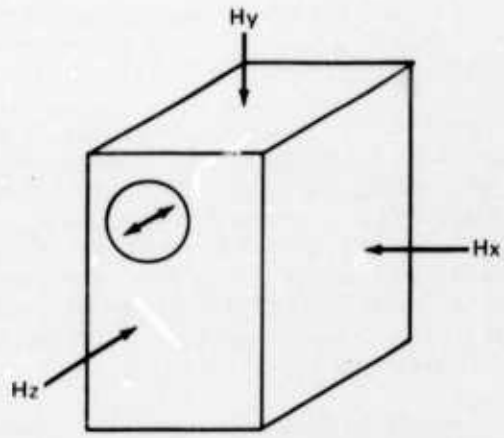

TYPE OF TEKTRONIX CRO	REQUIRED H (GAUSS) PER 0.1 CM PEAK-TO-PEAK DEFLECTION AND DIRECTION ON CRO SCREEN		
	Hx	Hy	Hz
515A	1.0 ↕	1.0 ↔	– [1]
422	0.8 ↕	1.6 ↔	1.0 ↗ [2]
547	1.0 ↕	1.5 ↘	5.5 ↖
549	2.0 ○	2.5 ↔	2.0 ↗

[1] NOT SENSITIVE TO SYMMETRICAL Z EXCITATION
[2] NULL DEFLECTION FOR FIELD ROTATED 30° TOWARD X AXIS

Figure 18. Susceptibility of Cathode Ray Oscilloscope

Besides the gross measurements listed in figure 18, some exploratory measurements were made inside the units. Large circulating currents in the frame of the units appeared to enhance the field inside, negating any shielding effect the cover would provide. Exploration with small probes (100 turns) carrying 1-amp currents indicated that a possible cause of deflection was leakage through the larger "windows" in the shield, particularly the circumferential slots illustrated in figure 15. Placing the same coil near the face or base of the tube had the same effect.

Quantitative explanation requires recourse to a well-known approximate formula (to be found in ref. 5) for magnetic deflection of CRTs:

$$d = \frac{0.3\ abH}{\sqrt{V}}$$

where d is the deflection in centimeters at the screen resulting from a field of H gauss applied for a distance b (in cm) at a distance a (in cm) from the screen where the accelerating potential is V volts.

A field of 1 gauss applied over 1 cm (representing a gap in a shield) at a representative distance 20 cm from the screen may be calculated to make d equal to 0.2 cm if V is 900 volts, representative of a first anode potential. Thus, 0.2 cm of jitter would result from a 1-gauss field. If the local attenuation at the slot (fig. 17) is on the order of 34 dB, the effect of a 1-gauss external field would be a deflection of 0.004 cm, which is much less than the 0.1-cm measured values of section 6.3. (The tube shield construction for the various CROs listed in fig. 14 is fairly similar, differing not so much in "windows" as in lengths of neck and bulb portions.)

Apparently, despite the observation of localized leakage at the slot, the principal cause of the observed deflections of figure 18 must be the general effect of fringing near the ends of the shield. At the base end, attentuation is 20 dB on figure 17, and accelerating voltage is low. At the face end, attenuation is less over a wider region, but voltage is higher.

6.7 CONCLUSIONS

Qualitatively and, to a lesser extent, quantitatively observed susceptibility aspects of avionics and other equipment employing CRTs and scan converters can be explained in terms of fairly simple theory and shielding tests. Mitigation of effects of SANGUINE system fields appears not to be required. This is because the same devices operate successfully in 60 Hz (and, in aircraft, 400 Hz) ELF magnetic field ambient environments comparable to maximum levels expected from SANGUINE system fields at locations where such devices could conceivably be located; either on the ground or on board airplanes. If mitigation were ever required, the solution would apparently not reside in the redesign of the CRT-using equipment. Since complete invulnerability could not be achieved due to the shield openings at the face and base of the CRT, only the shielding provided by such a large-scale metal structure as an airplane body or a shielded enclosure would solve problems for large-volume ambients greater than approximately 1 gauss.

7.0 COMPASS SYSTEM

7.1 INTRODUCTION

Two series of tests made on airplane compass systems were reported in monthly reports 11 and 12. These systems used the "flux valve" (which, depending on the manufacturer, and detailed construction, is otherwise known as a flux gate or a magnetic azimuth detector), and this element of the system proved very susceptible to ELF magnetic fields. This susceptibility is partially inherent in the principle of the flux valve, in that it is intended to determine the direction of the earth's field--hence, an alternating field of the same order of magnitude, and arbitrary direction, would *a priori* be expected to confuse such a system.

After a recapitulation of earlier findings, further tests are discussed in section 7.4 which had the objective of obtaining more detailed background.

7.2 RECAPITULATION OF EARLIER TESTS AND GENERAL BACKGROUND

The item tested was the Sp[illegible] Thin Flux Valve, Sperry Part No. 2591438-901, used in the Boeing 747 airplane. [illegible] is part of the magnetic heading reference system (MHRS) that also inlcudes a gyro heading reference, a slaving control unit (coupler), compass indicators (cockpit instruments), and a pilot's control panel with a null-type annunciator indicating whether the gyro and flux valve are in synchronization. In the 747 airplane, gyro heading is provided from an inertial navigation system. In addition, magnetically referenced navigation information may be derived from VOR or ADF systems and combined in various ways with the basic MHRS outputs.

The basic system (flux valve, coupler, gyro) obtains the magnetic heading of the airplane from the flux valve mounted in the wing, and updates the gyro heading data by slaving it in accordance with the measured magnetic information. The system can be pictured as a feedback loop, in which the gyro heading data are used to damp out the short-term fluctuations (noise) in the flux valve output. (See figure 20.)

The maximum rate at which the magnetic information can update the gyro signal is on the order of 1° per minute. Thus, on sharp turns (causing departure of the flux valve from horizontal) or during times when the magnetic information is unreliable, the annunciator indicates lack of synchronization. However, the cockpit instruments such as the horizontal situation indicator and the radio magnetic indicator (bearing relative to VOR or ADF) follow the direction change rapidly, being fed, in effect, information from the gyro. More important from a SANGUINE system investigation viewpoint, the information used to navigate the airplane on autopilot mode is also obtained from the gyro heading and therefore is not subject to erratic, short-term, confusing information from the flux valve.

The flux valve is mounted in the wing tip, in most airplane installations, away from magnetic material and current-carrying wiring because of the problems resulting from undesired magnetic fields. To give an idea of its sensitivity levels (or to what, in general, the flux valve may be susceptible), the horizontal component of the earth's field in the USA is in the range of approximately 0.15 to 0.29 gauss. Vector addition of quite small stray dc components can therefore cause errors in flux valve output. These errors can be compensated only if fixed and known.

If any published material exists on errors due to alternating fields, the engineers in The Boeing Company responsible for installation of the systems are unaware of it. Thus, to some extent, the effort reported is novel, in that a problem due to ac fields would usually be solved at the source--the offending wiring in the airplane.

Early tests with the flux valve installed in the test coil and exposed to SANGUINE system fields, while connected as in the Boeing 707 airplane, indicated:

- Flux valve output errors resulted from very small applied fields (< 0.1 gauss); errors were typically 40° for 0.4-gauss fields.
- With the flux valve coupled to the directional gyro, the symptom would be an off-null indication in the control panel. This system would not slave so as to correct the error despite a long wait (the error referred to in the note above is the amount of manual correction required to re-null).
- With frequency shift applied to the test signal, the steady "off-null" indication would be modulated at the shift rate.
- Near particular frequencies such as 100 Hz, 167 Hz, and so on (related by integer ratios to the 800-Hz fundamental output frequency of the flux valve), a beat-frequency oscillation of the annunciator often resulted.
- Some mitigation was obtained by shielding the flux valve with a 0.5-in.-thick aluminum enclosure. This provides eddy current shielding, more effective as frequency and enclosure dimensions increase. At 150 Hz, the incident field required for a given error level was only doubled.
- Self-contained airplane magnetic compasses (used as backup systems in case of loss of all power) were much less susceptible to ac fields up to at least 1 gauss, maintaining their average indication even if fluctuating, with frequency shift applied.

7.3 IMPACT OF SANGUINE SYSTEM ON NAVIGATION

The results of the extended investigation detailed below indicate that there is no potential problem for airplanes flying at any altitude over the site.

This reasoning is the collective impact of the following statements:

- The maximum field level at altitudes over 200 ft is expected to be less than 0.03 gauss*. At normal cruise altitudes, the field would be truly negligible.
- Some magnetic shielding must be attributed, at ELF, to the airplane wing (although not as much as the approximate 20 dB attributed to an aluminum airplane fuselage).
- Without any shielding, an incident field at the flux valve assumed horizontally polarized in the worst-case east-west direction could result in an error of as much as 3° in the flux valve output for the period the airplane was exposed to this level. This error would only occur at 200 ft altitude or less.
- At the rate of 1° per minute, the maximum heading reference change (if the system were left to synchronize itself) would be only 3°. This would only occur if the course were such that the interfering field were maintained in amplitude and direction for this time. After removal from the field, correction would occur.
- The amount of deflection on the annunciator for a 3° error is noticeable, but because of its short duration it is unlikely that the pilot would resynchronize the system (by commanding fast slaving) and thus introduce a step 3° error rather than the cumulative one in the note above. Even if the pilot made the erroneous correction, as soon as the extraneous field reduction occurred, a new off-null condition would arise and he would re-correct it.

It should be emphasized that the case chosen is a combination of hypothetical worst-case conditions not at all representative of typical situations. Yet resultant system changes are less than those due to typical anomalies in the earth's field and results of aircraft maneuvers.

Errors between flux valve and directional gyro headings which appear on the annunciator occur in flight for various reasons and are often larger than the 3° referred to. Causes of these errors include erroneous output of flux

---

*The worst-case number refers to the influence of a single conductor carrying 1,000 amp with the field computed 200 ft away and without considering the cancellation effect of any return current. In a grid antenna system, the separation is likely to be such that at 200 ft altitude, the worst-case field is that due to a conductor vertically below. SANGUINE system design is unlikely to involve currents as large as 1,000 amp in single conductors, so an extreme case is being cited. As shown in section 5.0 of this report, figure 10, the field at 200 ft altitude is more likely to be 1.6 mgauss above a conductor carrying 50 amp as part of a "grid."

valves due to displacement from horizontal during turns,* effects of turbulence, and gimbal errors found in unstabilized directional gyros. To quote reference 6: "Inflight-experience.....has indicated accuracies within two to five degrees..... are common."

A somewhat far-fetched case could be made that problems would arise if an airplane were being checked during preflight while parked directly over a buried antenna. In this case, using the 1,000-amp example cited, the field at the wing tip might amount to 300 mgauss, and difficulty would be encountered by the ground crew in initially synchronizing the system. However, it is presumably not contemplated that such a conductor would be buried directly under an airport.

It should also be noted that engineers familiar with compass systems have no record of preflight problems attributable to 60-Hz power wiring outside the airplane.

7.4 FURTHER TESTS

7.4.1 Introduction

The data summarized above (much of which was reported in monthly reports 11 and 12) are sufficient to indicate the order of magnitude of the field levels required for errors in the flux valve output, but do little to explain the phenomenon. There is also the possibility that, due to the complex factors involved, the "worst case" might not have been uncovered. Further, more sophisticated means of mitigation than using heavy aluminum boxes as shields might be desired if there were operational problems. It is concluded that there are no potential operational problems; however, this conclusion was reached only after the additional investigation reported in this section.

Thus, a fairly detailed experimental investigation was performed, one step supporting another as system characteristics were better understood. To follow the course of these tests requires some description of the flux valve principle.

7.4.2 Flux Valve Operation

References 6 to 12 give detailed background from which much of this description is taken. A three-branched magnetic core (120° between branches) is mounted pendulously in the horizontal plane, usually in the wing. A common 400-Hz excitation winding excites each core in the fashion shown in figure 19. The output winding for each phase has (at least, in principle) negligible 400-Hz output because the 400-Hz inductions are in opposition for this winding. The excitation saturates the core over part of the cycle. During such times, the

---

*The difference between flux valve instantaneous heading output and gyro during turns can be much larger than 3°, but the system error is limited by the slaving rate.

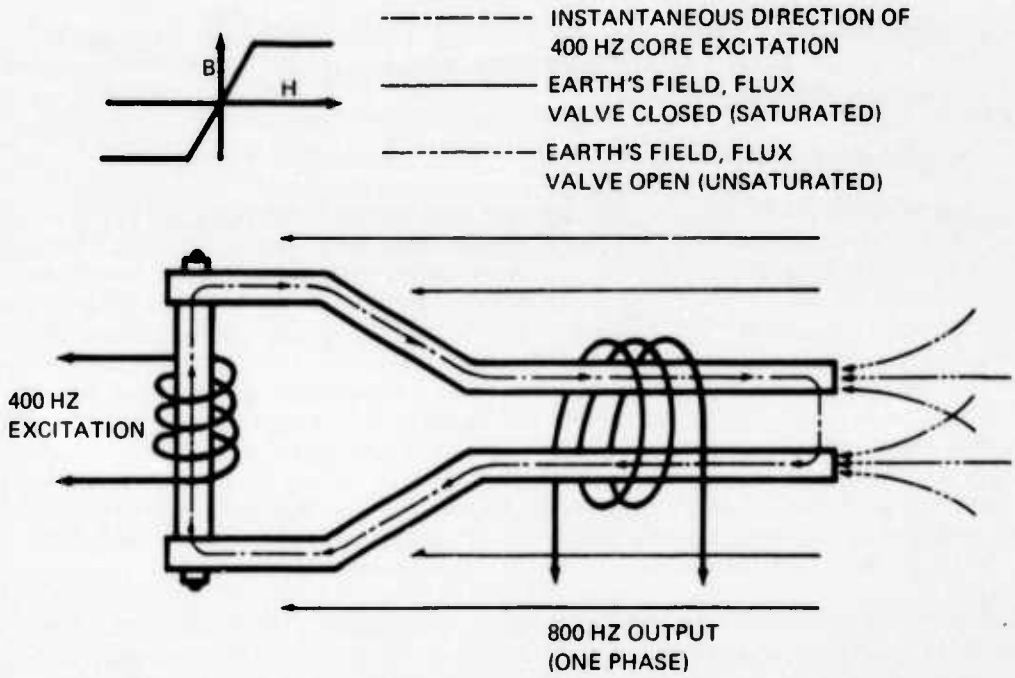

(DIAGRAM SHOWS ONE LEG AND COMMON EXCITATION WINDING OF 3 LEGGED CORE)

Figure 19. Flux Valve Principles

earth's field component along the axis of the branch has no effect on the core. During the rest of the cycle, the earth's field component contributes to the flux in the cores, as shown by the paths --------- , and the resulting 800-Hz voltage induced in the pickup winding has an amplitude related to that of the earth's field component and a phase depending on its direction. By combining the output of the three cores and synchronously demodulating, the direction of magnetic north can be sensed and presented in angular form relative to airplane heading.

The demodulation is accomplished in the compass coupler. Outputs from the coupler (stabilized by gyro heading information) supply flight instruments and flight control systems.

The flux valve is compensated for fixed and determinable errors when it is installed. This compensation is accomplished by injecting small amounts of dc into the windings.

A very crude analysis of the core operation can be performed using analytical representations of the core characteristic of figure 19. It can be shown that, if a sinusoidal interference component is present in addition to the dc component (earth's field) in the two branches in the same direction, products result which sinusoidally modulate the 800-Hz output at the interference frequency. Second harmonics of the interference frequency are also produced. Significantly, no change results in the basic carrier output (800 Hz), although a whole series of sidebands are produced.

It is apparent that nearby ac power wiring in the airplane (containing 400-Hz, and, usually, harmonic currents) can produce fields at the flux valve which would likely lead to errors.

7.4.3 Test Configuration

The block diagram of figure 20 and the photographs of figures 21, 22, and 23 illustrate the arrangement used in the supplementary tests. It will be noted that this arrangement did not include a directional gyro, and that headings were read out on an angle position indicator rather than on a flight instrument. This arrangement simulates the Boeing 747 navigation system rather than the one more frequently used in 707 airplanes, in that the test box provides a simulation of inertial navigation heading inputs. The tests described in monthly report 11 used a directional gyro, and simulated the Sperry C6-E compass system. In this system, the same type of slaving occurs to update the gyro output to correspond with magnetic information, but is physically accomplished in the compass indicator instrument rather than in the coupler. So far as the demonstration of flux valve behavior is concerned, there is no essential difference and the Boeing 747-type test equipment was more readily procured.

Figure 21 illustrates the overall test arrangement. Left to right are the test coil (rotatable in the earth's field by moving the wooden cart), sources of ac and dc coil excitation, an oscilloscope for monitoring test points in the compass coupler, and other system components enumerated in figure 22.

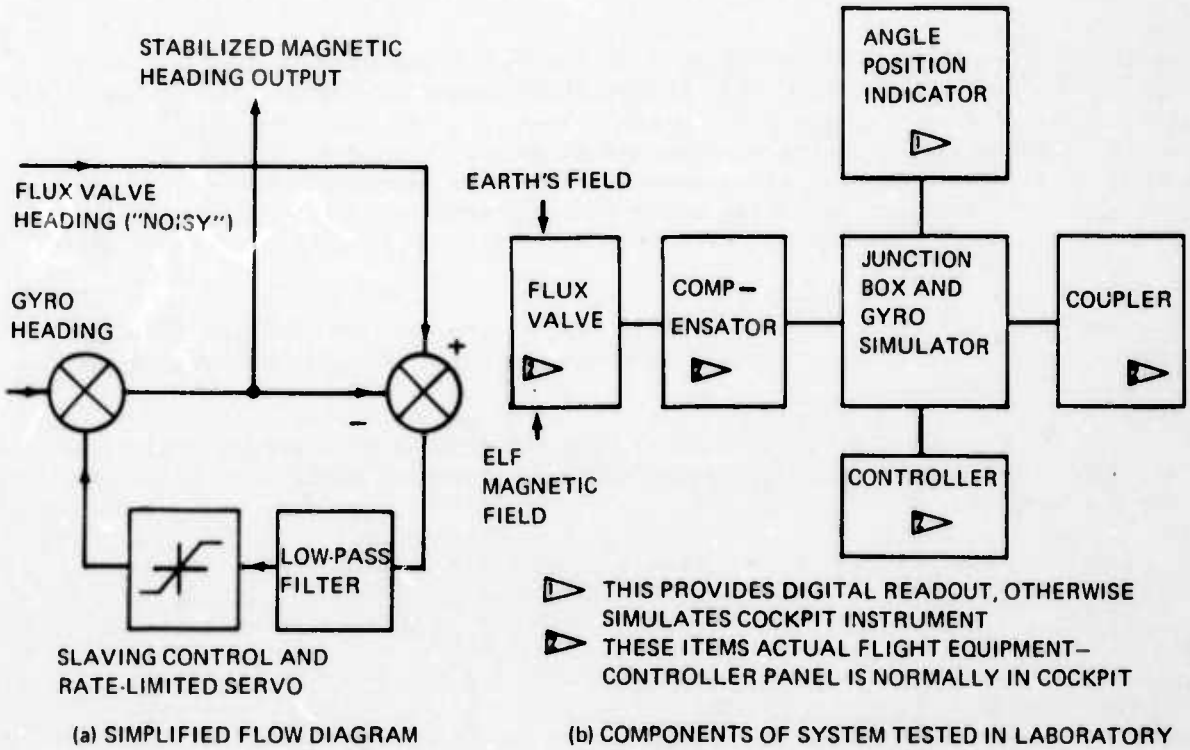

Figure 20. Compass System Block Diagrams

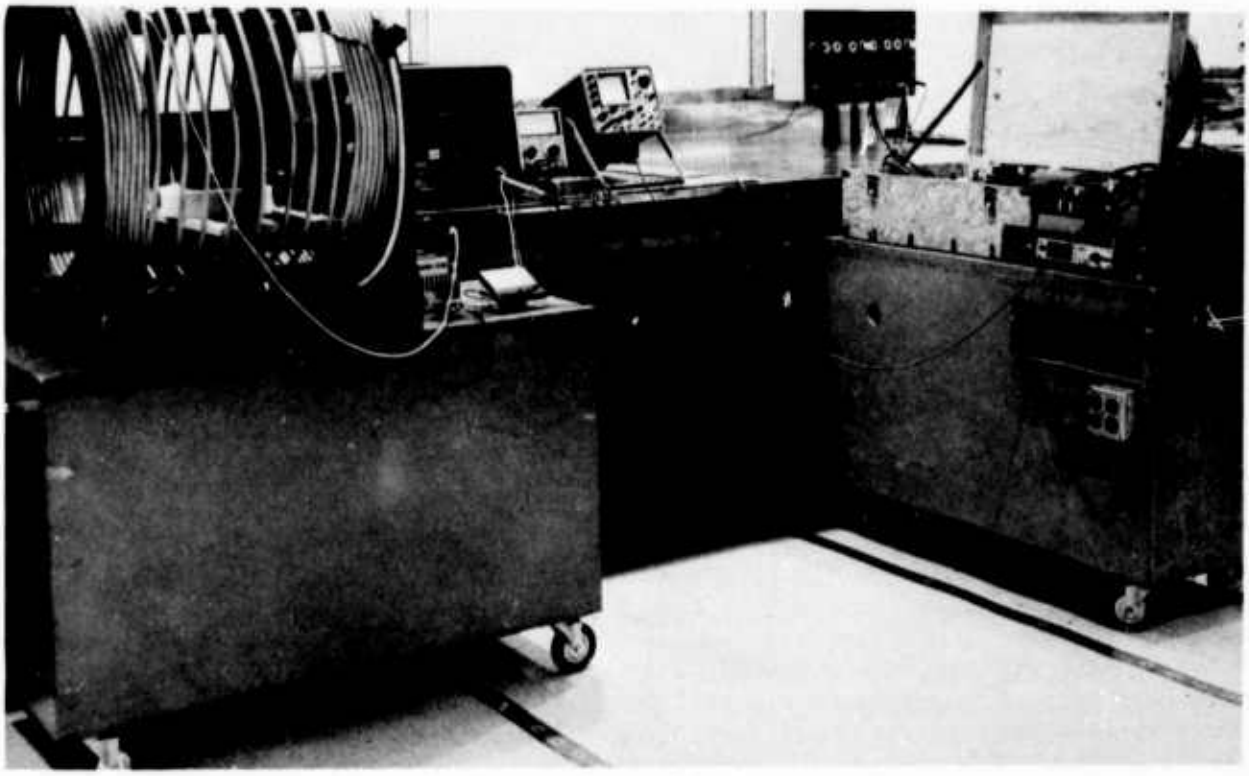

Figure 21. Compass System Test Arrangement

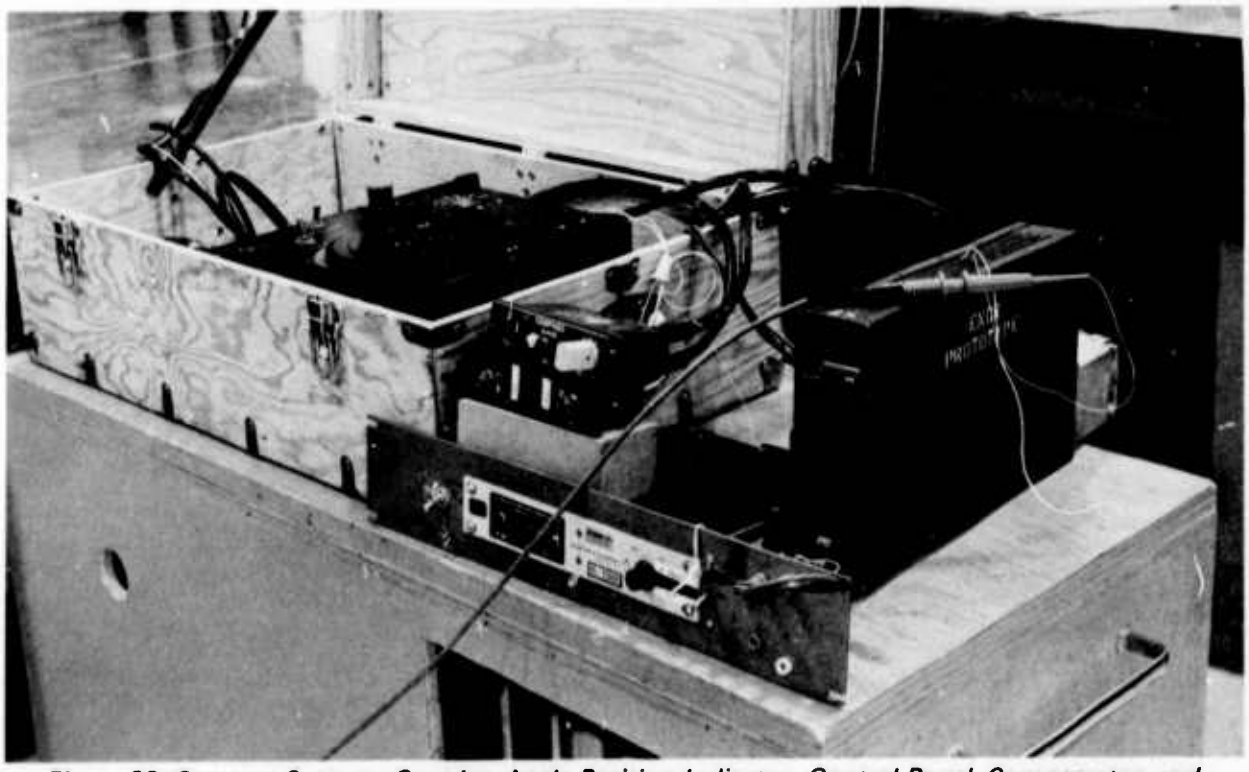

Figure 22. Compass System—Coupler, Angle Position Indicator, Control Panel, Compensator, and Inertial Navigation System Simulator

Figure 22 shows all the components needed to complete a test system to evaluate flux valve susceptibility. The compass coupler (on the right) was modified (for test purposes) to bring out certain circuit card points for connection to an oscilloscope probe.

Figure 23 illustrates the flux valve inside the test coil and a means of providing a small dc field (circulating battery current through coil) or small ac field (audio-oscillator current).

7.5 TEST RESULTS

7.5.1 Effects of Small DC Fields on Overall System

The application of fields as low as 0.06 gauss (dc) caused an error up to 5°. No error occurred when the axis of the coil was north-south, since this merely modified the apparent amplitude of the earth's field. The null indicator, as expected, showed left or right deflection according to the polarity of coil current at a fixed axis orientation. With any fixed polarity of coil current, the null indicator error direction was consistent no matter in which direction the flux valve was turned (to simulate airplane heading). This behavior, at small dc fields, is apparently correct since the effect is presumed to be a change in resultant vector field (earth plus applied), to simulate a new direction for north relative to the coil axis.

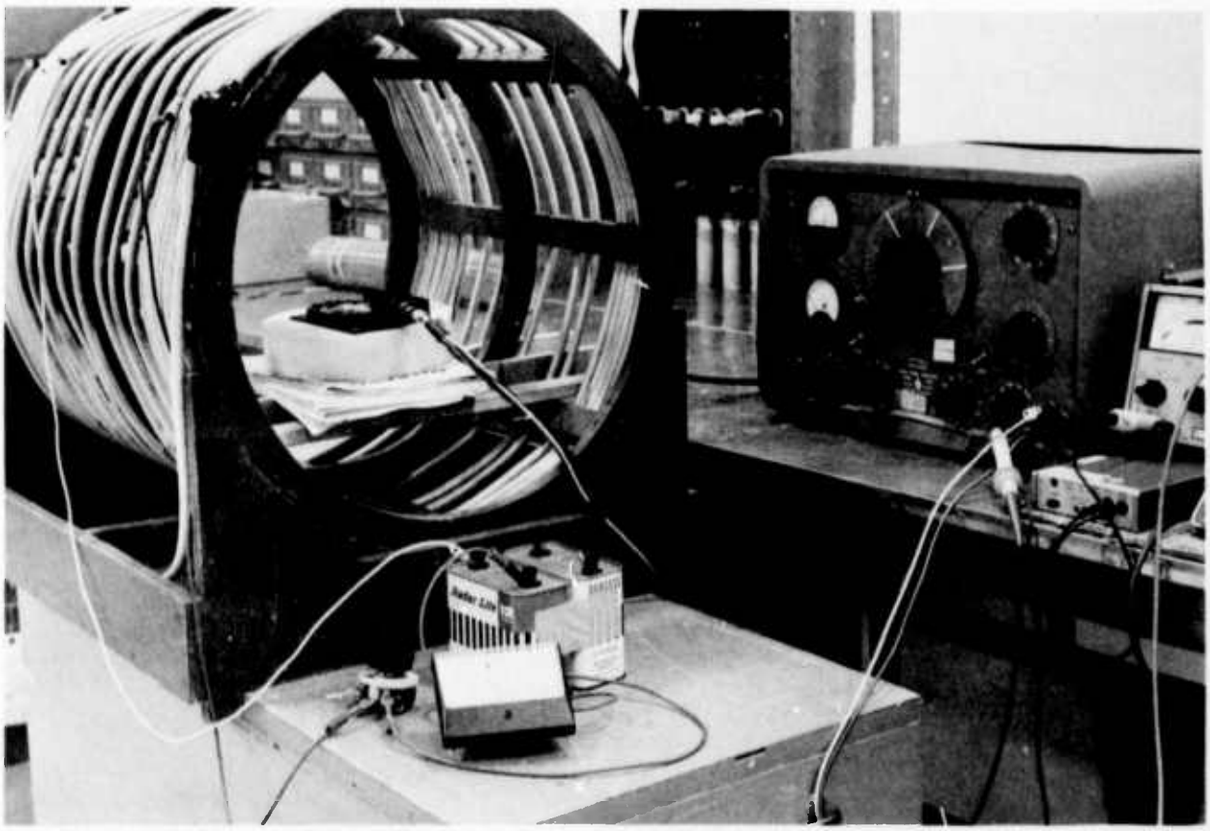

Figure 23. Flux Valve in Test Coil–DC Field Applied

The apparent direction of magnetic north having been changed by the dc field, either the system could be allowed to slave to resynchronize itself (which occurs in a minute or two), or could be manually corrected by commanding fast slaving in the appropriate direction to re-null. Either way, the final bearing readout was the same. Typically, a field of 0.05 gauss, at an angle less than 90° to north, yielded a 5° error.

Anomalous behavior was detected with one compass coupler unit; with one direction of applied dc field, the system would resynchronize; in the other direction, it would slave in the wrong sense and increase the error indefinitely. On the other hand, this same coupler behaved correctly if the flux valve were incrementally displaced about its vertical axis in the earth's field alone; it also responded correctly to manual inputs on the control panel. This symptom occurred only for small dc fields; larger dc fields (comparable to the earth's field) produced a response that was correct in that the system recognized the imposed field as the earth's field.

The anomalous behavior is closely related to a type of error (discussed in ref. 6) encountered during mechanical oscillation of the flux valve. In this particular case, the compass coupler itself probably had offset errors, although the error during oscillation in flight does not require an internal offset or asymmetrical condition in the compass coupler amplifiers. Subsequent problems with the compass coupler revealed that it was defective, so that in tests performed later with ac fields a more satisfactory coupler unit was used. The particular symptom--of slaving continuously in the wrong sense--is given some note here only because it is often observed during the application of alternating, SANGUINE-system-type fields to the flux valve.

Tests with dc fields were abandoned as being no longer productive after these investigations. However, a purpose had been served of becoming acquainted with some of the peculiarities of errors in static fields before proceeding to dynamic ones.

7.5.2 Effects of AC Fields on Overall System

For applied fields other than north-south greater than a threshold value of 0.007 gauss (at a representative frequency of 54 Hz), the system starts to slave slowly in one consistent direction; the null indicator shows no error at such low fields. (This was established as being due to inertia; at frequencies such as 1 Hz, the annunciator follows the field reversals.) More rapid slaving occurred at applied field levels such as 0.02 gauss. (In a complete operational system, as noted earlier, the gyro cannot be precessed more than 1° per minute.)

The cause of the unidirectional slaving was tentatively identified in this case by examining the waveforms inside the compass coupler. (Figure 21 illustrates the temporary connections to an oscilloscope.) After the flux valve input is applied to a control transformer, the resultant waveform is fed through an isolating amplifier to the demodulator. The isolating amplifier saturated on one side of the 800-Hz waveform, which was amplitude-modulated by the interference frequency (this form of output was predicted in 7.4.2 above). Only a very limited dynamic range appeared to exist.

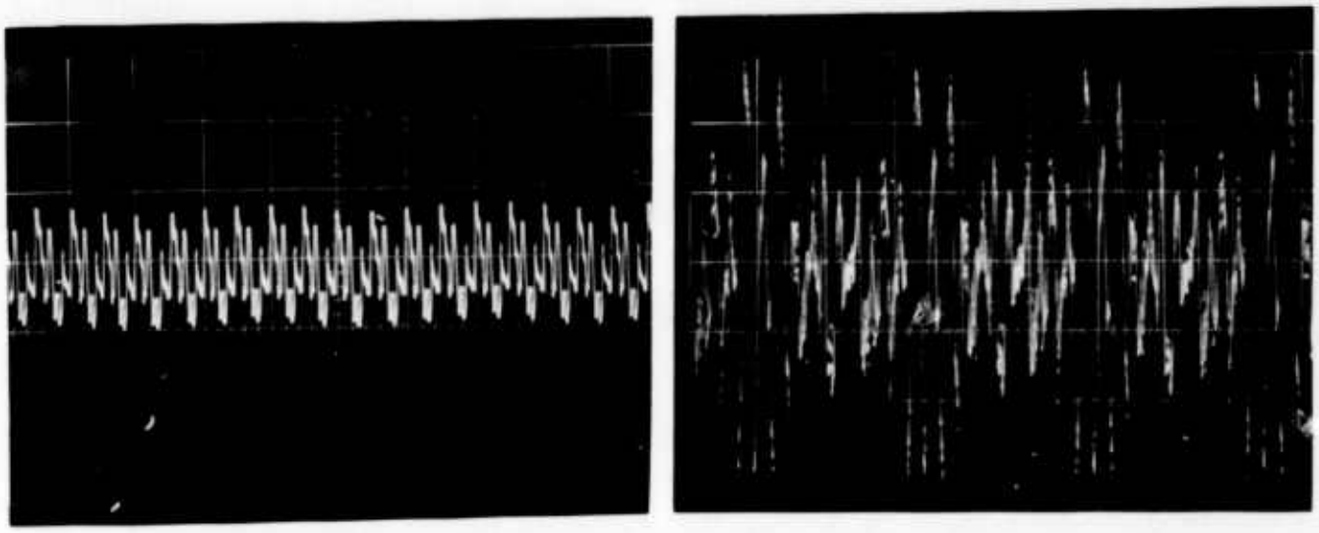

(a) TYPICAL CONDITION WHEN SYSTEM APPROACHES NULL.

(b) SAME AS (a), BUT 0.05-GAUSS FIELD AT 90 HZ APPLIED EAST-WEST. ISOLATION AMPLIFIER OUTPUT IS CLIPPED ON THIS INPUT.

SCALES: 500 μSEC/IN., 10 mV/IN.

Figure 24. Airplane Compass System—Oscillogram of Input to Isolation Amplifier Derived from Flux Valve Control Transformer

Figure 24 compares the input to the isolation amplifier before and after application of a 0.05-gauss interference field.

At large ac fields, greater than about 1 gauss, the system hunts in random directions to seek a null. Little or no deflection of the annunciator occurs, except when the applied frequency is integrally related to the excitation frequency, such as 200, 267, 400, 533, and 800 Hz. (In a complete operational system which included a gyro there was an off-null indication, as described.)

With ac fields applied, it was possible to test the analysis of core behavior. A Fairchild EMC-10 interference analyzer was connected line-to-line by specially fabricated breakout connections to the flux valve output, without disconnecting it from the compass coupler. The analyzer was tuned to the fundamental 800-Hz output, which is on the order of 100 mv at the azimuth of the flux valve which maximizes it. The output is nulled 90° away. Field levels up to 5 gauss had little effect on the maximum output (about 10%) but lessened the sharpness of the null. The sidebands (800 Hz plus or minus integers of the interfering frequency) were detectable on the EMC-10. The compass coupler does not have a bandpass filter to restrict the input to isolation amplifier and demodulator to the 800-Hz region only; thus, the modulation of the interfering field is seen in figure 24.

It is concluded that since the flux valve appears to be essentially linear in transfer characteristics, even when large ac fields are applied, the best approach to mitigation--if this were needed--would be to linearize the compass coupler input. This could be done by minimal redesign of the isolation amplifier for a dynamic range several times the earth's field requirement, or by installing an 800-Hz bandpass filter ahead of this stage. Reference 6 contains some discussion on two types of error encountered in flight which are relevant:

- If slaving rates for positive and negative errors differ due to such factors as unbalance in push-pull slaving amplifiers then with an oscillatory component of flux valve output due to vibration etc., causing periodic departure from horizontal, an error can develop because the resultant null is displaced from the one corresponding to an undisturbed flux valve.
- With large-amplitude mechanical oscillations of the flux valve, and the superimposed gyro drift which occurs in flight, even a coupler system that had perfect symmetry and thus equal positive and negative saturation inputs would produce an error. This is because an equilibrium condition between the unequal positive and negative amounts of slaving is reached, which corresponds to a greater error than that due to gyro drift, and in the same direction. (This process can be visualized in terms of the increase in dc unbalance in a push-pull amplifier stage when a symmetrical waveform drives the amplifier).

Since the mechanical oscillation of flux valves about the horizontal produces electrical oscillations (modulation of output), the types of error referred to above are really the same as those resulting from ELF alternating magnetic fields impinging on static flux valves. The analogy is limited because the mechanical oscillations are limited in frequency. The dynamic range or value of saturation input, and the stability with which it is centered about zero, is the characteristic in question for the compass coupler. Design improvements discussed by Sperry in reference 6 have the objective of minimizing errors in typical flight. Design for optimized behavior in strong ELF fields may well require different parameters. As stated earlier, the flux valve installation is made so as to avoid this problem.

It should also be noted that when the ac field is north-south, as with the dc field, minimal disturbance of operation of the flux valve was observed. The susceptibility of the wiring from flux valve to compass coupler to injected ELF as low as 50 mv (table 2) is not surprising in view of the isolation amplifier behavior. However, since twisted (and, incidentally, shielded) wiring is used in the airplane installation, any potential problems would be attributable to SANGUINE system fields at the flux valve rather than voltages induced on the wiring.

7.6 CONCLUSIONS

From the work reported in monthly reports 11 and 12 and the additonal tests and analysis reported here, it is concluded that:

- Compass systems for airplanes flying over the SANGUINE site will not be affected. (Note, however, that only the type of sensor in most common use has been tested. Slightly different principles are used in systems of other manufacturers.)
- The initial alignment of an airplane compass system would be a problem only if the airplane were virtually parked over the buried antennas.
- Mitigation, if ever required, would be fully successful only if the compass coupler circuitry were modified.

8.0 GROUND EQUIPMENT ENVIRONMENT MEASUREMENTS

As reported in detail in monthly report 11, surveys were made at three Seattle-area FAA air traffic control installations to determine the level of ambient power frequency fields which represent the environment in which the equipment performs satisfactorily. As with any such undertaking, we can only summarize in terms of maxima and averages, and add a caution to the effect that this is not necessarily representative of a larger population.

The highest level encountered in an equipment area was 22 mgauss. This represents the root of the sum of the squares of horizontally and vertically polarized components at 60, 180, and 300 Hz, which are the predominant contributions to an overall spectrum of H-fields up to 25 kHz, since harmonic amplitude diminishes rapidly with increasing order. Considering the 60-Hz components alone, the highest level would have been 15 mgauss (the highest level encountered in a nonequipment area was 62 mgauss, 2 ft in front of a large power transformer in a substation).

The average for all readings in the equipment areas was 1.7 mgauss for the 60-Hz field components (root of the sum of squares of horizontally and vertically polarized values, the former being in the direction for maximum).*

It is estimated that the representative environment at ELF due to power frequency current-carrying conductors is 3 mgauss.

For SANGUINE system purposes, it may be stated that location of ATC facilities (including sophisticated installations with displays) within distances from the antennas where the SANGUINE system field would be 3 mgauss would cause no problems whatsoever, and while "environment" would be more intense than "representative," ATC installations with 20 mgauss SANGUINE system levels should not encounter equipment problems due to the field. It is assumed the incoming power and telephone circuits would be mitigated to the level relevant for the most susceptible ground equipment. Insufficient data are available to state with certainty whether the mitigation levels now contemplated are sufficient to take care of all air traffic control equipment at the interface with power and telephone lines.

---

*The survey used a loop antenna approximately 20 in. in diameter. A survey with a smaller sensor would undoubtedly have uncovered points where fields were larger, but localized to power wiring, etc. It is more meaningful to obtain an environment averaged over equipment-sized dimensions.

9.0 RESULTS AND RECOMMENDATIONS FOR CONTINUED RESEARCH

9.1 STUDY RESULTS

A summary of study results follows:

In-depth testing of representative "safety-of-flight-critical" avionics demonstrates that, except for two categories of equipment noted below, a large safety margin (one order of magnitude or more) exists between the ELF field strengths (30 mgauss) anticipated from a SANGUINE system and the susceptibility thresholds of the equipment tested.

Systems using cathode-ray tubes (CRTs) as display elements are an order of magnitude more susceptible to ambient ELF fields than are the majority of avionics systems. However, the margin of protection for such equipment when airborne is still very high--20 dB or more between anticipated SANGUINE system field strengths and the threshold of susceptibility of CRTs. (MIL-E-6051D, a military EMC specification, requires a minimum demonstrated 6-dB "safety margin" for critical systems.)

Magnetic field sensors (flux valves) of airplane compass systems evidenced susceptibility to very low ambient field levels in the ELF region, i.e., levels of magnitude that might readily be encountered in the immediate vicinity of a SANGUINE system antenna. However, from a consideration of total system operational characteristics (chiefly the inertia or inability of associated components to respond to very rapid changes) there is substantial protection against significant errors in airplane navigation. This is true even under the worst-case assumption of an airplane flying at a very low altitude (200 feet) over a SANGUINE system antenna element. Difficulties may be encountered, however, in synchronizing a Gyrosyn (Sperry Rand) compass system on the ground, if the airfield is located over an antenna wire, a situation of extremely low probability.

Ground-based air traffic control equipment operates satisfactorily in an ELF magnetic environment (60 Hz) whose strength is equal to or greater than that close to a SANGUINE system antenna, although the latter is at a different frequency. Only equipment using CRTs or scan converters was adversely influenced by fields of magnitudes similar to those very close to a SANGUINE system antenna. Again, this would pose a problem only if the ground control installation were virtually on top of a SANGUINE antenna.

Limited and preliminary testing was performed on ground equipment at an air traffic control center for susceptibility to ELF signals injected or superimposed on incoming power and telephone lines. Though admittedly inconclusive, test results suggest that the mitigation criteria currently envisioned by other investigators for protection of personnel and commercial equipment are also adequate for air traffic control installations.

9.2 RECOMMENDATIONS FOR CONTINUED RESEARCH

To resolve marginal or questionable areas of extreme susceptibility to ELF fields, the following areas of continued research are recommended as a minimum:

1) Investigation of airplane compass systems other than the Sperry type tested
2) Further investigation of susceptibility of ground-based control equipment to ELF voltages superimposed or injected on incoming power and telephone lines
3) A study of the potential effects of SANGUINE system fields on light airplane avionics
4) A more detailed "refined" analysis of fields near a SANGUINE system antenna, including earth-return currents and earth ionosphere cavity excitation, but only if higher antenna currents are considered
5) Extension of airframe ELF shielding measurements to airplanes other than the Boeing 747 and 737, specifically including equipment locations

Research on the first item will be greatly expedited by the extensive study already performed and described herein on a system employing a Sperry flux valve (or flux gate). Insights gained in the study will permit the timely disclosure of compass system susceptibilities to a SANGUINE system field and will enable the development of mitigative procedures as required.

Continued investigation on the second item will profit greatly by use of a "susceptibility voltage tester" perfected at the close of this study (described in section 3.1.1). This device is based on similar items used in routine electromagnetic compatibility testing of avionics, modified to the ELF requirements of this study. It will enable injection of controlled ELF voltages into incoming power and communication lines common to ground-based groups of control equipment, and afford isolation to signals already contained in those lines. (This is accomplished essentially through the use of large, balanced transformers in opposition, and a dummy load equal in impedance to that of the equipment under test.)

The third item is to provide assurance that nothing of significance has been overlooked in the extrapolations of section 4.5 of this report, to cover this case. While avionics equipments for light aircraft must comply with FAA requirements--and are therefore to some extent electromagnetically compatible--they tend to be less sophisticated than those tested to date.

REFERENCES

1. *Environmental Compatibility Assurance Program (ECAP) Status Report,* Department of the Navy, Electronic Systems Command, December 1970

2. R. D. Teasdale, "Magnetic Alloy Shields for Color Television Tubes," *Proc. National Electronics Conference,* Chicago, 1953

3. *Electromagnetic Shielding Design Manual,* Magnetic Metals Company, Camden, New Jersey, 1969

4. *Designers Handbook--The When, Why and How of Magnetic Shielding,* Westinghouse Metals Division, Blairsville, Pennsylvania, 1966

5. D. G. Fink, *Television Engineering Handbook,* McGraw-Hill.

6. *Compass System Errors and Compensation Techniques: Introducing the Pre-Indexed Pre-Calibration Flux Valve,* Sperry Rand Technical Newsletter, Field Engineering, TA-595-TN-1, Revision 2, Sperry Flight Systems Division, Phoenix, Arizona, October 1969

7. *Overhaul Manual, Magnetic Field Sensor, Part No. 2591438-901,* Publication No. 15-3141-12, Sperry Flight Systems Division, Phoenix, Arizona

8. *Overhaul Manual, Compass Coupler, Part No. 2591201-901,* Publication No. 15-3131-02, Sperry Flight Systems Division, Phoenix, Arizona

9. U.S. Patent 2,476,273, July 19, 1949

10. U.S. Patent 2,383,460, August 28, 1945

11. U.S. Patent 2,047,609, July 14, 1936

12. U.S. Patent 2,383,461, August 28, 1945

APPENDIX A

The following is a list of publications which have been reviewed for pertinence to this study.

Abraham, L. G., Jr., "Aspects of Terrestrial ELF Noise Spectrum When Near the Source or its Antipode," *Radio Science J. Res.*, NBS/USNC-URSI, Vol. 69D, No. 7, July 1965

Alpert, Y. A., et al., *Propagation of Low-Frequency Electromagnetic Waves in the Earth-Ionosphere Waveguide*, AD665 698, N68-21354, Akademia Nauk USSR, Moscow, 129 pages, Trans 1967

Bahar, E., "Propagation of VLF Radio Waves in a Model Earth-Ionosphere Wave Guide..," *Radio Science*, Vol. 1 (New Series) No. 8, August 1966

Bahar, E., "Model Study of Ionosphere Perturbations and Propagation of RF Between Two Sites," AD813 917, X67-19921, 5 pages, April 1967

Berry, L. A., and M. E. Chrisman, "The Path Integrals of VLF Wave Hop Theory," *Radio Science J. Res.*, NBS/USNC-URSI, Vol. 69D, No. 11, November 1965

Bitterlich, Dr. W., *Determination of Rock Conductivity from VLF-Propagation Measurements*, Technical Note No. 3, AFCRL-63-383, AD420 597, July 1963

Brock-Nannestad, L., *EM Phenomena in the ELF Range; Natural Background Noise and Instrumentation for its Measurement*, AD472 613, 93 pages, June 1965

Budden, K. G., "The 'Waveguide Mode' Theory of the Propagation of Very-Low Frequency Radio Waves," *Proc. IRE*, June 1957

Burgess, B., "Propagation of VLF Waves Under Disturbed Conditions," *Radio Science J. Res.*, NBS/USNC-URSI, Vol. 68D, No. 1, January 1964

Burgess, B., *The Influence of Propagation Conditions on the Design of VLF Radio Wave Long Range Navigation*, X66-14503, 26 pages, October 1965

Carson, J. R., "Wave Propagation in Overhead Wires with Ground Return," *Bell System Tech. J.*, Vol. 5, 1926, pp 539-554

Carter, R. O., "The Mutual Impedance Between Short Earth-Return Circuits," *J. IEEE*, Part I, Vol. 93, 1946, pp 275-277

Chapman, F. W., and R. C. V. Macario, "Propagation of Audio-Frequency Waves to Great Distances," *Nature*, May 19, 1956

Crain, C. M., and H. G. Booker, "The Effects of Ions on Very Low Frequency Propagation in an Abnormally Ionized Atmosphere," *J. Geophys. Res.*, Vol. 69, No. 21, November 1, 1964

Crombie, D.D., and A.G. Jean, *The Guided Propagation of ELF and VLF Radio Waves Between the Earth and the Ionosphere,* Central Radio Propagation Laboratory, NBS, Boulder, Colorado

Egeland, Alv, *ELF (500-1000) CPS Emissions at High Latitude,* Kiruna Geophysical Observatory, Kiruna, C Sweden

Egeland, Alv, et al., *Measurements of the Earth-Ionospheric Cavity Resonance Frequencies at High Latitudes,* Report No. N66-29259, AF61(052)811, 42 pages, February 21, 1966

English, W. N., et al., *Equipment for Observation of the Natural Background in the Frequency Range 0.01-30 Cycles per Second,* AD 450 173, Reprint 6103, Pacific Naval Laboratory, Esquimalt, B. C., June 1961 (a reprint of a paper presented at the Instrument Society of America Conference)

Foster, R. M., "Mutual Impedance of Ground Wires Lying on the Surface of the Earth," *Bell System Tech. J.,* July 1931, pp 408-419

Galejs, J., "On the Terrestrial Propagation of ELF and VLF Waves in the Presence of a Radial Magnetic Field," *Radio Science J. Res.,* NBS/USNC-URSI, Vol. 69D, No. 5, May 1965

Galejs, J., "ELF and VLF Fields of a Horizontal Electric Dipole," *IEEE Trans on Ant. and Prop.,* Vol. AP-16, No. 6, November 1968

Galejs, J., *ELF and VLF Fields of a Horizontal Electric Dipole,* AD672 548, Sylvania Electronics Systems, July 1968 (expanded version of the above paper)

Galejs, J., *Terrestrial Extremely-Low-Frequency Propagation,* Sylvania Electronics Systems, Waltham, Mass. (a 55-page report containing extensive bibliography)

Galejs, J., *Near Fields and Antipodal Fields in the Terrestrial Earth-to-Ionosphere,* AD679 164, N9-16826, 36 pages, November 1968

GiaRusso, D. P., and J. E. Bergson, *Studies of VLF Radiation Patterns of a Dipole Immersed in a Lossy Magnetoplasm,* D1-820797, Boeing Scientific Research Laboratories, March 1969

Gibbons, J. J., *The Ionosphere: Propagation Theory,* Pennnsylvania State University, Ionosphere Research Laboraotory, University Park, Pennsylvania

Gyunnien, E. M., and I. N. Zabavina, "The Propagation of Long Radio Waves and the Nonhomogeneous Ionosphere," *Problems of Wave Diffraction and Propagation,* NASA TTF-591, NASA Technical Translation from the Russian, November 1969*

*This collection of sixteen papers treats the problems of super-long radio waves in the waveguide channel earth-ionosphere. The collection is of interest to those specializing in the field of the radiophysics of radio-wave propagation.

Harrison, R. P., and E. A. Lewis, "A Method for Accurately Measuring the Vertical Electric Field Strength of a Propagating VLF Wave," *IEEE Trans. on Instrumentation and Measurement*, March-June 1965

Higgins, T. P., *Magnetic Compass Deviations Produced by Magnetic Loads*, D1-82-0932, Boeing Scientific Research Laboratories, November 1969

Jean, A. G., et al., "Observed Attenuation Rate of ELF Radio Waves," *J. Res. Nat. Bur. Std.*, Vol. 65D, No. 5, September 1961

Katz, A. H., *Multifrequency Observations of Extremely Low Frequency Electro-Magnetic Radiation*, AD615 972, AFCRL-65-118, March 1965 (35 pages plus extensive bibliography)

Katz, A. H., et al., *Observations of Sub ELF Emissions in the 2-16 Hz Frequency Range*, AD648-716, N67-26746, 60 pages, October 1966

Kellner, Walter, *Electrical Rock Characteristics From the Field Structure of a Magnetic Dipole Immersed in a Conducting Medium*, AD690 167, N69-39993, AFCRL-69-0281, 48 pages, April 1969

Kitchen, F. A., et al., "A Review of Present Knowledge of the Ionospheric Propagation of Very Low- and Low-Frequency Waves," *Proc. IEE*, March 1953

Krakowski, M., "Mutual Impedance of Crossing Earth-Return Circuits," *Proc. IEE*, Vol 114, 1967, pp 253-258

Lacey, L. S., "The Mutual Impedance of Earth-Return Circuits," *Proc. IEE*, Vol. 69, Part 4, 1952, pp 156-167

Large, D. B., and J. R. Wait, "Theory of Electromagnetic Coupling Phenomena in the Earth-Ionosphere Cavity," *J. Geophys. Res.*, Space Physics, Vol. 73, No. 13, July 1, 1968

Liebermann, L., "Extremely Low-Frequency Electromagnetic Waves I: Reception from Lightning," and "...II: Propagation Properties," *J. Appl. Phys.*, Vol. 27, No. 12, December 1956

Liemohm, H. B., *ELF Propagation and Emission in the Magnetosphere*, D1-82-0890, Boeing Scientific Research Laboratories, August 1969

Lokken, J. E., and J. A. Shand, "Man-Made Electromagnetic Interference at Extremely Low Interference," *Can. J. Phys.*, Vol. 42, October 1964

Makarov, G. I., and V. V. Novikov, "Propagation of Electromagnetic Waves in Planes and Spherical Impedance Waveguides," *Problems of Wave Diffraction and Propagation*, NASA TTF-591, NASA Technical Translation from the Russian, November 1969

Morgan, R. R., *World-Wide VLF Effective Conductivity Map*, AD675-771, N69-11499, 63 pages, January 1968

Nessler, Norbert, *Measurement of the Conductivity and Dielectric Constant of a Homogeneous Medium by Means of Wave Propagation,* AD677 587, N69-14172, 24 pages, July 1968

Mott, H., and A. W. Biggs, "Very-Low-Frequency Propagation Below the Bottom of the Sea," *IEE Trans. on Ant. and Prop.,* May 1963

Omura, J. K., *Statistical Analysis of LF/VLF Communication Modems,* AD857 630, X69-19386, 105 pages, August 1969

Pierce, E. T., *The Thunderstorm as a Source of Atmospheric Noise at VLF Frequencies...,* AD854 636, Stanford Research Institute, June 1969

Pierce, E. T., "Propagation of Radio Waves of Frequency Less than IKC," *Proc. IRE,* March 1960

Robinson, N., and U. Valil, *Research on Electromagnetic Noise at Extremely Low Frequencies,* AD39640, AFCRL-64-352, Summary Report No. 1, Technion R&D Foundation, Haifa, Israel, August 1961--May 1963 (a bibliography of papers on the subject for the period shown)

Seeley, E. W., *Optimum Antenna Arrangement for a VLF Vertical-Incidence Ionospheric Sounding System,* NWCCL TP 777, Naval Weapons Center, Corona Laboratories, May 1968

Shaffer, J., et al., *Propagation of Very Low Frequency CW Signals in the Deep Ocean,* AD689 744, Columbia University, Hudson Laboratories, April 1969

Sheddy, C. H., et al., *A Fortran Program for Mode Constants in an Earth-Ionosphere Waveguide,* AD837 562, X68-20099, 64 pages, May 1968

Spogen, L. P., et al., *HF and LF Propagation Models for Interference Prediction,* AD820 109, Bell Aerosystems, August 1967

Wait, James R., "Mutual Electromagnetic Coupling of Loops over a Homogeneous Ground," *Geophysics,* Vol. XX, No. 3, July 1955

Wait, James R., "Expected Influence of a Localized Change of Ionosphere Height on ELF Propagation," *J. Geophys. Res.,* Vol. 66, No. 10, October 1961

Wait, James R., "Transmission Loss Curves for Propagation at VLF," *IRE Trans. on Comm. Sys.,* December 1958

Wait, James R., "Propagation of Very-Low Frequency Pulses to Great Distances," *J. Res. Nat. Bur. Std.,* Vol. 61, No. 3, September 1958

Wait, James R., "A New Approach to the Mode Theory of VLF Propagation," *J. Res. Nat. Bur. Std.,* Vol. 65D, No. 1, January 1961

Wait, James R., "An Analysis of VLF Mode Propagation for a Variable Ionosphere Height," *J. Res. Nat. Bur. Std.,* Vol. 67D, No. 4, July 1962

Wait, James R., "Influence of the Lower Ionosphere on Propagation of VLF Waves to Great Distances," *J. Res. Nat. Bur. Std.*, Vol. 67D, No. 4, July 1963

Wait, James R., "The Attenuation vs Frequency Characteristics of VLF Radio Waves," *Proc. IRE*, June 1957

Wait, James R., "The Mode Theory of VLF Ionospheric Propagation for Finite Ground Conductivity," *Proc. IRE*, June 1957

Wait, James R., and A. Murphy, "The Geometrical Optics of VLF Sky Wave Propagation," *Proc. IRE*, June 1957

Wait, James R., *Survey and Bibliography of Recent Researches in the Propagation of VLF Radio Waves*, National Bureau of Standards Technical Note 58, May 1960

Wait, James R., "Some Remarks on Mode and Ray Theories of VLF Radio Propagation," *Radio Science J. Res.*, NBS/USNC-URSI, Vol. 68, No. 1, January 1964

Wait, James R., Two-Dimensional Treatment of Mode Theory of the Propagation of VLF Radio Waves," *Radio Science J. Res.*, NBS/USNC-URSI, Vol. 68D, No. 1, January 1964

Wait, James R., "Earth-Ionosphere Cavity Resonances and the Propagation of ELF Radio Waves," *Radio Science J. Res.*, NBS/USNA-URSI, Vol. 69D, No. 8, August 1965

Wait, James R., "On the Mode Theory of VLF Ionospheric Propagation," paper presented at Colloque Internationale sur la Propagation des Ondes Radio Electriques, Paris, 1956

Watt, A. D., and R. D. Croghan, "Comparison of Observed VLF Attenuation Rates and Excitation Factors with Theory," *Radio Science J. Res.*, NBS/USNA-URSI, Vol. 68D, January 1964

Waynick, A. H., "The Present State of Knowledge Concerning the Lower Ionosphere," *Proc. IRE*, June 1957

Yabroff, I. W., "Reflection at a Sharply-Bounded Ionosphere," *Proc. IRE*, June 1957

AD 251 074, "Subsurface Propagation Studies," November 1960

AD291 179, Bibliography: "Electromagnetic Phenomena with Special Reference to ELF," September 1962 (over 1,000 entries, most with abstracts)

AD448 427, "Relative Effectiveness of Magnetic Shielding," Minneapolis-Honeywell, June 1964

AD462 719, "Electromagnetic Compatibility of Equipment and Systems," Moore School of EE Report 65-23

AD482 683, "Analytical Investigation of EM Interference Measurements; Susceptibility of Digital Circuits," AFAL-TR-66-117, Technology, Inc., 1966

AD800 090, "Variable-μ Receiver for Measurement of Magnetic Induction Fields; Susceptibility of Integrated Circuits," AFAL-TR-66-281, Electro-Mechanics Co.

AD821 531, "Electromagnetic Compatibility Between the AN/ARC-96 VLF/LF System and OT," Electronics, Comm., Inc., St. Petersburg, Fla., March 1967

Document D2-2302, *Low Frequency Propagation,* The Boeing Company, November 1957

Document D6-4345, *Low Frequency Ground Wave Propagation Analysis,* The Boeing Company, January 1963

Mathematical Note No. 166, *Bibliography and Comments on Important Recent Research in the Field of VLF Propagation,* The Boeing Company, March 22, 1957

Mathematical Note No. 181, *Propagation Characteristics of L-F Communication,* The Boeing Company, October 6, 1957

DASA Report No. 2181, *Effect of Ionospheric Depression on Long-Range Communications at Very-Low Frequencies,* Defense Atomic Support Agency, October 1968

Technical Note 319, *Numerical Values of the Path Integrals for Very-Low Frequencies,* National Bureau of Standards, September 1965

Report No. 801, *An Empirical Study of ELF and VLF Shield Cans,* Navy Underwater Sound Laboratory

Propagation of Radio Waves at Frequencies Below 300 Kc/s, Proceedings of the Seventh Meeting of the AGARD Ionospheric Research Committee, Munich, 1962 (contains 30 papers, 11 on VLF propagation)

APPENDIX B

This appendix consists of a representative set of photographs and schematics relating to the tests summarized in tables 1 and 2.

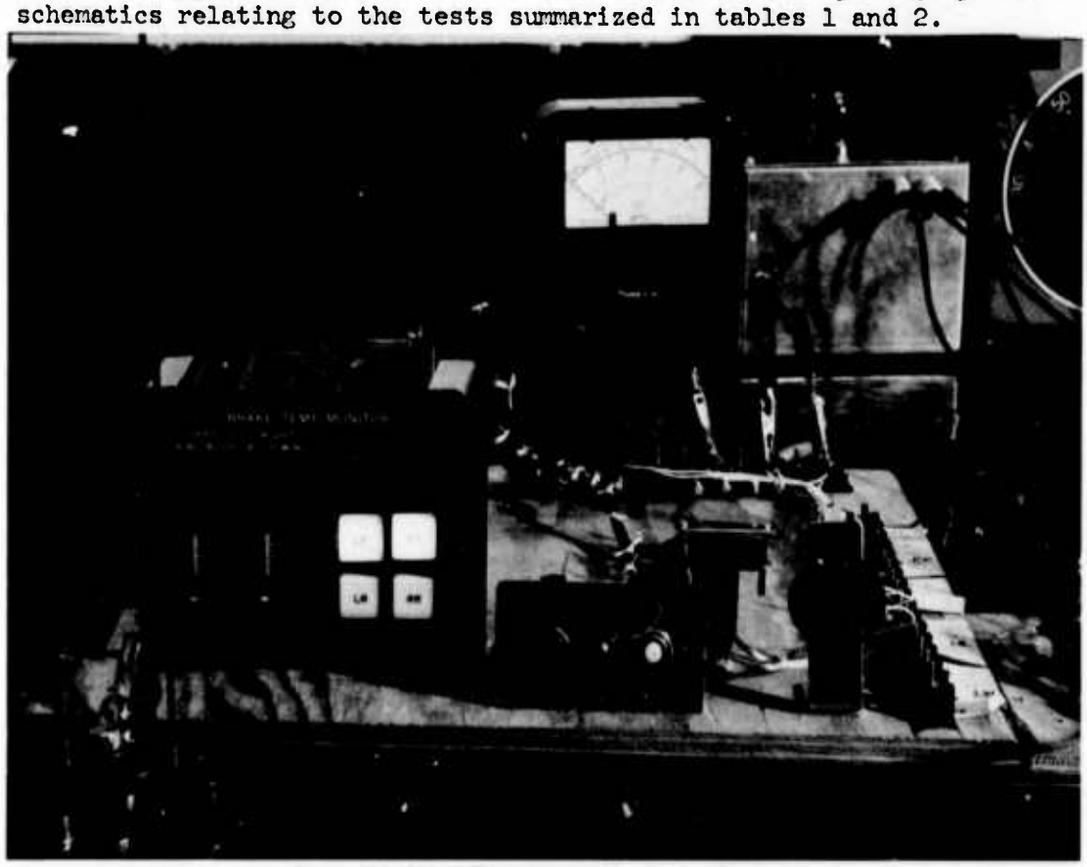

Figure B1. Brake Temperature Monitoring System

Test run at 400° F, sensors heated by attaching electrodes to them and passing current through them (400~); 28 VDC rheostat for lamp brightness.

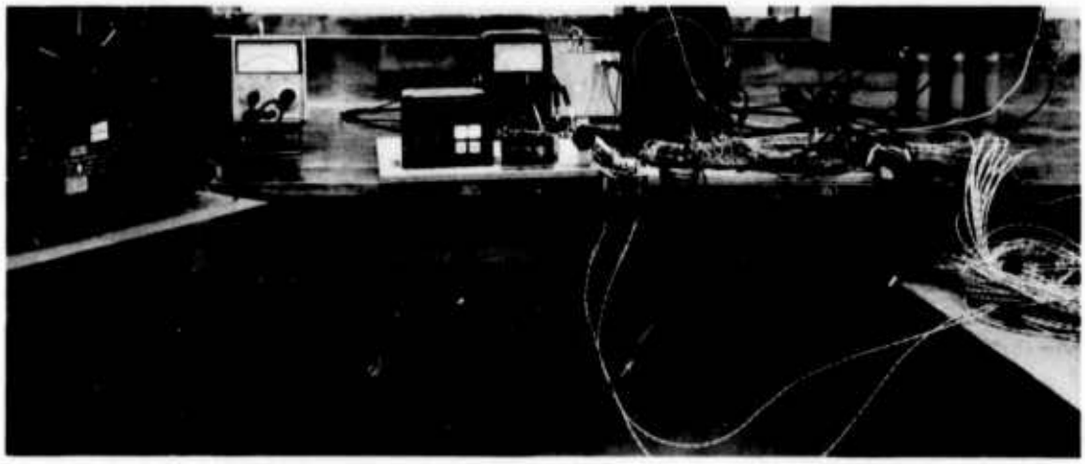

Figure B2. Test Setup for Brake Temperature Monitor (Wire-by-Wire Voltage Injection Test)

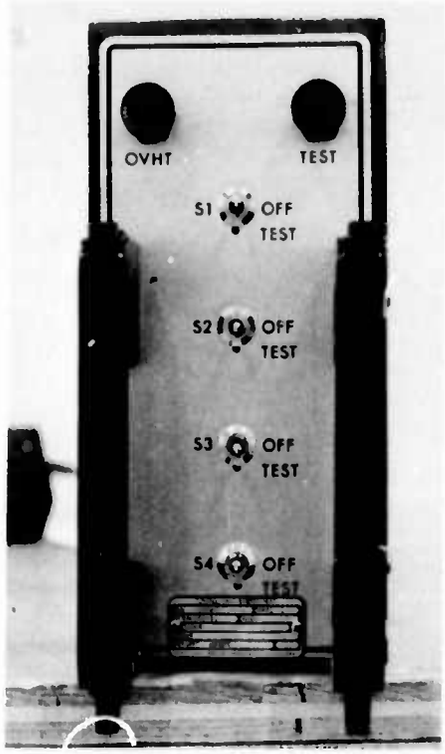

Figure B3. Window Heat Control Unit

Figure B4. Cockpit Voice Recorder and Control Unit

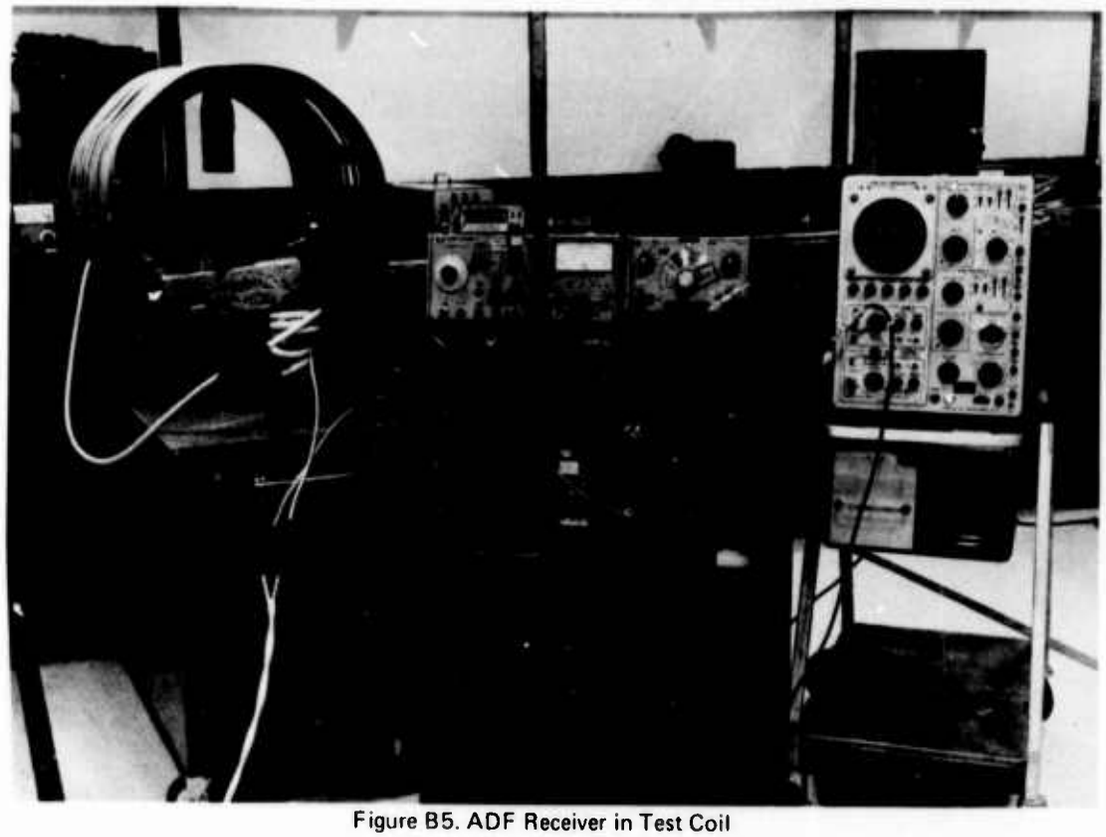

Figure B5. ADF Receiver in Test Coil

Shown are: special Z-match transformer (in front of coil); frequency-shift adjuncts (on top shelf of roll-about cart); gaussmeter (on shelf in cart); gaussmeter probe in coil. Power oscillator is not shown.

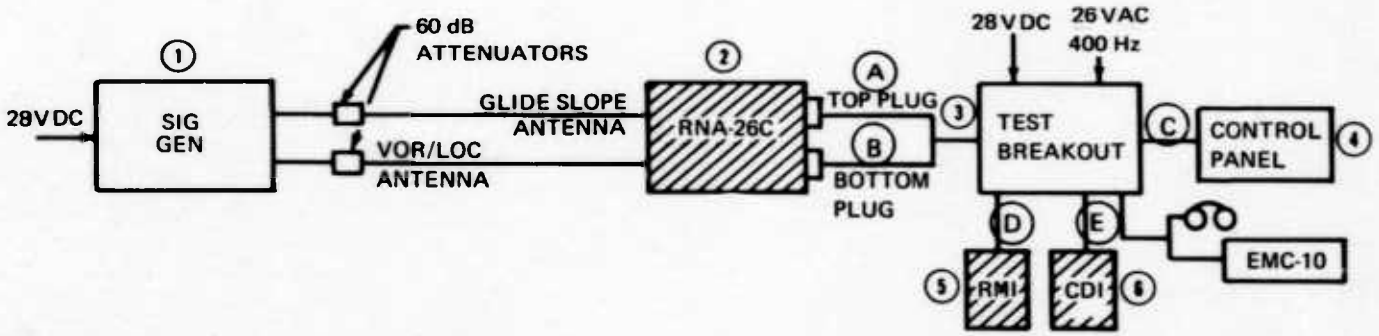

1. Precision ILS/VOR Signal Generator, Cossor Company, Type CRM 555 (See Fig. B7)
2. RNA-26C, Bendix Avionics Products
3. RNA-26C Test Breakout Box, Boeing Built
4. VOR/ILS Control Panel, Boeing Built
5. Gyrosyn Compass Indicator, Sperry, Model C-6E
6. Course Indicator, Collins, Type 331A-6D

Note: Shaded boxes indicate items under test.

Figure B6. Block Diagram of Test Setup: RNA-26C VHF Navigation Receiver (Bendix)

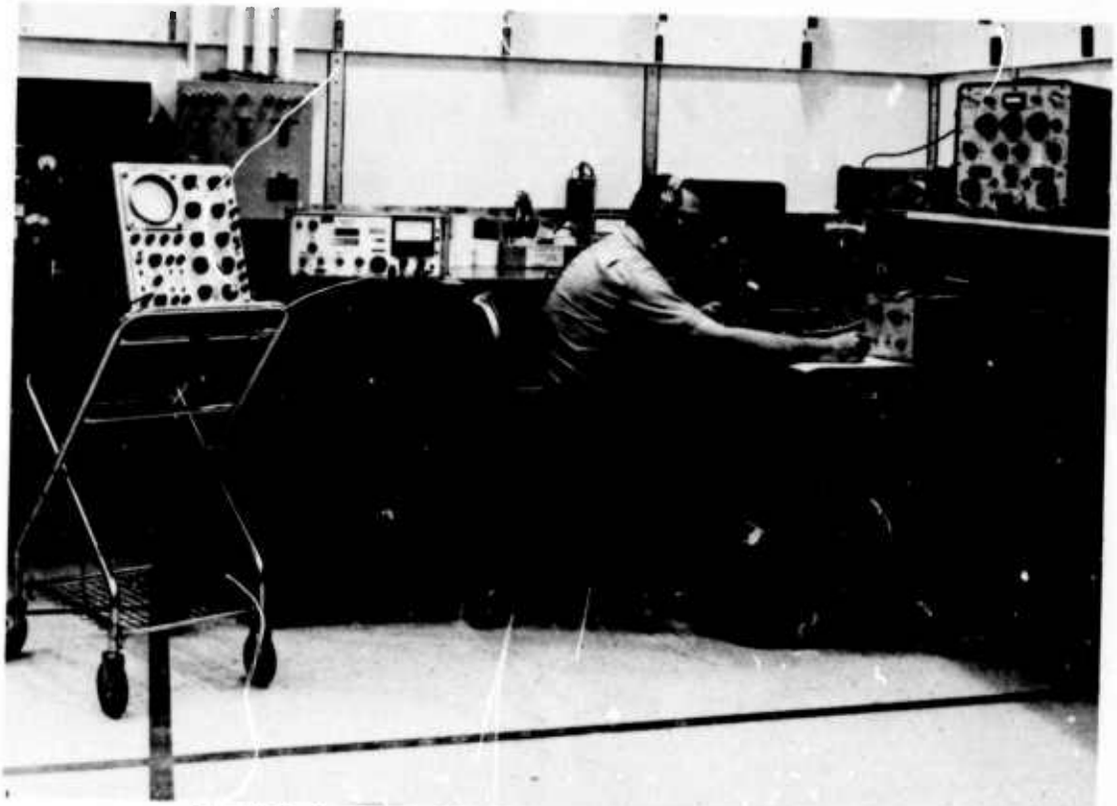

Figure B7a. Test Setup: RNA-26C VHF Navigation Receiver (Bendix)

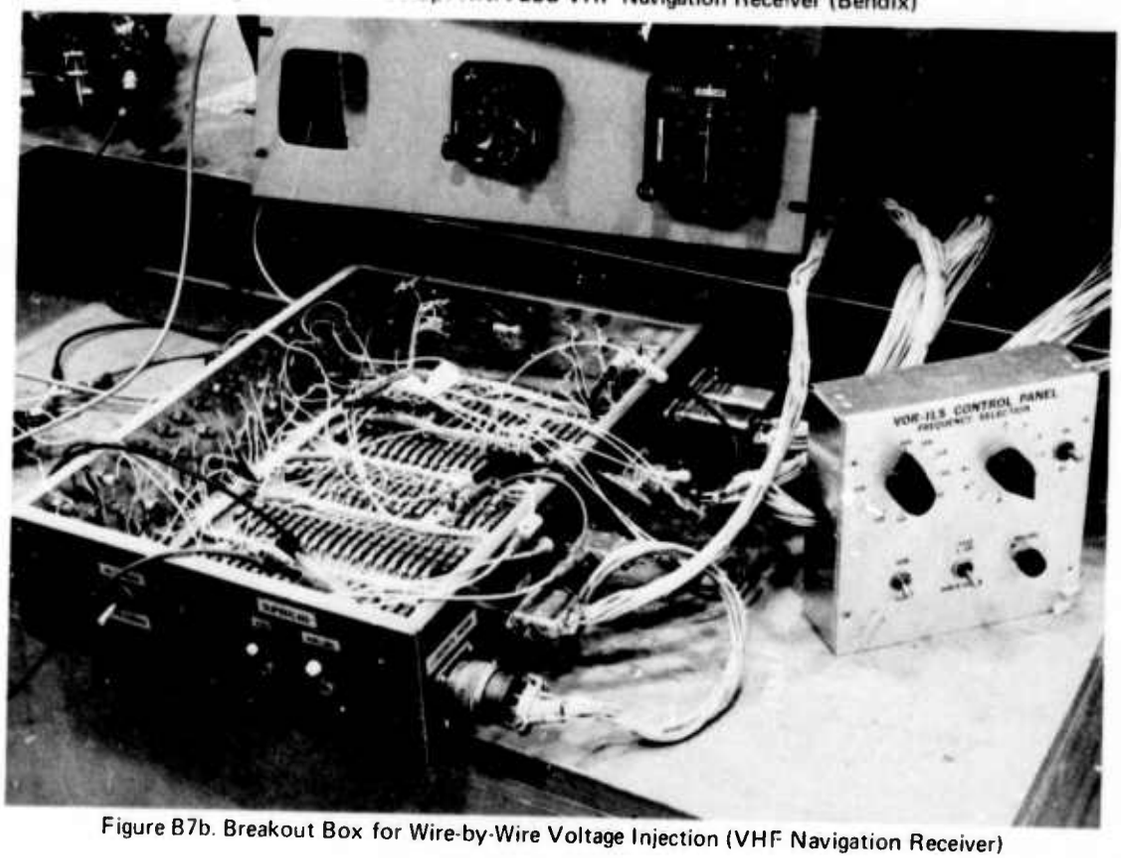

Figure B7b. Breakout Box for Wire-by-Wire Voltage Injection (VHF Navigation Receiver)

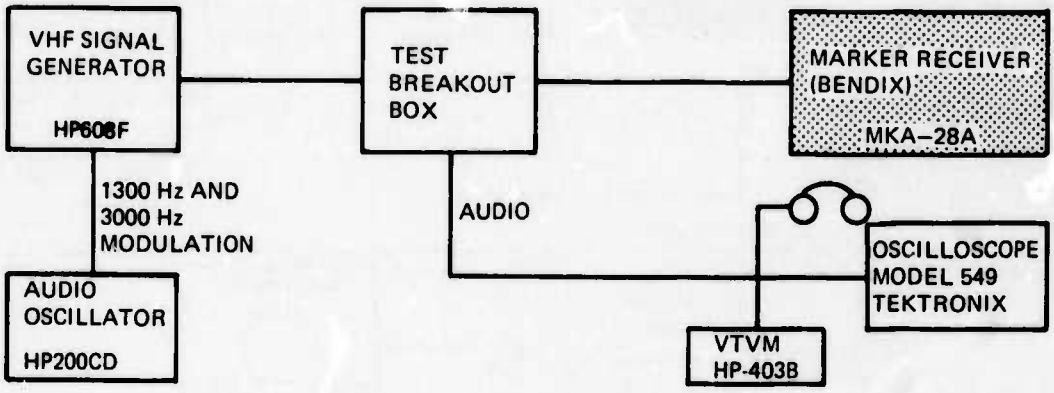

Figure B8. Test Setup: MKA-28A, Marker Receiver (Bendix)

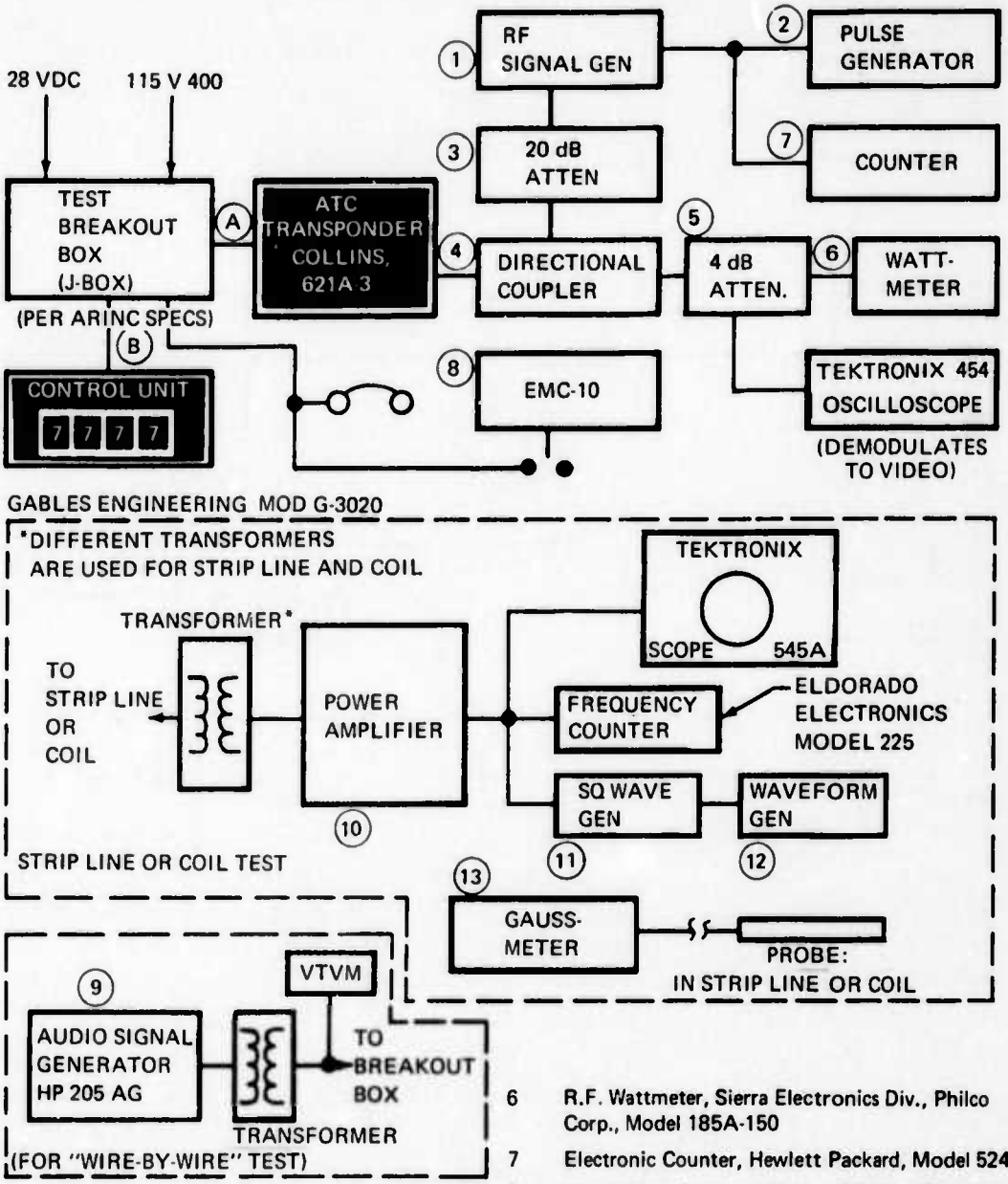

1 UHF Signal Generator, Hewlett Packard, 612A

2 Pulse Generator, Datapulse 110B

3 Attenuator, PRD, Type 1300 (19.6 dB at 4 GHz)

4 Directional Coupler, Hewlett Packard, 766D

5 Microwave Power Attenuator, Empire, Singer Co., Metrics Div. Model AT-70-4(4 dB)

6 R.F. Wattmeter, Sierra Electronics Div., Philco Corp., Model 185A-150

7 Electronic Counter, Hewlett Packard, Model 5245-L

8 Interference Analyzer 20 Hz—50 KHz, Fairchild, Model EMC-10

9 Audio Signal Generator, Hewlett Packard, 205 AG

10 Power Amplifier, Communications Measurements Lab., Model 1432D-750 (250 VA)

11 Square Wave Generator, Hewlett Packard, 211B

12 Waveform-Generator Data Royal, F210A

13 Gaussmeter, RFL, Model 1890

Figure B9. Test Setup: 621A-3 ATC Transponder (Collins)

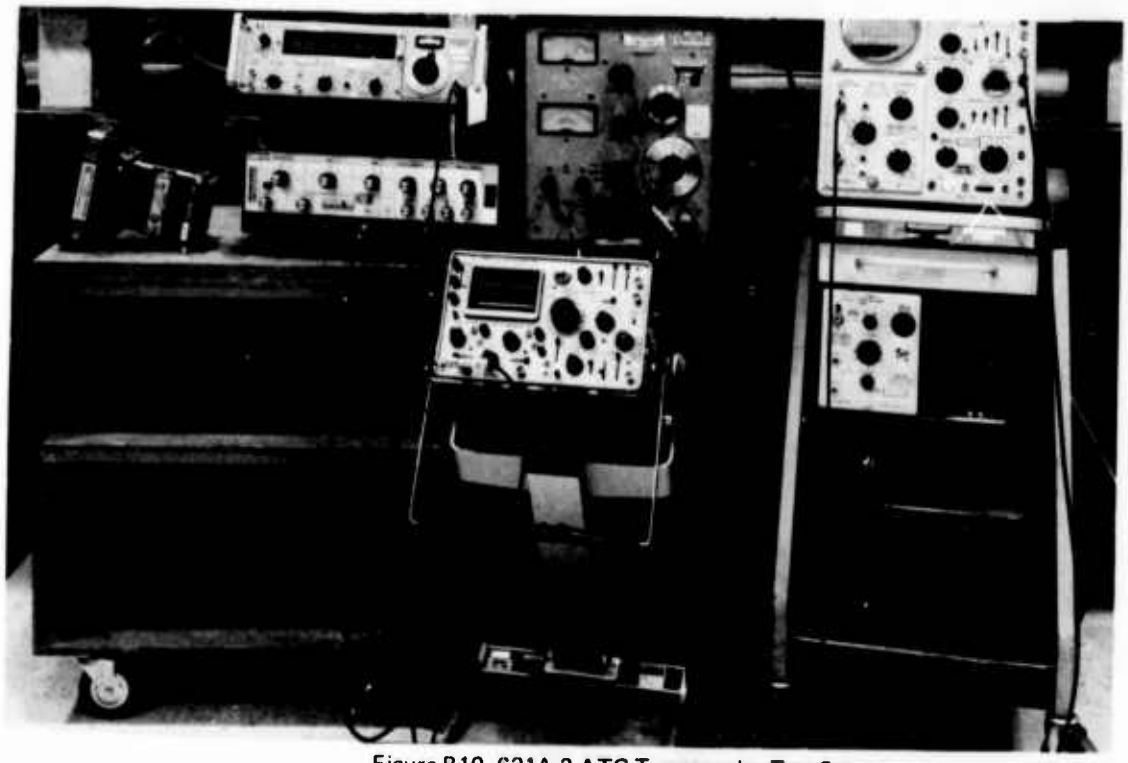

Figure B10. 621A-3 ATC Transponder Test Setup

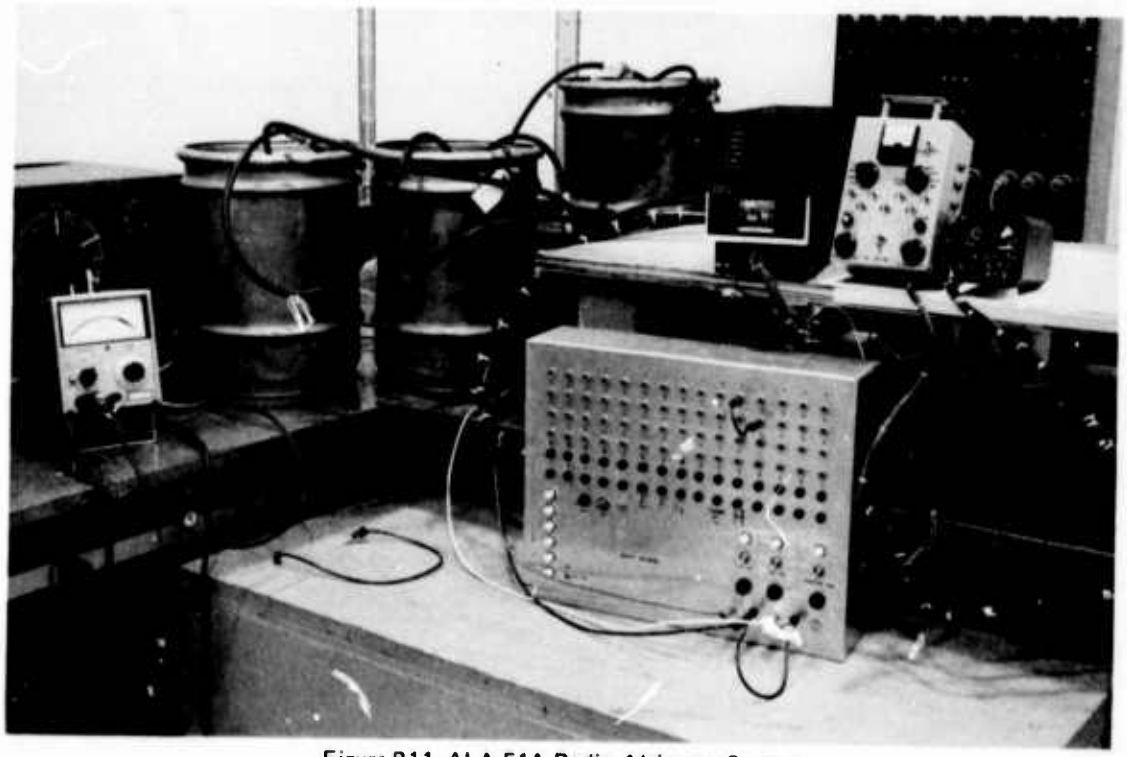

Figure B11. ALA-51A Radio Altimeter System

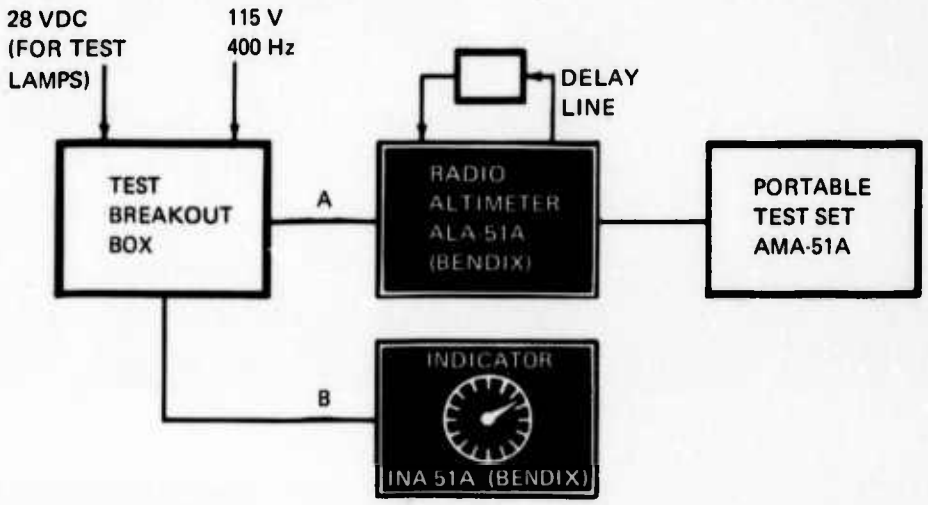

Figure B12. Test Setup: ALA-51A Radio Altimeter System (Bendix)

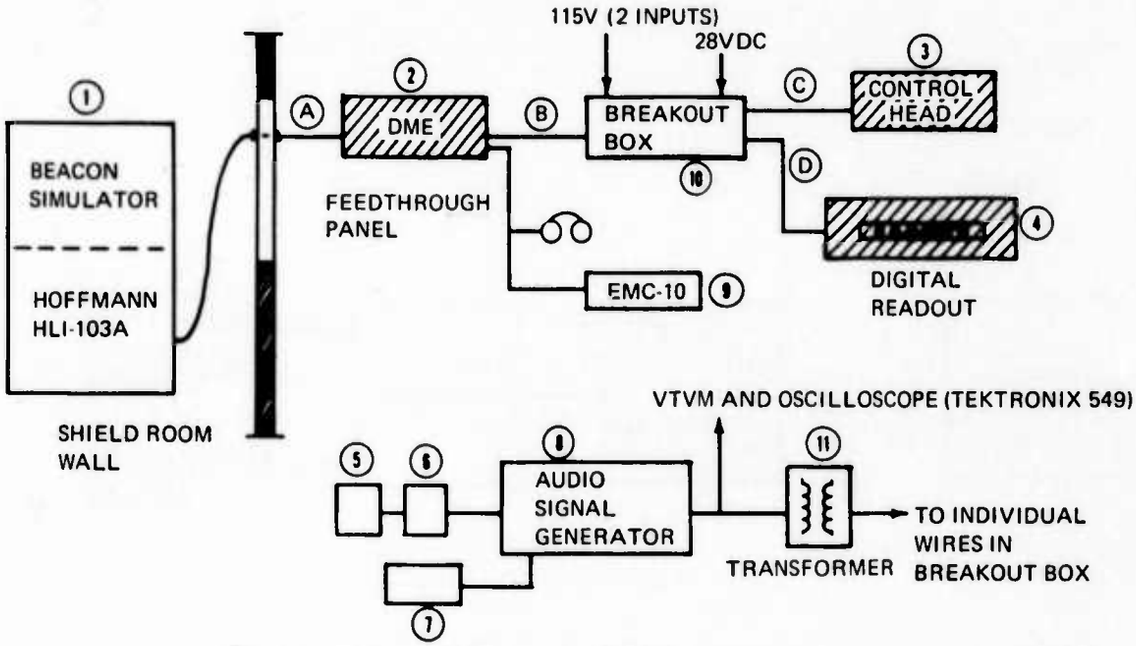

1. Beacon Simulator; Hoffmann, HLI-103A
2. Distance measuring equipment; Collins, 860E-2
3. Nav-Comm Control Head; Gables, G-1982
4. Distance Indicator (Digital); Collins, 339D-1
5. Square Wave Generator; Hewlett-Packard, 211B
6. Waveform Generator; Data Royal Corporation, Model F210A
7. Frequency Meter; Eldorado Electronics, 225
8. Audio Signal Generator; Hewlett Packard, 205AG
9. Interference Analyzer; Fairchild, Electro Metrics Corp., Model EMC-10
10. Boeing built test breakout box.
11. Secondary of this transformer inserted serially in leads in breakout box.

Note: Cross hatched boxes indicate items under test.

Figure B13. Test Setup: Distance Measuring Equipment

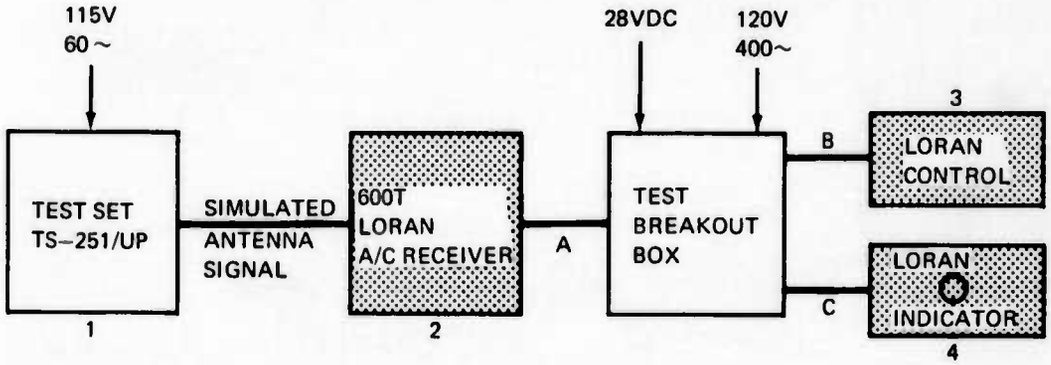

1 AIRPLANE AND MARINE INSTRUMENTS CORP., CLEARFIELD, PA.

2 LORAN A/C RECEIVER, 600T (ECC–00176) EDO COMMERCIAL CORP., MELVILLE, L.I.

3 LORAN CONTROL, 600T (ECC–0150-3)

4 LORAN INDICATOR, 600T (ECC–00105-1)

NOTE: SHADED BOXES INDICATE UNITS UNDER TEST

Figure B14. Test Setup: Loran System 600T, Edo Commercial Corp.

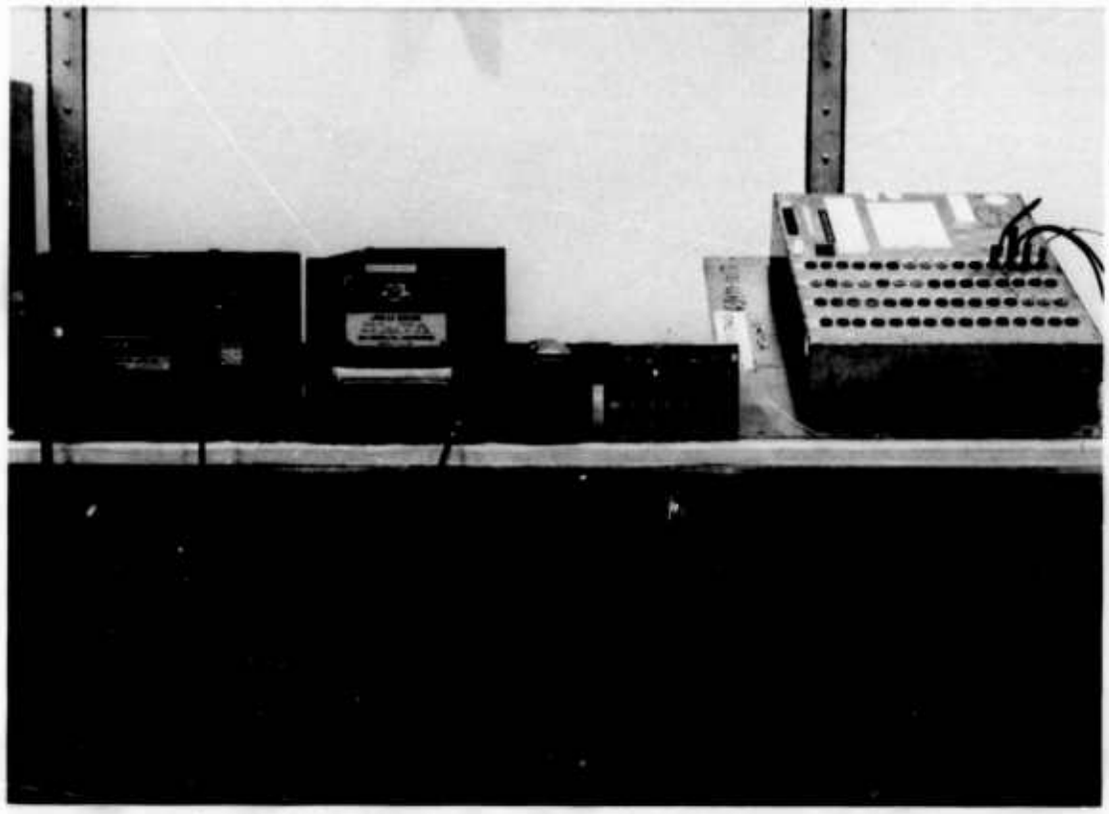

Figure B15. Test Setup: Loran Receiver 600T, Edo Commercial Corp.

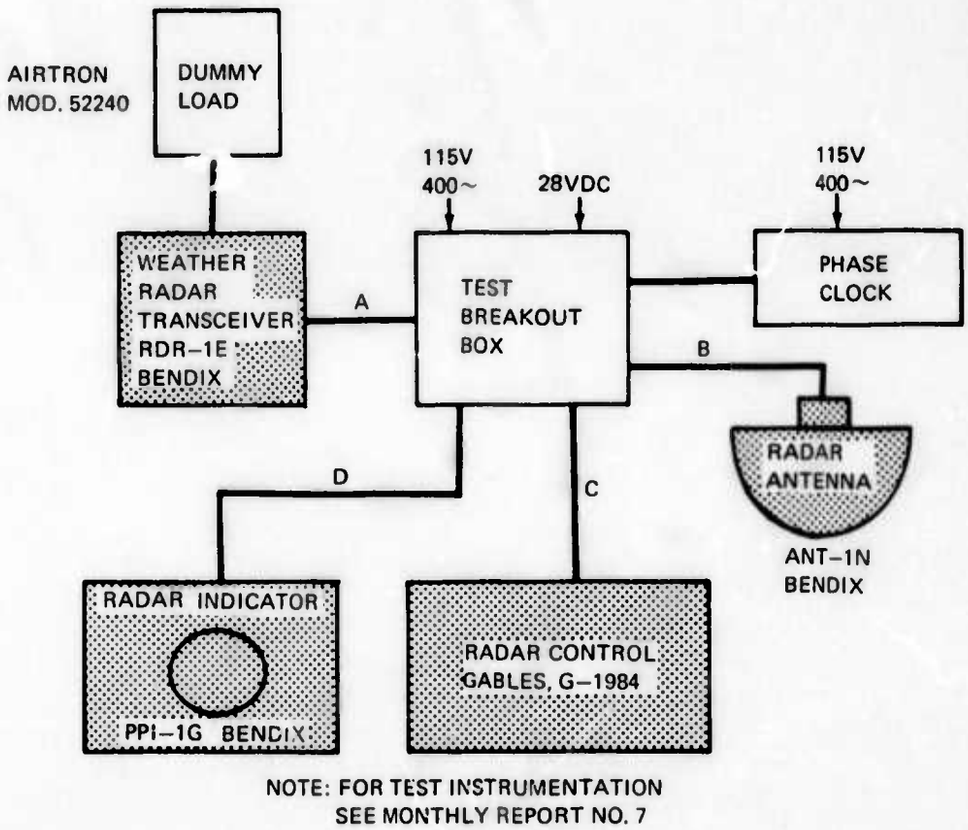

NOTE: FOR TEST INSTRUMENTATION
SEE MONTHLY REPORT NO. 7

Figure B16. Block Diagram of Test Setup: Weather Radar System RDR-1E (Bendix)

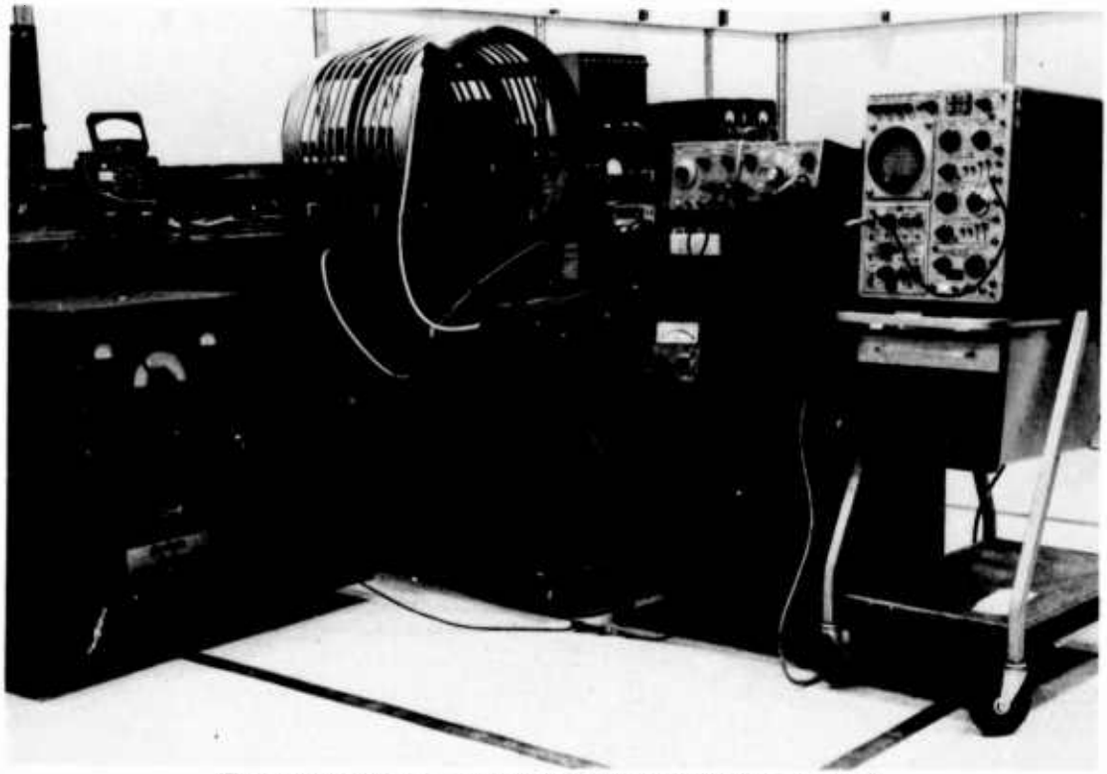

Figure B17. Test Setup: Weather Radar (Coil), RDR-1E (Bendix)

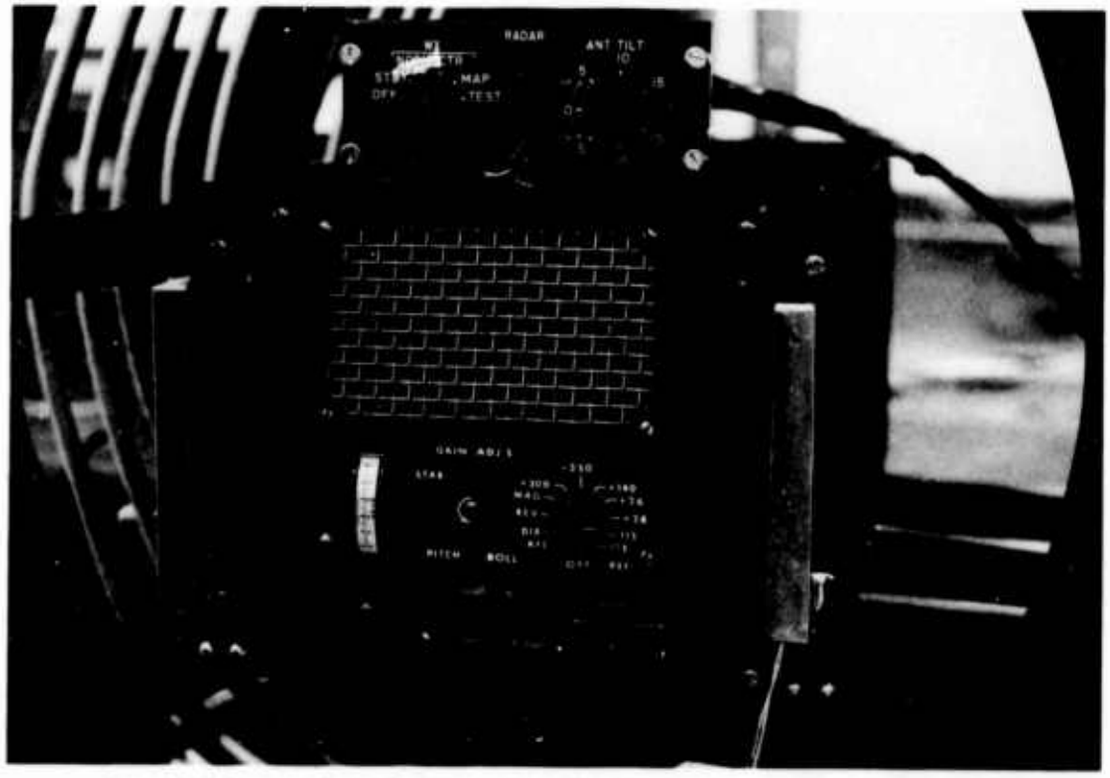

Figure B18. Weather Radar System RDR-1E, Main Unit and Radar Control in Coil for Test

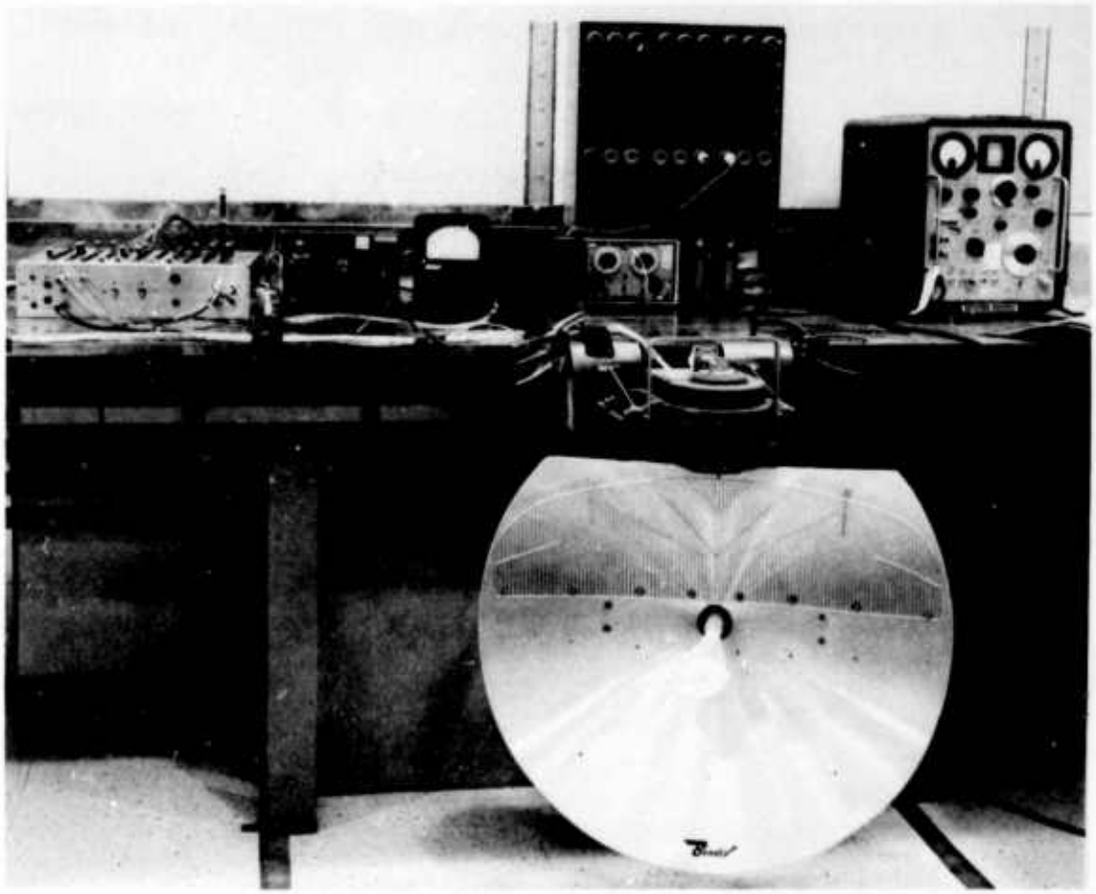

Figure B19. Weather Radar System RDR-1E Radar Antenna

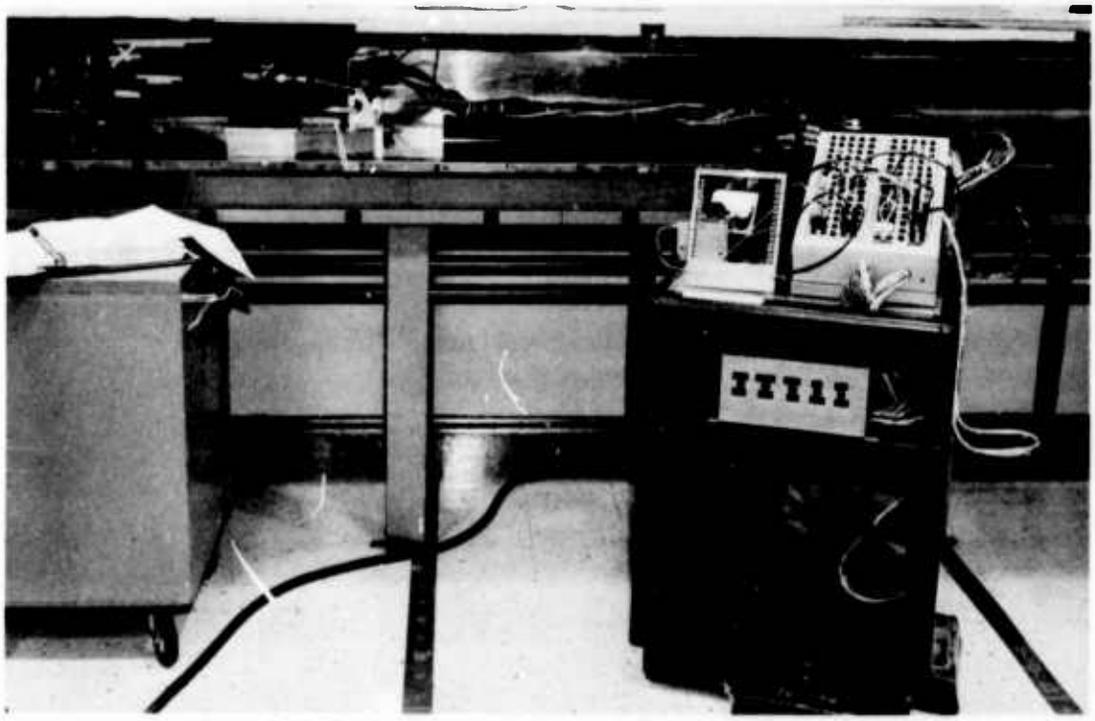

Figure B20. Test Setup: Inertial Navigation System, Strip-Line Testing

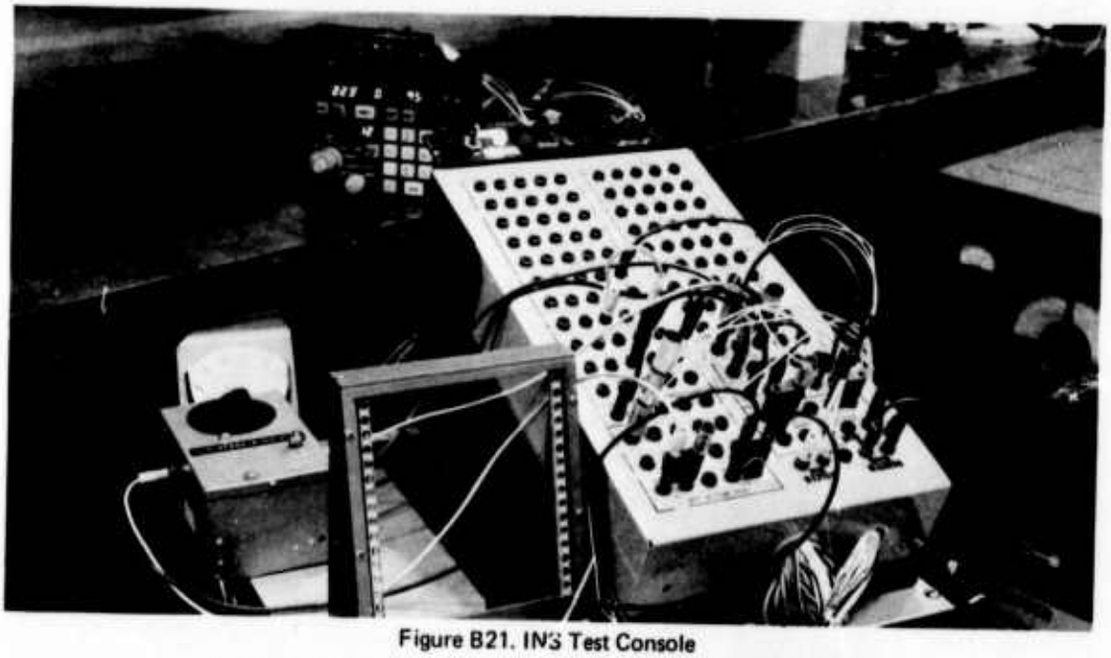

Figure B21. INS Test Console

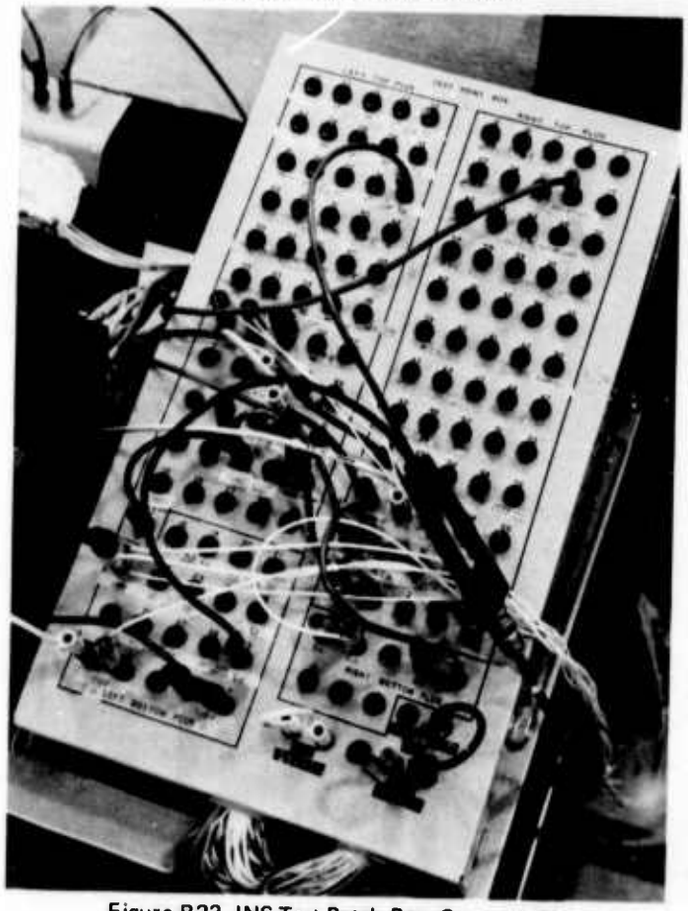

Figure B22. INS Test Patch Box, Carousel IV

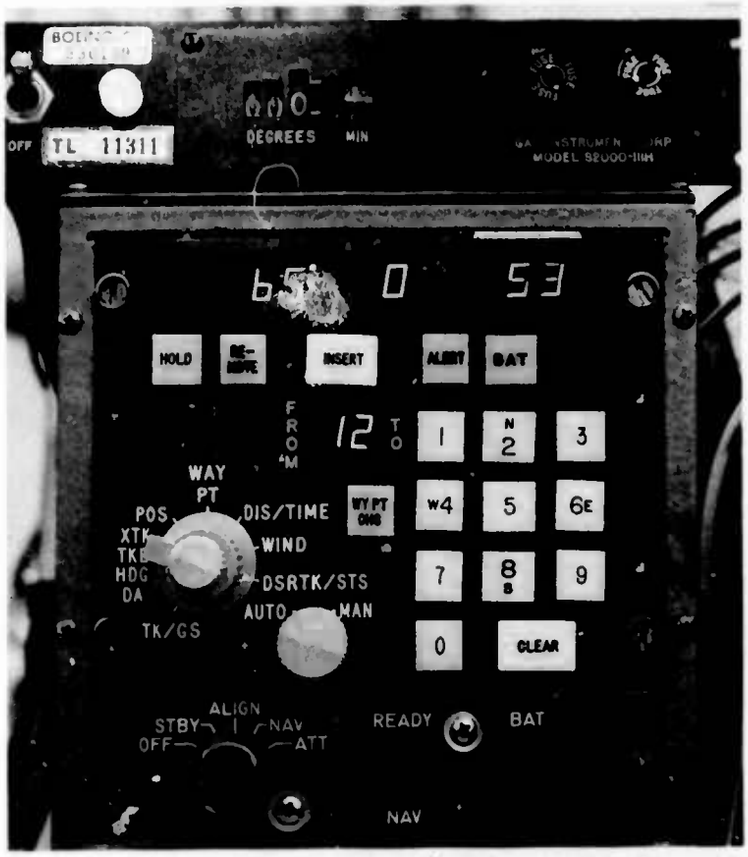

Figure B23. INS Control/Display Unit and Mode Selector Unit, Carousel IV

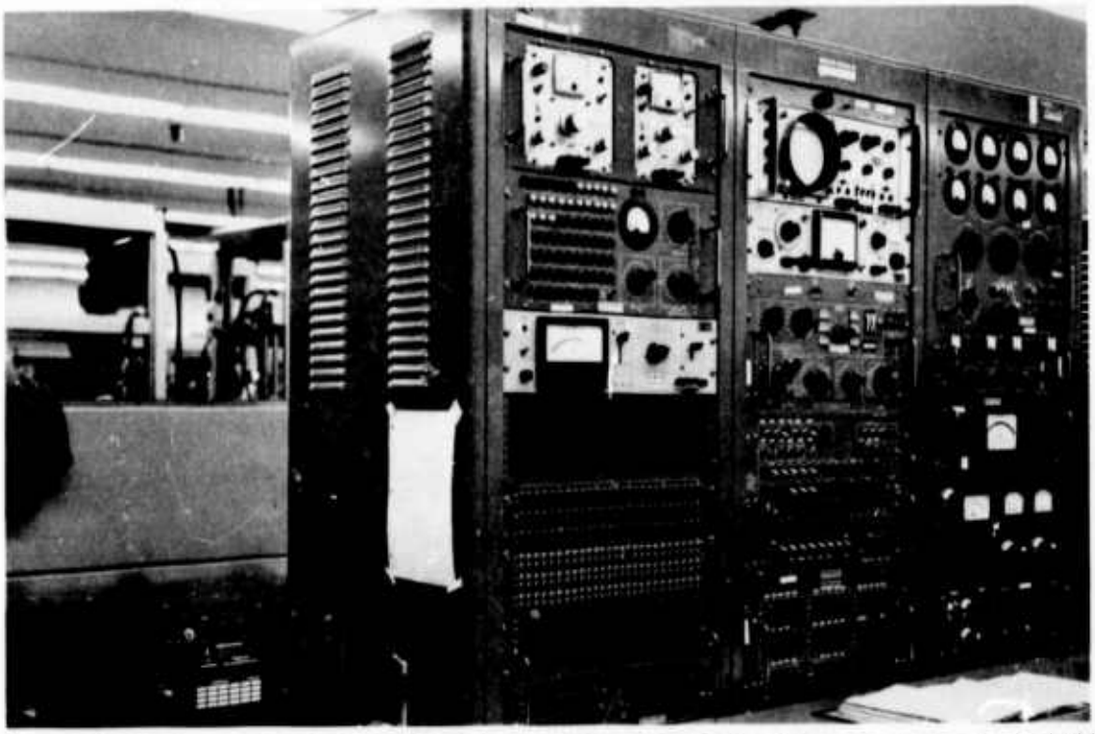

Figure B24. Test Equipment for Bendix PB-20 Autopilot Computer (Airborne Computer Unit at Lower Left)

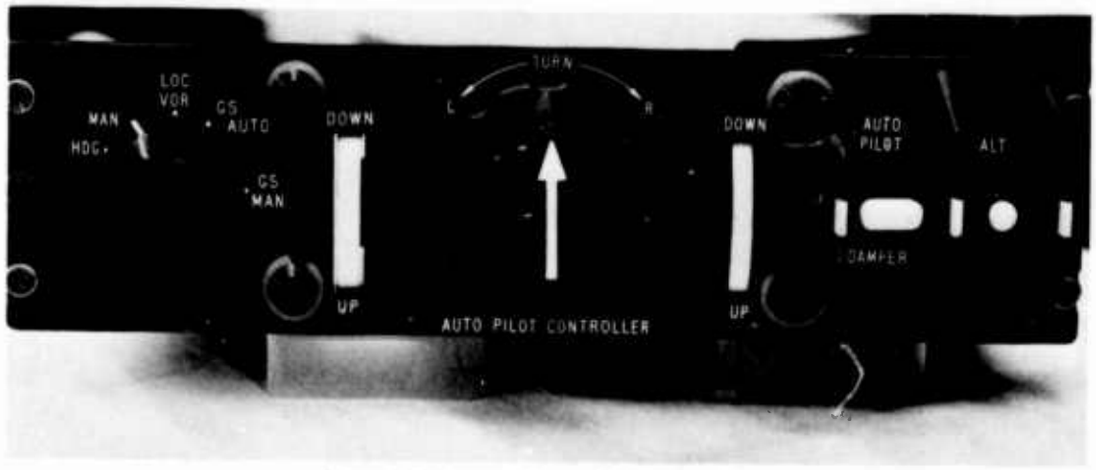

Figure B25. Control Panel, PB-20 Autopilot

Figure B26. Roll Control Channel for Sperry SP-77 Flight Control System

Figure 27a. P13-20 Autopilot Control Panel (in Coil). Servos on Test Bench at Left. Computer in Rack at Right of Coil

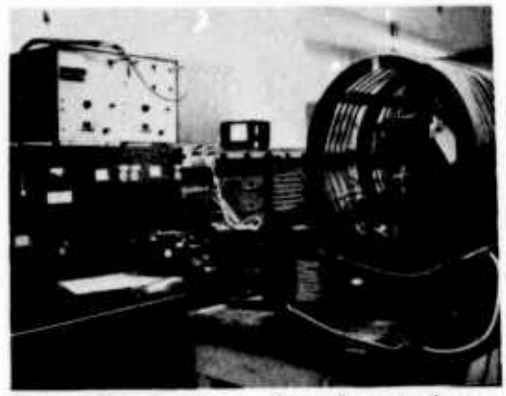

Figure B27b. Test Setup: Flight Recorder System

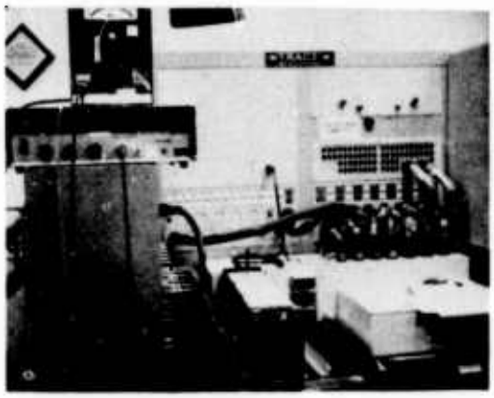

Figure B28. Automatic Test Equipment, (T.R.A.C.E.) for Air Data Computer

Figure B29. Test Equipment Required to Exercise Air Data Computer

Figure B30. Horizontal Display Cabinet – Radar Bright Display, RBDE-4

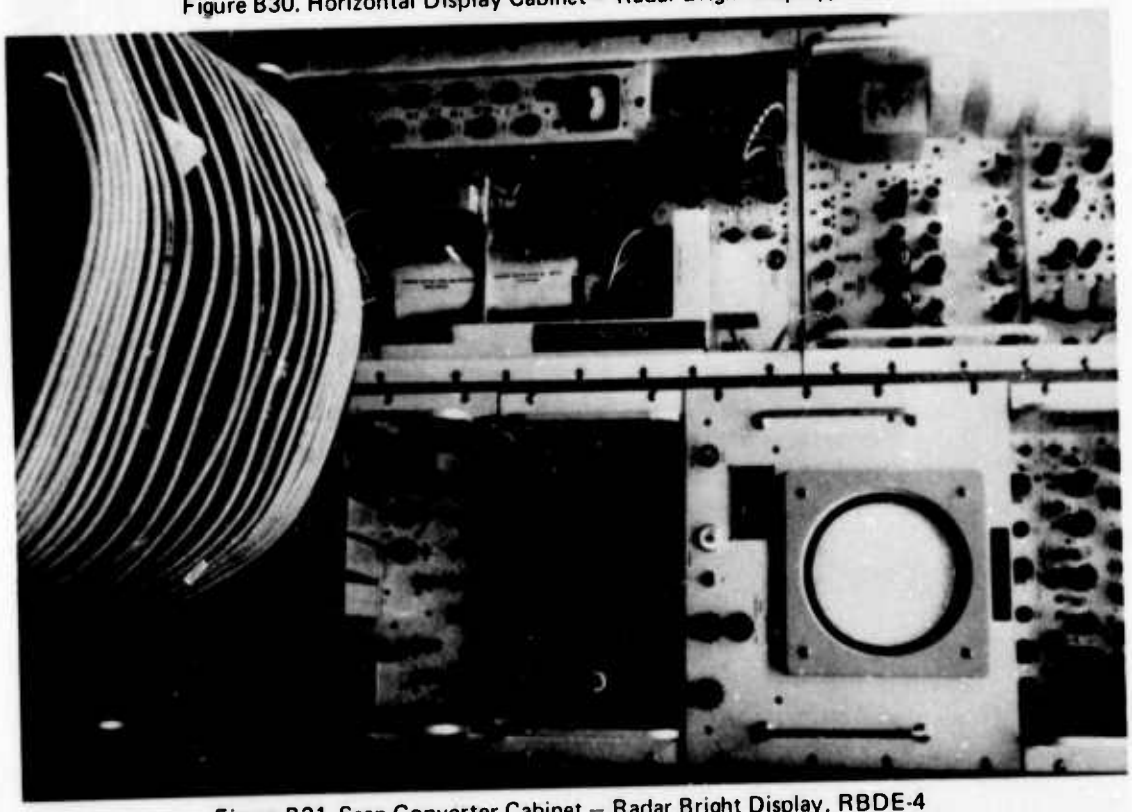

Figure B31. Scan Converter Cabinet – Radar Bright Display, RBDE-4

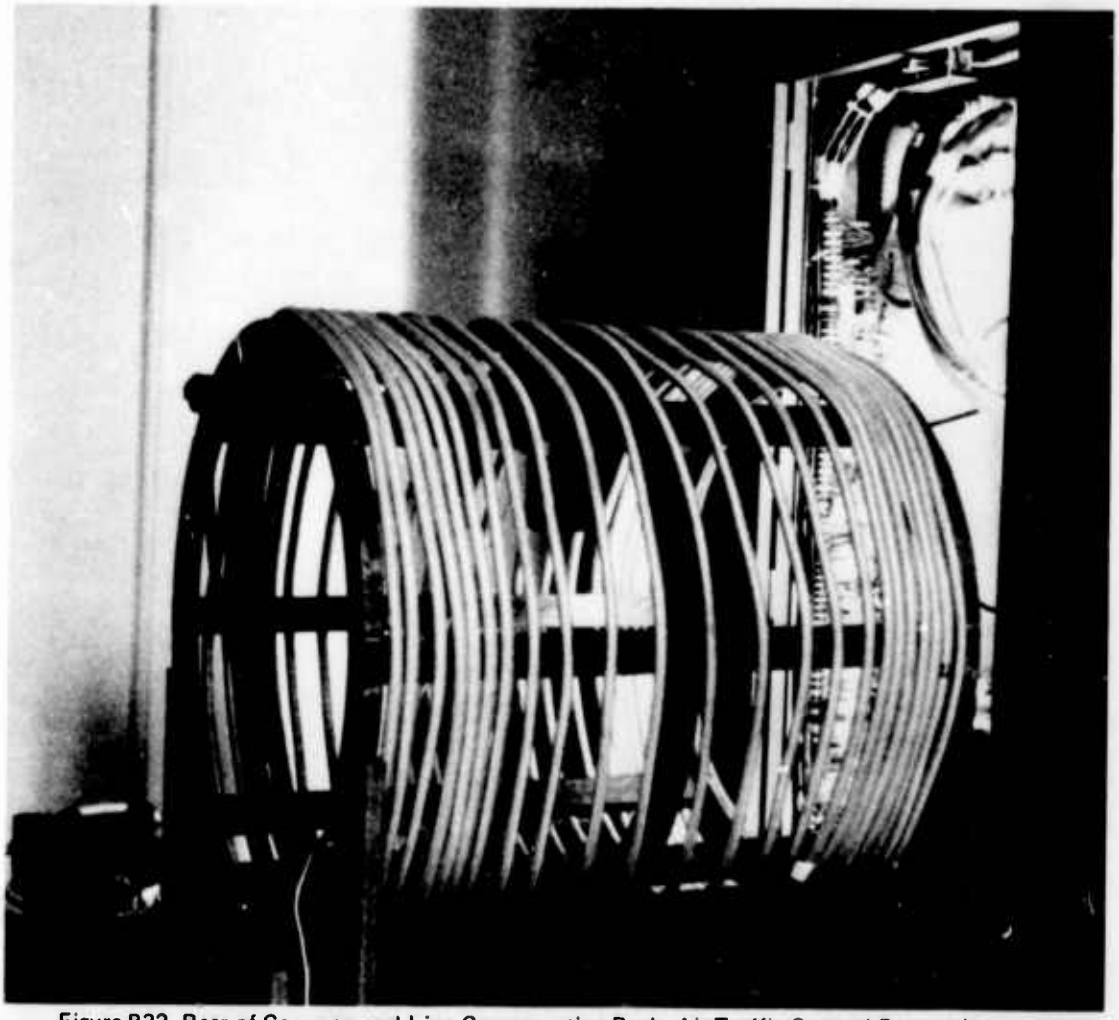

Figure B32. Rear of Common and Line Compensating Rack, Air Traffic Control Beacon Interrogator, ATCBI-2

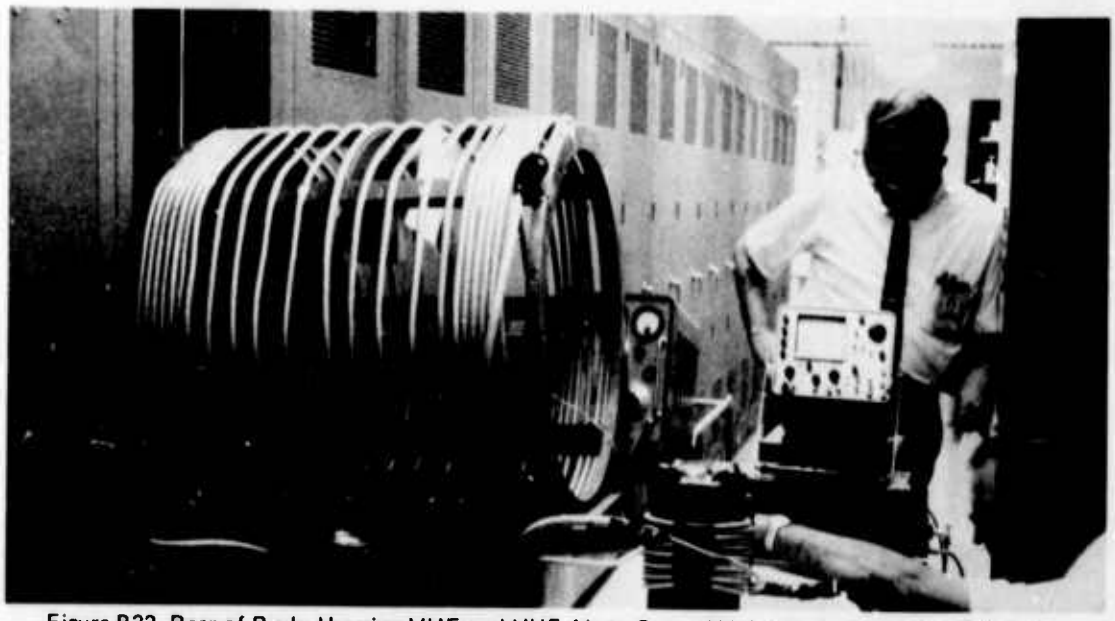

Figure B33. Rear of Racks Housing VHF and UHF Air-to-Ground Voice Communication Receivers

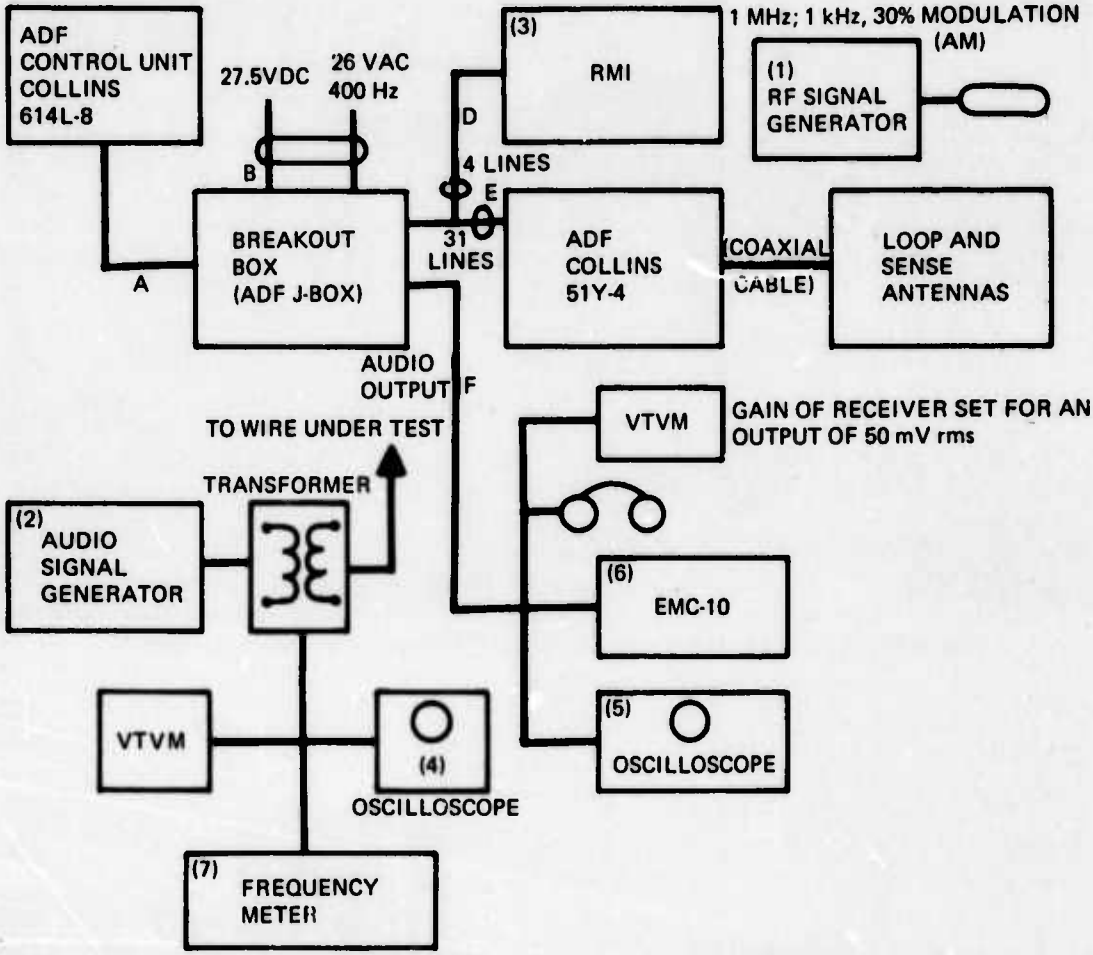

(1) SIGNAL GENERATOR, HEWLETT-PACKARD MODEL 606A
(2) AUDIO SIGNAL GENERATOR, HEWLETT-PACKARD MODEL 205AG
(3) GYROSIN COMPASS INDICATOR, SPERRY-RAND, MODEL C-6E
(4) OSCILLOSCOPE, TEKTRONIX TYPE 549
(5) OSCILLOSCOPE, TEKTRONIX TYPE 545
(6) INTERFERENCE ANALYZER, FAIRCHILD, ELECTRO-METRICS CORP., MODEL EMC-10
(7) DIGITAL FREQUENCY METER, ELDORADO ELECTRONICS, MODEL 225

NOTE: VTVM's are Hewlett-Packard, Model 403B

Figure B34. Test Setup: ADF 51Y-4

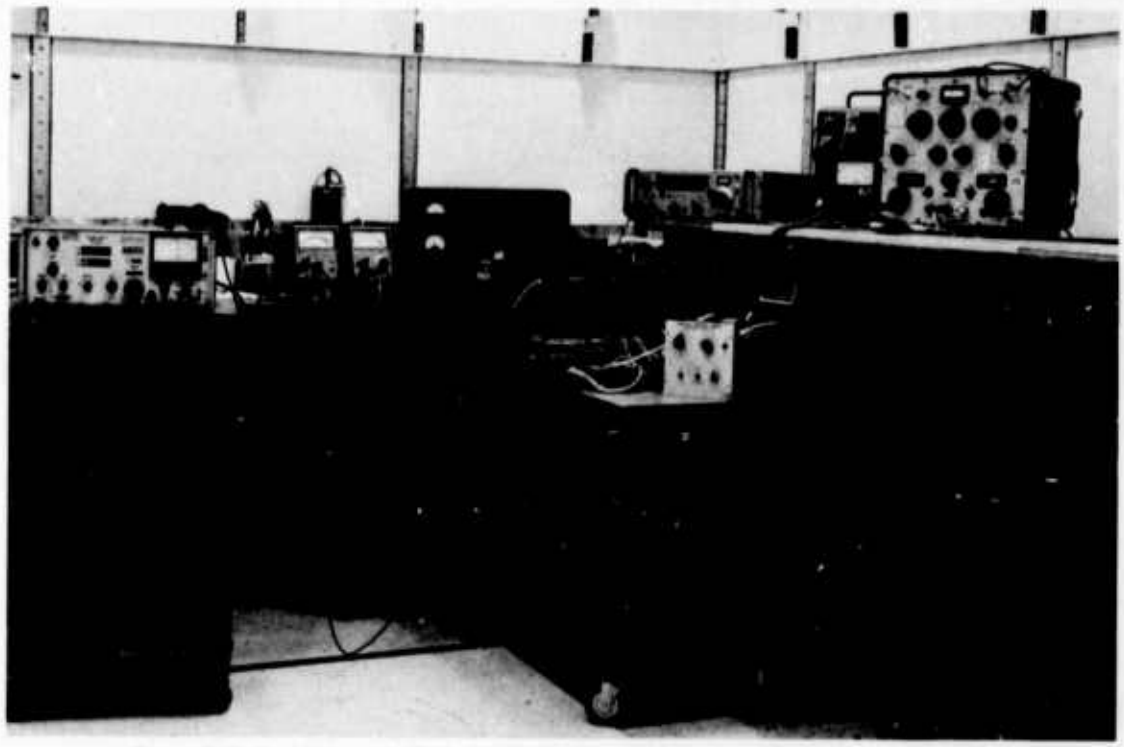

Figure B35. Test Setup: VHF Navigation Receiver (Equipment in Strip-Line Cavity)

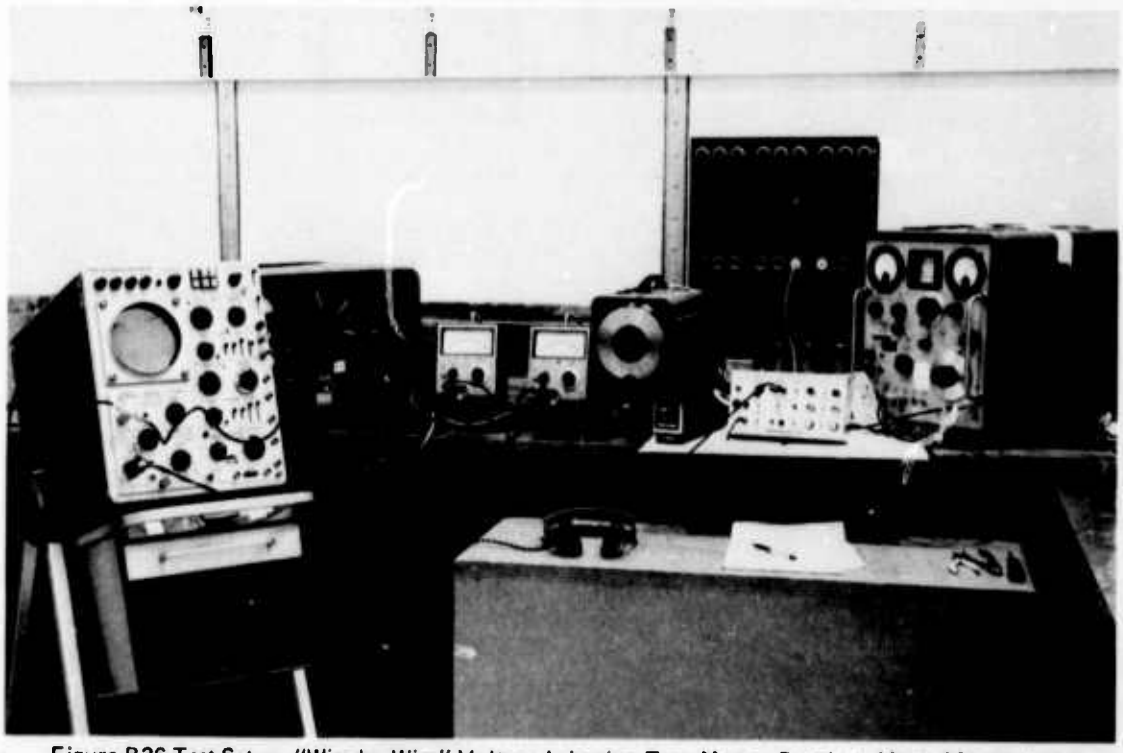

Figure B36 Test Setup: "Wire-by-Wire" Voltage Injection Test; Marker Receiver, MKA-28A (Bendix)

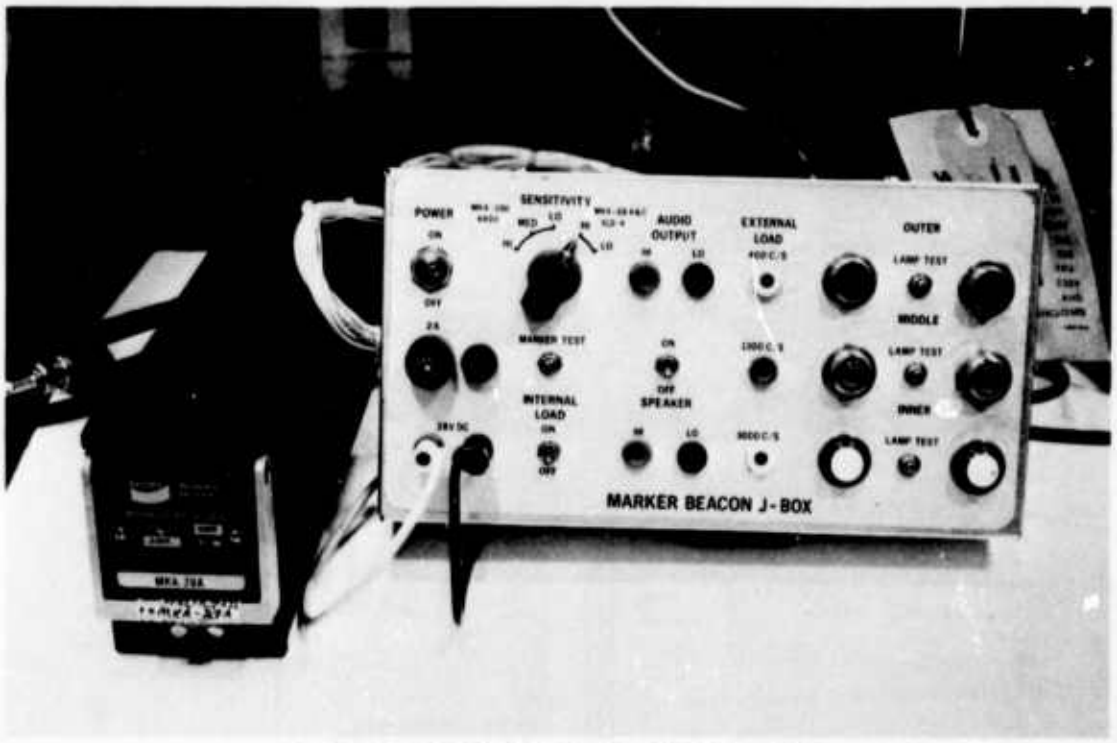

Figure B37. Marker Receiver and Test Breakout Box

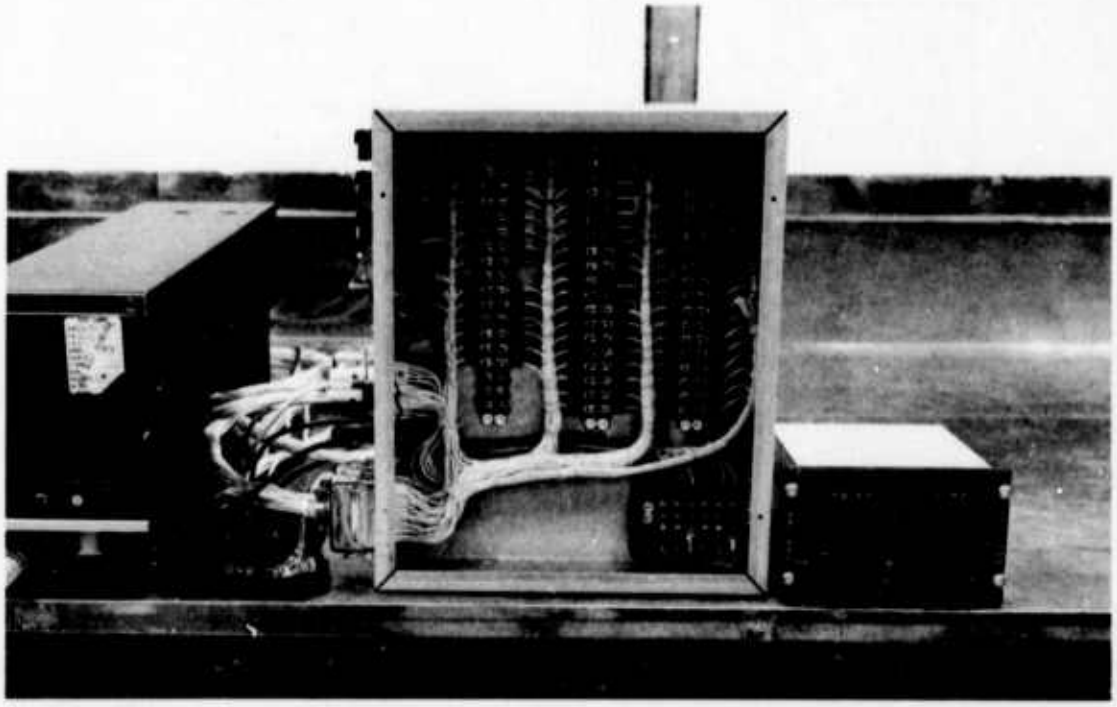

Figure B38. Test Setup and Breakout Box for Distance Measuring Equipment DME 860-2 (Collins)

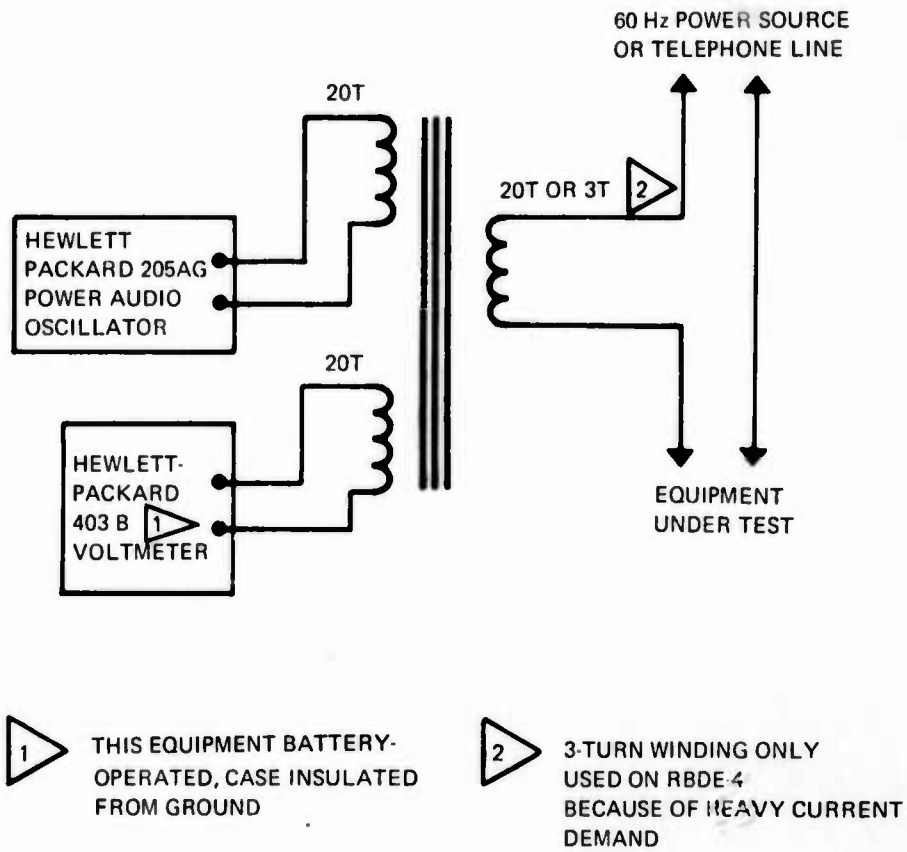

Figure B39. Test Setup: Voltage Injection in Power Lines

Figure B40. Air Route Surveillance Radar Display

Figure B41. Power Line Voltage Injection; Air Route Surveillance Radar

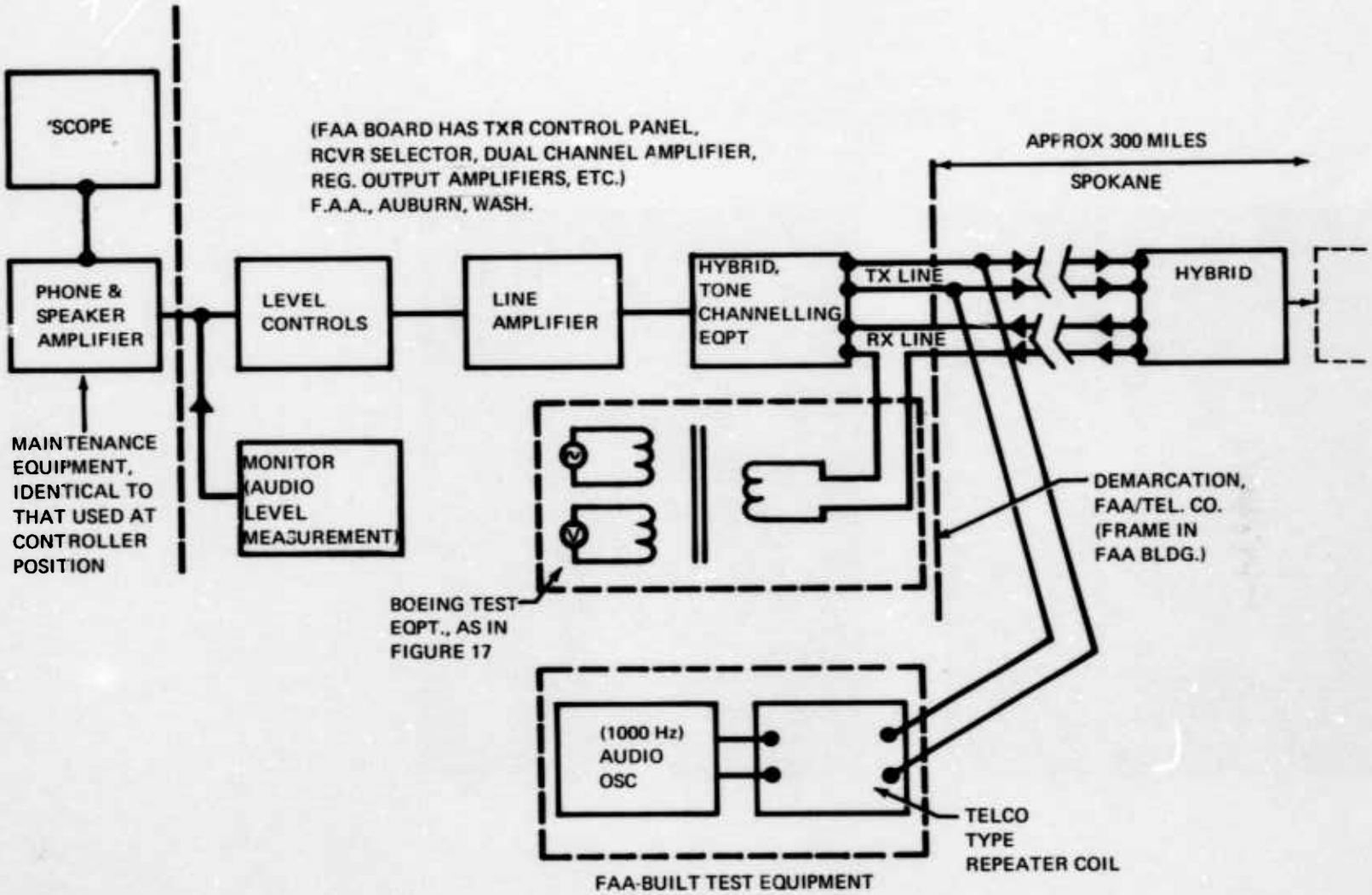

Figure B42. Telephone Circuit Test Arrangement

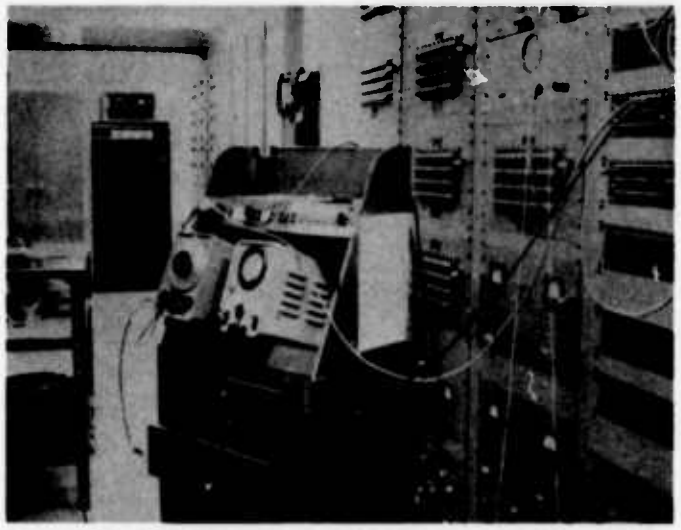

Figure B43. FAA Equipment Feeding 1000 Hz Test Signal Into Transmit Line

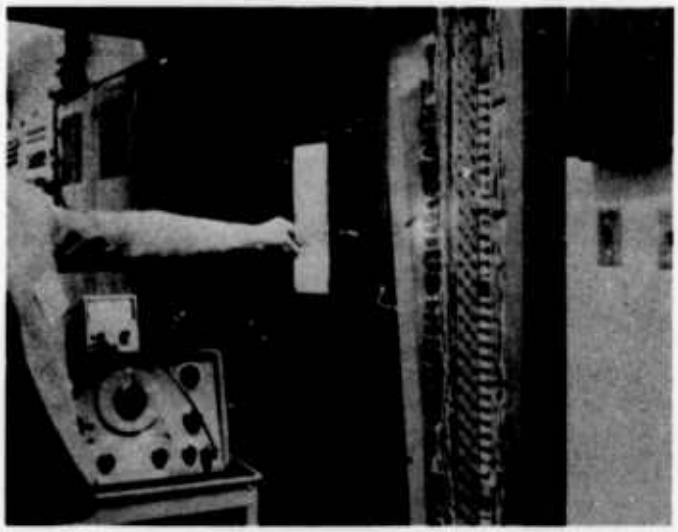

Figure B44. Boeing Test Equipment Injecting Voltages Into Receive Line on FAA Side of Demarcation to Telephone Company Facilities

Figure B45. Telephone Type Level Measuring Equipment

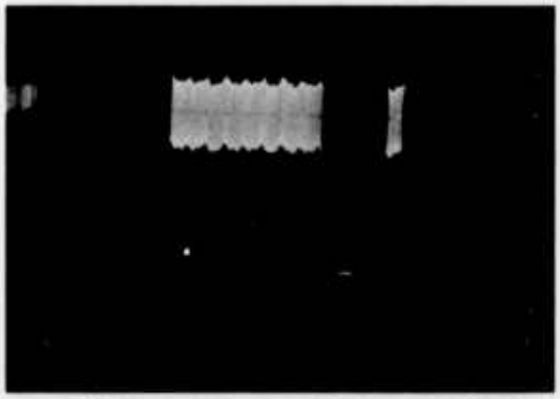

Figure B46. Received Signal on Monitor, With 60 Hz Superimposed on 1000 Hz Test Signal (20 ms/cm; 200 mv/cm)

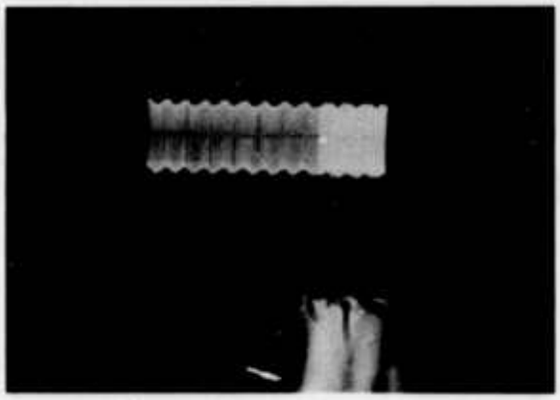

Figure B47. Received Signal on Monitor, With 60 Hz Superimposed on 1000 Hz Test Signal (700 mv, 60 Hz injected)

Security Classification

DOCUMENT CONTROL DATA - R & D

(Security classification of title, body of abstract and indexing annotation must be entered when the overall report is classified)

1. ORIGINATING ACTIVITY (Corporate author)
The Boeing Company
Commercial Airplane Group
P.O. Box 3707
Seattle, Washington 98124

2a. REPORT SECURITY CLASSIFICATION
U

2b. GROUP

3. REPORT TITLE
Aircraft Navigation and Communication Interference Mitigation–FINAL REPORT

4. DESCRIPTIVE NOTES (Type of report and inclusive dates)
FINAL REPORT December 11, 1969–March 11, 1971

5. AUTHOR(S) (First name, middle initial, last name)
Alfred Eckersley
Reuben Goldman
William W. Cooley

6. REPORT DATE

7a. TOTAL NO. OF PAGES
106

7b. NO. OF REFS
12

8a. CONTRACT OR GRANT NO.
N00039-70-C-1513

b. PROJECT NO.

c.

d.

9a. ORIGINATOR'S REPORT NUMBER(S)
D6-60134

9b. OTHER REPORT NO(S) (Any other numbers that may be assigned this report)

10. DISTRIBUTION STATEMENT

DISTRIBUTION STATEMENT A
Approved for public release;
Distribution Unlimited

11. SUPPLEMENTARY NOTES

12. SPONSORING MILITARY ACTIVITY
Department of the Navy
Naval Electronics System Command
Washington, D.C. 20360
(Navelex PME117-21)

13. ABSTRACT

The research described here is but one facet of an overall project–SANGUINE Environmental Compatibility Assurance Program (ECAP)–to ensure that an environmentally compatible, extremely low-frequency (ELF) communication system is feasible.

Described here are the experimentally determined effects of ELF fields on aircraft navigation and communication subsystems and on elements of ground control equipment. The ELF range of interest in this research is 40 to 150 Hz. Discrete test frequencies were frequency-shifted +5 Hz about nominal or center test values at a 5-Hz-per-second rate to simulate one possible SANGUINE system data transmission condition.

Magnetic fields were generated in two devices: a strip-line and a large solenoidal coil. The strip-line was 10 ft long, 2 ft wide, and 2 ft high, permitting the simultaneous immersion of several units of a subsystem under test within the field. Various permutations of equipment component orientation with respect to field direction were explored. Field strengths to 10 gauss were generated within the strip-line cavity (40 to 150 Hz) with the oscillator-amplifier used in these tests. Test coil diameter was 2 ft. Uniform field intensities to 20 gauss within the coil were attainable using the same amplifier.

Additionally, ELF voltages were injected directly into leads comprising interconnecting cables for avionic and ground control equipment under test. This test simulated voltages that may be induced in cabling with a SANGUINE system field and disclosed potential equipment susceptibilities.

Fifteen avionics systems and five ground control units (at a regional air traffic control center) were tested for susceptibility to ELF fields. Avionics items tested ranged in complexity from relatively simple oil and fuel quantity indicator subsystems to complex, flight-critical items such as inertial navigation, Loran, and Gyrosyn compass systems. A summary tabulation of all test results is given. An analysis is made of marginally susceptible items: the flux valve of the compass system and cathode-ray tube displays.

A simplified theoretical analysis was performed to determine levels of expected SANGUINE system fields at various altitudes over the antenna. Data were obtained, by test, on shielding effectiveness of large transport airplanes to ELF magnetic fields. Another analysis related magnetic field intensity external to a Boeing 747 airplane and "worst case" induced voltages in wiring inside the airplane.

Ambient field surveys at 60 Hz were performed in the vicinity of concentration of aircraft ground control equipment (FAA control towers and a regional control center) to determine field levels observably compatible with equipment operation.

A bibliography of documents pertinent to this study is appended.

DD FORM 1 NOV 65 1473

Security Classification

Security Classification

14 KEY WORDS	LINK A ROLE	LINK A WT	LINK B ROLE	LINK B WT	LINK C ROLE	LINK C WT
Extremely Low Frequency (ELF) Transmission						
SANGUINE System						
Mitigation						
Electromagnetic Compatibility (EMC)						

Security Classification